Fall 1974

SUBMERSIBLE MANEUVERING AND CONTROL

GREGORY JOHN SCHOENAU

INFORMATION TO USERS

This material was produced from a microfilm copy of the original document. While the most advanced technological means to photograph and reproduce this document have been used, the quality is heavily dependent upon the quality of the original submitted.

The following explanation of techniques is provided to help you understand markings or patterns which may appear on this reproduction.

1. The sign or "target" for pages apparently lacking from the document photographed is "Missing Page(s)". If it was possible to obtain the missing page(s) or section, they are spliced into the film along with adjacent pages. This may have necessitated cutting thru an image and duplicating adjacent pages to insure you complete continuity.

2. When an image on the film is obliterated with a large round black mark, it is an indication that the photographer suspected that the copy may have moved during exposure and thus cause a blurred image. You will find a good image of the page in the adjacent frame.

3. When a map, drawing or chart, etc., was part of the material being photographed the photographer followed a definite method in "sectioning" the material. It is customary to begin photoing at the upper left hand corner of a large sheet and to continue photoing from left to right in equal sections with a small overlap. If necessary, sectioning is continued again — beginning below the first row and continuing on until complete.

4. The majority of users indicate that the textual content is of greatest value, however, a somewhat higher quality reproduction could be made from "photographs" if essential to the understanding of the dissertation. Silver prints of "photographs" may be ordered at additional charge by writing the Order Department, giving the catalog number, title, author and specific pages you wish reproduced.

5. PLEASE NOTE: Some pages may have indistinct print. Filmed as received.

SUBMERSIBLE MANEUVERING AND CONTROL

by

Gregory J. Schoenau

B.Sc., University of Saskatchewan, 1967

M.Sc., University of Saskatchewan, 1969

A THESIS

Submitted to the University of New Hampshire

In Partial Fulfillment of

the Requirement for the Degree of

Doctor of Philosophy

Graduate School

Engineering Ph.D. Program

Systems Design Area
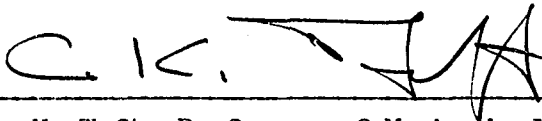
October 1974

This thesis has been examined and approved.

_____
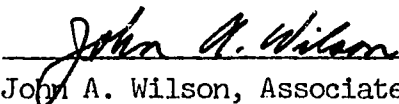Robert W. Corell, Professor of Mechanical Engineering

_____
David E. Limbert, Associate Professor of Mechanical Engineering

_____
Charles K. Taft, Professor of Mechanical Engineering

_____
Robin D. Willits, Associate Professor of Business Administration

_____
John A. Wilson, Associate Professor of Mechanical Engineering

ABSTRACT

Improving the maneuverability of a submersible offers
a number of advantages. Principal among these is a reduction
in the amount of manhours spent operating the submersible,
thus freeing the operator's time for other tasks. This also
enhances the capability of the submersible to perform tasks
where precise control is required.

Feedback control laws are derived in this thesis to
aid the operator in controlling the motion of a submersible.
The objective of these control laws is to automatically com-
pensate for the coupling effects between the motions in the
various degrees of freedom, thus providing the operator with
single - output control. To accomplish this, a general theory
for decoupling some classes of nonlinear systems is derived.
Decoupling is achieved by nonlinear feedback of measurements
of the states of the system. For a submersible, the system
states are the velocities and displacements in each degree of
freedom. Within certain practical constraints, nonlinear un-
stable coupled systems can be compensated to behave as stable
decoupled systems exhibiting linear input - output transfer
relationships.

The theory is used to successfully decouple the roll
and surge equations for a particular submersible; the U.S.
Navy's Deep Submergence Rescue Vehicle (DSRV). Computer simu-
lations are conducted to verify the results. These results
are extended to develop a set of generalized feedback equations
for the complete decoupling of the motion of the DSRV in all
six degrees of freedom. Some limitations associated with imple-
menting this scheme, such as the effect of control input
saturation, are discussed. Methods of satisfactory control
system design within these limitations are proposed.

Submersible maneuverability can also be improved by adhering to a vessel design which offers a high degree of geometric symmetry. The wake steering nozzle (WSN) is a new method of steering submersibles which has the potential of improving the geometric symmetry of a submersible as well as reducing the number of thrusters required. The WSN consists basically of a conventional propeller surrounded by an accelerating type flow nozzle. In a properly designed flow nozzle, opening a port located just aft of the propeller plane induces flow into the nozzle deflecting the wake producing a steering force.

The operation of several propeller-nozzle combinations is investigated at zero and nonzero forward velocity. A series of tests are conducted at zero forward velocity to determine the effects of major parameters of propeller-nozzle geometry on reliability, propeller torque and the axial and radial thrusts developed. The parameters varied in the tests are nozzle length, nozzle divergence and propeller pitch. These tests reveal that the radial steering thrust of the nozzles increases with the nozzle divergence. However, higher nozzle divergence results in an unreliable mode of operation where the wake remains deflected after the control port is closed producing an erratic radial thrust. The tests do define a set of nozzles which operate reliably while producing reasonably large radial thrusts. These combinations are the longer nozzles and are about midrange in terms of divergence and propeller pitch.

Two nozzles from the static tests which were midrange in terms of divergence are chosen for forward velocity testing. The reliability of these nozzles shows an increase with forward velocity. Locating a series of ports axially along the nozzle surface is shown to be an effective means of controlling the magnitude of the radial steering force.

Based on the test results, a preliminary comparison is made between the WSN and some conventional submersible propulsion and steering systems. The comparison is made using computer simulations. The WSN is shown to possess the same steering characteristic as a conventional tail mounted steering device. Although the efficiency of the WSN as a basic thruster is less than that of a conventional nozzled propeller, it can be expected to improve with further optimization of the basic design.

The research on the wake steering nozzle reported in this thesis represents the organized efforts of a number of people. The role of the author in this project was that of project coordinator. In this dissertation, the writer's experience in the management structure of the project is related to certain aspects of organizational behavior theory to formulate some key concepts considered relevant in managing research projects of this type. This covers concepts on the organizational level such as project planning and goal setting, to interpersonal considerations such as the type and style of leadership provided.

ACKNOWLEDGEMENTS

TABLE OF CONTENTS

LIST OF FIGURES

LIST OF TABLES

LIST OF SYMBOLS

Symbol	Definition
A_c	Characteristic surface area of the tiltable shroud (ft^2)
b_s	Shroud span (ft)
C_d	Shroud drag coefficient
C	Shroud lift coefficient
C_s	Shroud chord (ft)
D	Propeller/nozzle inside diameter (in)
F	Thrust (lbs)
F_d	Drag force developed by shroud (lbs)
F	Lift force developed by shroud (lbs)
I_x	DSRV roll moment of inertia ($slug\text{-}ft^2$)
I_y	DSRV pitch moment of inertia ($slug\text{-}ft^2$)
I_z	DSRV yaw moment of inertia ($slug\text{-}ft^2$)
J	Advance ratio
K_{TA}	Axial thrust coefficient of propeller and nozzle
K_{TR}	Radial thrust coefficient of propeller and nozzle
K_{TR-A}	Steering ratio of propeller and nozzle
K_p	Roll moment due to DSRV main propeller (ft-lbs)
K_{pc}	Pressure coefficient of propeller and nozzle
K_t	Roll moment due to DSRV ducted thrusters (ft-lbs)
K_Q	Torque coefficient of propeller and nozzle
L	Nozzle length (in)
L_a	Length of nozzle aft section (in)

Symbol		Definition
L_b	-	Distance from the origin of the axis system to the tip of the bow of the submersible (ft)
L_p	-	Axial length of the propeller hub (in)
L_s	-	Distance from the tip of the bow of the submersible to the leading edge of the shroud (ft)
L_v	-	DSRV overall length (ft)
m	-	DSRV mass in the submerged state including entrained water (slugs)
M_p	-	Pitch moment due to DSRV main propeller (ft-lbs)
M_t	-	Pitch moment due to DSRV ducted thrusters (ft-lbs)
n	-	Propeller speed (rev/sec)
N_p	-	Yaw moment due to DSRV main propeller (ft-lbs)
N_t	-	Yaw moment due to DSRV ducted thrusters (ft-lbs)
p	-	Angular velocity relative to the DSRV roll axis (radians/sec)
P	-	Propeller pitch (in)
P_a	-	Ambient pressure of fluid (lbs/in^2)
P_s	-	Pressure at any point on the nozzle surface a distance Z_a from the nozzle entrance (lbs/in^2)
P_v	-	Vapor pressure of fluid (lbs/in^2)
q	-	Angular velocity relative to the DSRV pitch axis (radians/sec)
Q	-	Torque (ft-lbs)
r	-	Angular velocity relative to the DSRV yaw axis (radians/sec)
r_h	-	Radius of the propeller hub (in)
R_c	-	Radius of curvature of the nozzle aft section inside surface (in)

Symbol		Definition
R_{co}	–	Radius of curvature of nozzle aft section outside surface (in)
t	–	Time
t_p	–	Propeller blade thickness (in)
u	–	Linear velocity along the DSRV surge axis (ft/sec)
$\bar{u}$	–	mx1 vector representing the inputs of a system with components $u_1, u_2, \ldots \ldots, u_m$
v	–	Linear velocity along the DSRV sway axis (ft/sec)
V	–	Fluid velocity (ft/sec)
w	–	Linear velocity along the DSRV heave axis (ft/sec)
$\bar{w}$	–	mx1 vector representing the new inputs to a decoupled system with components $w_1, w_2, \ldots \ldots, w_m$
$\bar{x}$	–	nx1 vector representing the states of a system with components $x_1, x_2, \ldots \ldots, x_n$
$\bar{y}$	–	mx1 vector representing the outputs of a system with components $y_1, y_2, \ldots \ldots, y_m$
x_G, y_G, z_G	–	Coordinates of the center of mass relative to the body axes (ft)
X_{oi}, Y_{oi}, Z_{oi}	–	Initial values of the DSRV position in the fixed coordinate frame (ft)
X_p, Y_p, Z_p	–	Forces due to the main propeller along the surge, sway and heave axes respectively (lbs)
X_s, Y_s, Z_s	–	Forces produced by the tiltable shroud along the surge, sway and yaw axes respectively (lbs)
X_t, Y_t, Z_t	–	Forces due to the ducted thrusters along the surge, sway and yaw axes respectively (lbs)
x_{ti}, y_{ti}, z_{ti}	–	Coordinates of the ballast tanks relative to the vehicle axes (ft)

Symbol		Definition
Z_a	-	Axial distance along the nozzle surface (in)
α_s	-	Angle of attack of the fluid relative to the shroud (degrees)
δ_y	-	Angle of deflection of the shroud relative to the DSRV surge axis (degrees)
θ	-	Angular displacement relative to the DSRV pitch axis (radians)
θ_d	-	Nozzle divergence angle (degrees)
θ_r	-	Angle of rotation of the thrust vector (degrees)
ϕ	-	Angular displacement relative to the DSRV roll axis (radians)
ψ	-	Angular displacement relative to the DSRV yaw axis (radians)
ρ	-	Fluid density (slugs)
μ	-	Fluid viscosity (lbs-sec/ft^2)
η	-	Efficiency

CHAPTER I

INTRODUCTION

1-A General

There has been a recent expanded usage of small sub-
mersibles such as Alvin, Dolphin and Deep Quest for research,
rescue and recovery operations. These Deep Submergence Vehicles
(DSV) belong to a new class of submersibles. Characteristic of
this group are mission requirements calling for control with
precise spatial orientation and maneuverability of the vehicle
in all the six degrees of freedom. Precise positional navigation
is essential for such operations as e search for and recovery
of objects from the ocean bottom. Wiv! the resulting emphasis on
control as opposed to speed, the DSV is generally equipped with
more thrusters and steering surfaces than the fleet or attack
submarines.[1-2]*

The propulsion-steering system of one of the more sophi-
sticated submersibles, the U.S. Navy's Deep Submergence Rescue
Vehicle (DSRV) is shown in Figure 1. The reversible main propeller
provides for thrusts along the vehicle surge axis. The tiltable
shroud provides yaw and pitch turning moments during cruising. For
hovering maneuvers, the tiltable shroud is largely ineffective and
the ducted thrusters are used to provide yaw and pitch moments as
well as sway and heave forces. Steady state roll and pitch moments
are achieved by pumping mercury between the tanks. Vehicle neutral
buoyancy at any depth is achieved by controlling the amount of
water in the variable ballast tanks.

* Numbers in brackets refer to references.
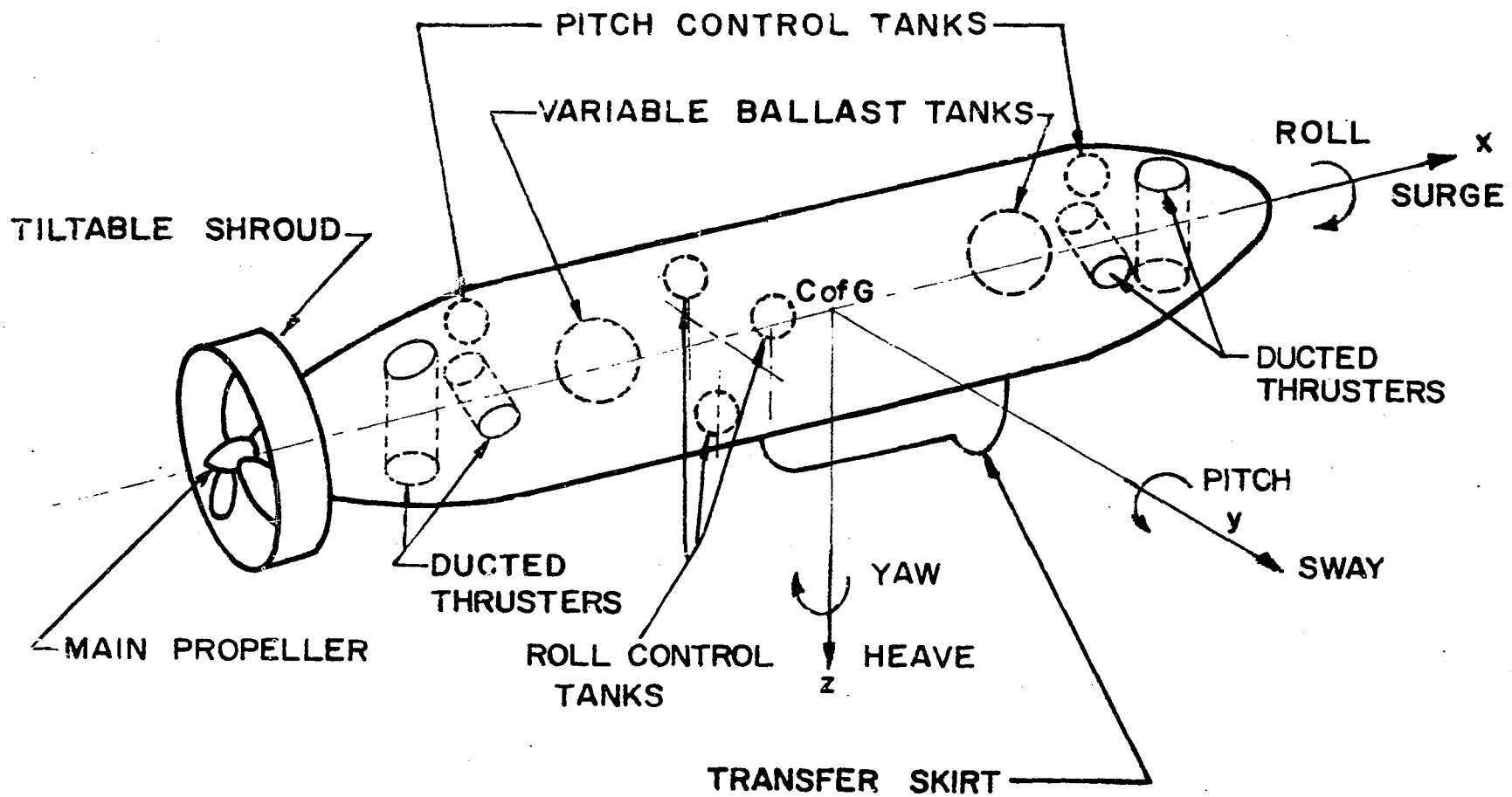
Figure 1   The Propulsion and Steering System of the DSRV

It has been observed that even when equipped with suf-
ficient thrusters to maneuver in six degrees of freedom, a sub-
mersible such as the DSRV, cannot be controlled by a human operator
within the prescribed error envelope for some maneuvers regardless
of the degree of sophistication built into the operator display
system. The primary reason for this is that the operator is unable
to continuously compensate for the hydrodynamic and inertial cross
coupling between the various motions.[3-4] A familiar example of
inertial coupling between the motions is the centripetal force
exerted on the vessel during a turning maneuver. An example of
hydrodynamic coupling is that which exists between the roll and
surge degrees of freedom. Rotation of the main propeller to produce
a force in the surge direction also produces a roll moment which
the operator must offset by pumping mercury between the roll control
tanks.

To summarize, although motion in only one degree of
freedom is desired, motion in several degrees of freedom may occur
with the result that the operator is required to manipulate several
inputs simultaneously to eliminate these cross-coupling effects. To
perform effectively, the operator should be concerned with a mini-
mum of coupled control tasks, hopefully only a single axis uncoupled
control task. This could be achieved by designing a feedback control
system to dynamically compensate the system with the primary design
objective of having one system input controlling one and only one
motion in each degree of freedom. This would relieve the operator
of the burden of continuously controlling the DSRV thus increasing
the payload objectives by freeing his time to carry out other tasks.

1-B Decoupled Control

Compensating multivariable systems,such as the DSRV, to achieve independent or decoupled input-output control has been the objective of researchers in feedback control systems.[5-7] However, the results published to date are limited by the lack of a unified body of knowledge concerning the decoupling of multivariable systems Significant progress towards the development of a unified theory for the decoupling of linear multivariable systems has occurred in last few years. Morgan was the first to study the problem using the state space approach.[8] He developed sufficient conditions under which certain sytems described by linear time-invariant differential equations could be compensated to behave as noninteracting or decoupled systems. Using different approaches, Falb and Wolovich[9] and Gilbert[10] significantly extended decoupling theory by developing necessary and sufficient conditions for decoupling a large class of linear time invariant systems. As a consequence of these papers, numerous results have appeared dealing with various facets of linear decoupling theory and applications.[11-19]

The currently existing forms of equations considered adequate for describing the motion of the DSRV are a complex, coupled and highly nonlinear set of equations.[20] The linear decoupling procedure of Wolovich and Falb has been evaluated by applying it to a linearized version of the equations for roll-surge motion of the DSRV.[21] The theory was shown to be effective when applied to the roll-surge equations only if an excessive number of linearized operating points were used in the development of decoupling feedback controllers.

These results prompted the investigation and the sub-
sequent development of a theory for the direct decoupling of non-
linear systems. Two classes of nonlinear systems are considered
in Chapter II and conditions under which these systems can be
decoupled are developed separately. The distinguishing character-
istic between these two classes is that the first class (Class 1)
is restricted to systems in which the inputs or forcing functions
appear linearly while the second class (Class 2) includes systems
which have nonlinear inputs. Class 2 systems are the general class
of systems which can be modelled by nonlinear time-varying ordinary
differential equations.

Using the theory, decoupling is achieved by nonlinear
feedback of measurements of the states of the system. For the DSRV,
the system states are the velocities and displacements in each
degree of freedom. Within certain practical constraints, nonlinear
unstable interacting systems can be compensated to behave as stable
decoupled systems exhibiting linear input-output transfer relation-
ships. A block diagram representation of a decoupled system is
shown in Figure 2. For this decoupled system each input w_i effects
only one output y_i.

The inputs to the DSRV system consist of propeller speeds
and mercury pump rates. Since the propeller forces are quadratic
functions of propeller speed, the DSRV equations of motion must be
analyzed as a Class 2 system. In Chapter III the decoupling theory
for Class 2 systems is used to successfully decouple the roll-
surge equations. Some practical limitations associated with imple-

COMPENSATED SYSTEM

$\overline{w}$ NEW INPUTS

NONLINEAR PROCESSOR

SUMMER Σ

INPUTS $\overline{u}$

NONLINEAR SYSTEM

OUTPUTS $\overline{y}$

$f(\overline{x})$

$\overline{x}$ MEASUREMENTS OF THE SYSTEM STATES

NONLINEAR PROCESSOR
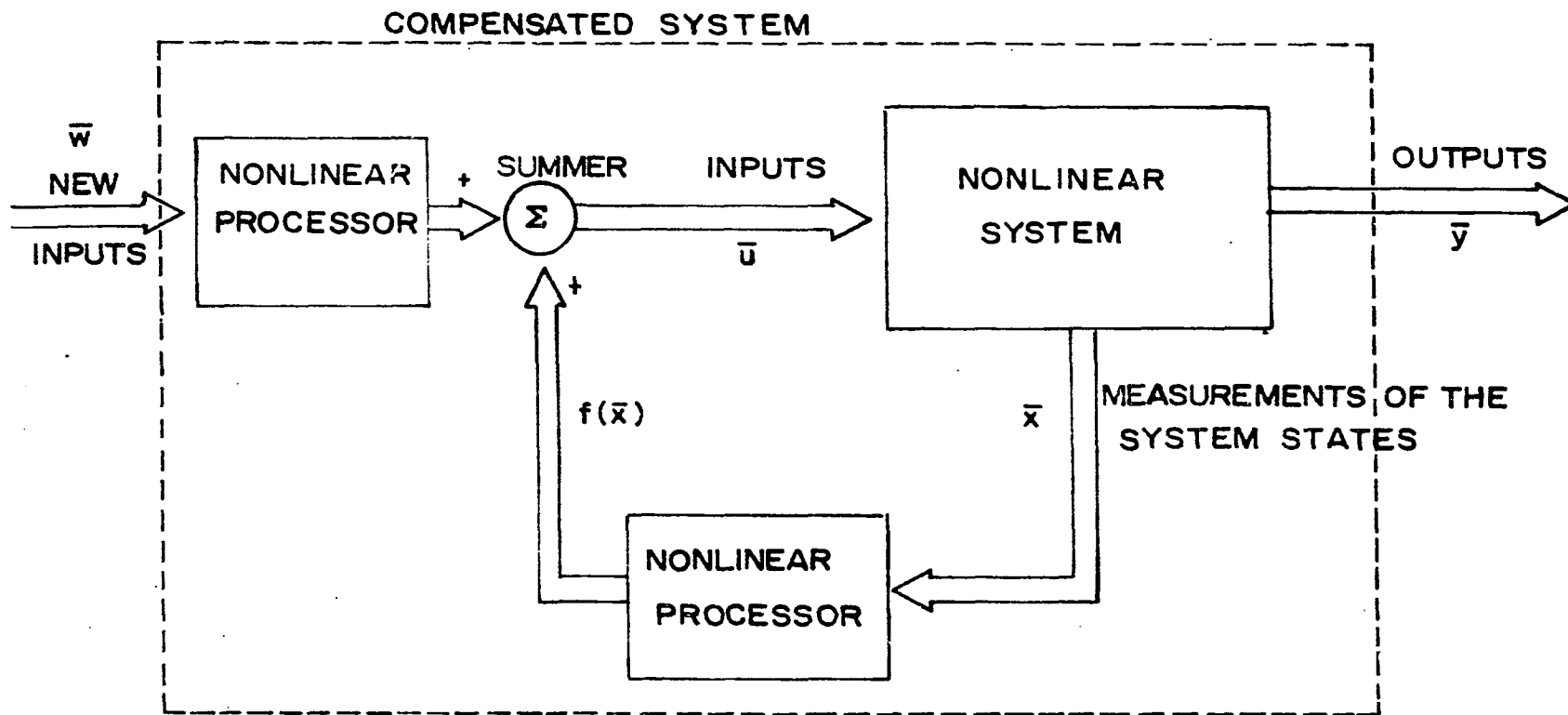
Figure 2   A Block Diagram Representation of a Nonlinear Decoupled System

menting this scheme are presented and satisfactory control system
design within these limitations is discussed. This discussion
includes such factors as guaranteeing system stability subject to
physical constraints on the system inputs. A set of generalized
feedback equations are also derived for the complete decoupling
of the dynamic motion in all six degrees of freedom.

1-C   The Wake Steering Nozzle

Another approach to reduce the degree of cross-coupling
between the motions is to adhere to a high degree of geometric
symmetry in the vehicle design. This reduces the amount of hydro-
dynamic coupling which is basically proportional to the distance
between the vehicle center of gravity and center of geometry.
Asymmetrically mounted steering surfaces tend to increase this
distance because of their low weight to area ratio. For example,
the use of tail mounted thrusters and steering surfaces such as
the main propeller and shroud of the DSRV, results in a vehicle
fore and aft asymmetry. It has, in fact, been shown that the use
of only tail mounted thrusters and steering surfaces can result in
the submersible becoming dynamically unstable during a hovering
maneuver.[22]

In order to improve the geometric symmetry of a sub-
mersible and reduce the number of thrusters required, an alternative
method of obtaining thrusts and steering moments was devised, known
as the wake steering nozzle. The wake steering nozzle (WSN) is a

new method of steering submersibles. It offers the potential to
reduce the number of thrusters as compared with a conventional
system while maintaining a comparable level of maneuverability
and increasing vessel geometric symmetry. The WSN, shown in Figure
3, consists of a propeller surrounded by an accelerating type flow
shroud. This nozzle or shroud has the effect of increasing the
velocity through the duct enabling it to operate under a favorable
loading criterion. The use of shrouded propellers as thrusters is
not new and has been explored both experimentally and analytically.[3-
What is unique about the WSN as proposed by Wozniak, Taft and
Alperi is its ability to develop a steering force as well as an
axial thrust.[29-30] The concept is based on the fact that a shrouded
propeller can be designed which has a pressure distribution down-
stream of the propeller plane which is lower than ambient pressure.
Providing an open slot or control port downstream of the propeller
thus allows flow to be induced into the shroud causing a separation
of the wake from one side of the nozzle. This is illustrated by
the streamlined pattern shown in Figure 2. This results in an asym-
metry in the pressure distribution inside the shroud producing a
radial steering force. From another viewpoint, the wake is deflected
through an angle relative to the propeller axis causing a radial
momentum force. Thus by locating a set of slots downstream from
the propeller and opening and closing these slots, the wake can be
steered.

Assuming a strategy for controlling the direction of
the wake, two WSN mounted on a submersible, one fore and one aft,
would provide the same capability to generate independent control

OPEN PORT

S

CLOSED PORT
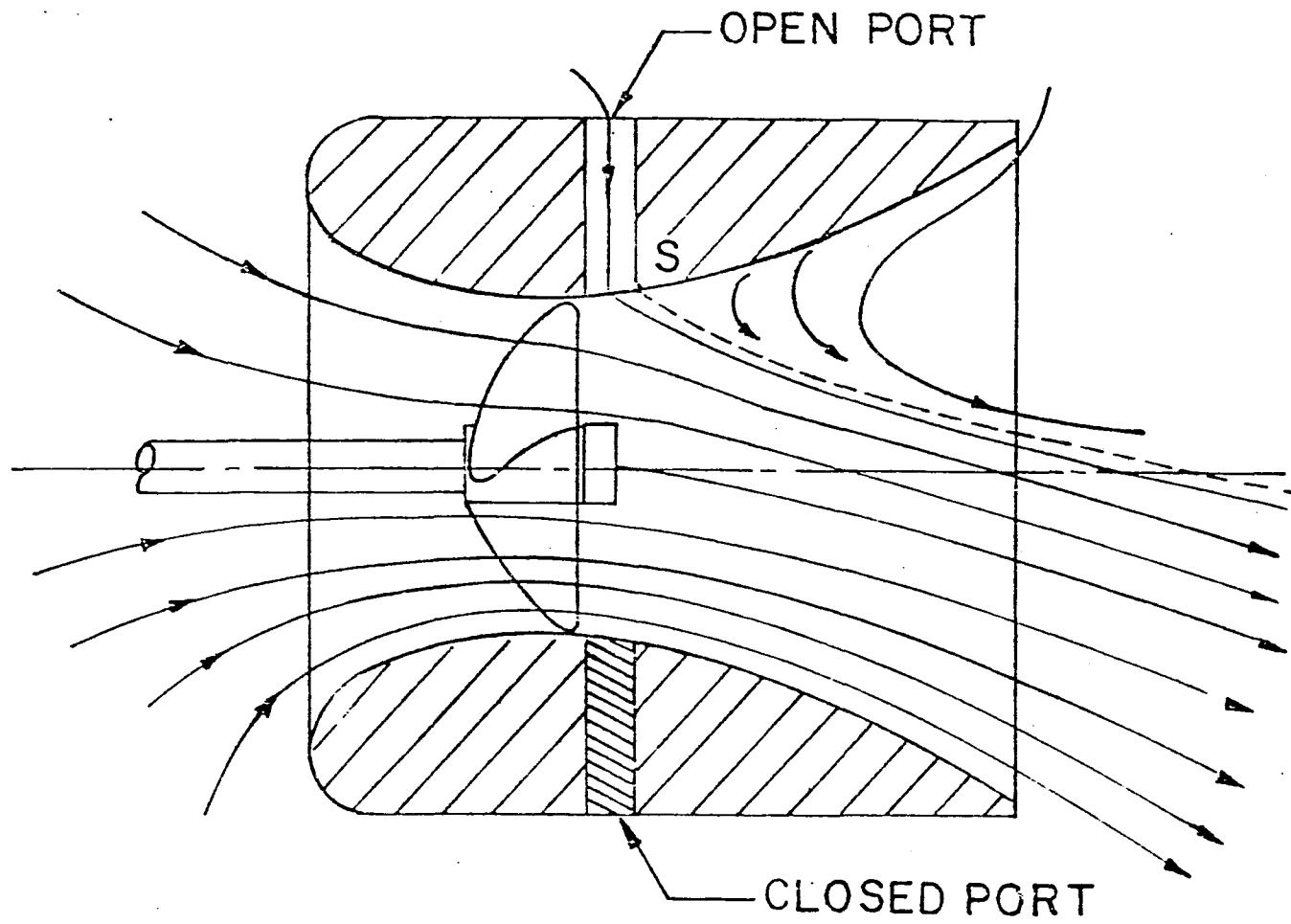
Figure 3   The Wake Steering Nozzle

forces and moments in each degree of freedom as the thrusters now
on the DSRV. The resulting increase in submersible fore and aft
geometric symmetry is apparent in Figure 4 which shows the configura-
tion. The ability of the wake steering shroud to generate steering
forces at vessel zero forward velocity is an additional advantage
over steering surfaces such as rudders.

The objective of the research on the WSN was to gain an
improved understanding of the phenomena to enable assessment of
its potential use in a propulsion-steering system for submersibles.
The performance of the WSN was evaluated experimentally at both
zero and nonzero forward velocity.

Wozniak, in his static or zero forward velocity tests
on the WSN, found a propeller shroud combination which appeared to
work reasonably well.[29] Wozniak calculated the thrusts being pro-
duced by this WSN from pressure measurements on the inside surface
of the shroud. This method was cumbersome and time consuming. There-
fore the first goal was to design and build a test system which
would enable the direct measurement of the WSN radial and axial
thrusts. The system basically consists of a beam with strain guages
mounted on the surface.[31] The necessary peripheral equipment was
provided for dynamic recording. A shroud holder into which wax inserts
could be placed was also designed and constructed. The use of these
wax inserts enabled the shroud inside shape to be changed easily.
The measurement system is described in detail in Chapter IV.

Using this system, preliminary static tests were conducted
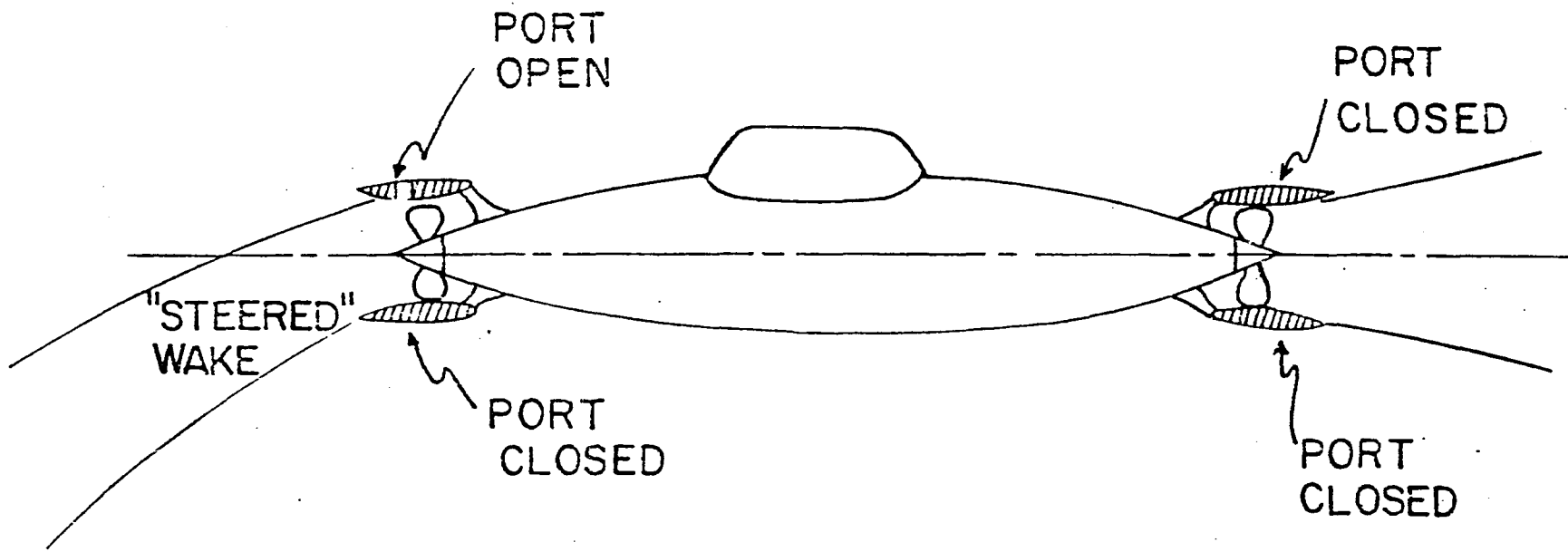
Figure 4   Proposed Submersible Propulsion and Steering System Using Two
Wake Steering Nozzles

on a group of highly divergent shrouds. Many of these shrouds exhibited uncontrolled separation of the wake from the inside surface of the shroud producing an erratic radial force. These tests led to the definition of a number of states of operation and the emergence of the concept of reliability of operation of the WSN. Roughly speaking, a shroud is said to operate reliably if, only when a control port is open, does it develop a radial thrust.

A further series of static tests were then conducted to determine the effects of major parameters of propeller-shroud geometry on reliability, propeller torque and the axial and radial thrusts developed. The parameters varied in the tests were shroud length, shroud curvature or divergence and propeller pitch.[32-33] This testwork served to define a number of propeller-shroud combinations which operate reliably. The static test results are contained in Chapter IV.

To extend these results to include the effects of forward velocity, a water tunnel was designed and constructed. A set of propeller-shroud combinations which exhibited reliable operation during the static testing were selected for evaluation at nonzero velocity.[34] To minimize the fluid drag on the shroud, the outside surface and force balance beam were streamlined. Tests were conducted over a range of forward velocities and the results non-dimensionalized for comparison with the results of other researchers on shrouded propellers used for propulsion.[23-26] This enabled a comparative evaluation of the WSN for use as an axial thruster.

In Chapter VI, the steering effectiveness of the WSN
is compared with a conventional steering device. The comparison
is made using computer simulations of the DSRV equations of motion
in the horizontal plane. The simulations were first conducted using
the existing DSRV propeller-tiltable shroud and then replacing it
with a WSN and the simulations repeated. Three basic maneuvers are
considered; an accelerating turn, a decelerating turn and a con-
stant velocity turn. The axial thrusting efficiency of the WSN is
examined by comparing it to the efficiency of some of the combina-
tions of propellers and nozzles tested by Van Manen. [24,25]

1-D Project Management

The investigation of the WSN reported herein was a
project involving a number of people. The role of the writer of
this thesis was that of a project coordinator. Therefore, the
results on the WSN presented in this thesis are, for the most
part, an overview of this project.

Most of today's research problems require a combina-
tion of effort from many people. The ability of these people to
work together requires considerable integrated effort and mana-
gerial skill. Most engineers gain this skill as a result of purely
experience based learning. In Chapter VII, the writer's experience
inthe management structure of the wake steering project is combined

with certain aspects of organizational behavior theory to formulate some key concepts considered relevent in managing research projects of this type. This includes the evaluation of such elements as project planning and leadership style.

CHAPTER II

A THEORY FOR THE DECOUPLING OF NONLINEAR SYSTEMS

2-A General

One of the more severe forms of hydrodynamic cross-coupling in a submersible occurs between the roll and surge motions.[2,3,35] This particular type of coupling is a problem in fleet or attack submarines as well as submersibles such as the DSRV. Decoupling of the DSRV roll and surge motions was first attempted using existing linear theory. The nonlinear equations of motion were linearized about several operating points and the linear decoupling theory of Wolovich and Falb was applied to develop decoupling controllers.* The linear theory was found to be satisfactory only if a very large number of operating points were used. Application of the linear theory was further complicated by the fact that each maneuver required a different set of operating points thus requiring operating points to be established for the set of all possible combinations of variables. These difficulties, combined with the fact that calculating some of the operating point values required solving nonlinear algebraic equations, led to exploring the possibility of direct decoupling of nonlinear systems.

Two classes of nonlinear systems are considered and conditions for the design of decoupled systems are developed

---

* The details of the application of the linear theory by the
  author are contained in Reference 21.

separately for each class. Both classes of systems fall into the general class of systems which can be modelled by nonlinear time-varying or nonautonomous ordinary differential equations. The first class (Class 1) is restricted to systems for which the input variables or forcing functions appear linearly in the differential equations. This class of systems has recently been considered by other authors.[37-38] The end results are similar to those derived in this thesis but the method by which they are derived is different. Necessary and sufficient conditions for decoupling are developed herein using an approach which in one respect parallels that used by Wolovich and Falb for linear systems; the system outputs are differentiated. Other aspects of the development are based on matrix algebra. The derivation herein is relatively simple and straightforward compared with the derivation of Tokumaru and Iwai[38] who flatly state that the approach taken here will not work and proceed to solve the problem by introducing a concept of relative orders.

Sufficient conditions for decoupling to be possible are derived in a similar manner for a class of systems in which the input variables appear nonlinearly in the differential equations (Class 2). The equations of motion for the DSRV are of this class. This class of systems has also been investigated by Tubalkain and Limbert.[39] By expressing the system equations in vector form, conditions for decoupling are developed in this thesis in a more direct manner to include systems which may not be decoupled by

the methods presented in Reference 39.

Decoupling is achieved in each class of systems by nonlinear feedback of measurements of the states of the system. A synthesis procedure is given which enables the poles of the closed loop input-output transfer relationships to be chosen by the designer. The theory is extended to develop a feedback control law for the regulatory control of both classes of nonlinear systems. A method is also outlined for the investigation and guarantee of system stability subject to certain practical constraints.

2-B Class 1 Systems

This is the class of systems which can be adequately modelled by a set of nonlinear time-varying ordinary differential equations in which each term involving the forcing function is linear.

2-B.1 Definitions and Notations - Class 1

The class of systems under consideration can be represented in state variable vector form as

$$\dot{\bar{x}} = a(\bar{x},t) + B(\bar{x},t)\bar{u}$$

$$\bar{y} = c(\bar{x},t)$$

(2.1)

where $\bar{x}$ is a real nx1 vector representing the state of the system, $a(\bar{x},t)$ and $c(\bar{x},t)$ are nx1 and mx1 vector functions of $\bar{x}$ and time t, $B(\bar{x},t)$ is an nxm matrix function of $\bar{x}$ and t and $\bar{u}$ and $\bar{y}$ are mx1 vectors representing the system inputs and outputs respectively. The input vector $\bar{u}$ is assumed to be unbounded.

The vector functions $a(\bar{x},t)$ and $c(\bar{x},t)$ are assumed to have entries which are continuous or piecewise continuously differentiable functions of the state vector $\bar{x}$ and time t. The entries of all vector and matrix functions of $\bar{x}$ and t are finite for finite $\bar{x}$ and t.

The general nonlinear state variable feedback equation for a system such as (2.1) is

$$\bar{u} = f(\bar{x},t) + G(\bar{x},t)\bar{w} \tag{2.2}$$

where $f(\bar{x},t)$ is an mx1 vector function of $\bar{x}$ and t, $G(\bar{x},t)$ is an mxm matrix function of $\bar{x}$ and t, and $\bar{w}$ is a new m dimensional input vector.

Combining (2.1) and (2.2) gives the following closed loop system equations

$$\dot{\bar{x}} = a(\bar{x},t) + B(\bar{x},t)f(\bar{x},t) + B(\bar{x},t)G(\bar{x},t)\bar{w}$$

$$\bar{y} = c(\bar{x},t) \tag{2.3}$$

A block diagram representation of a decoupled Class 1 system is shown in Figure 5.
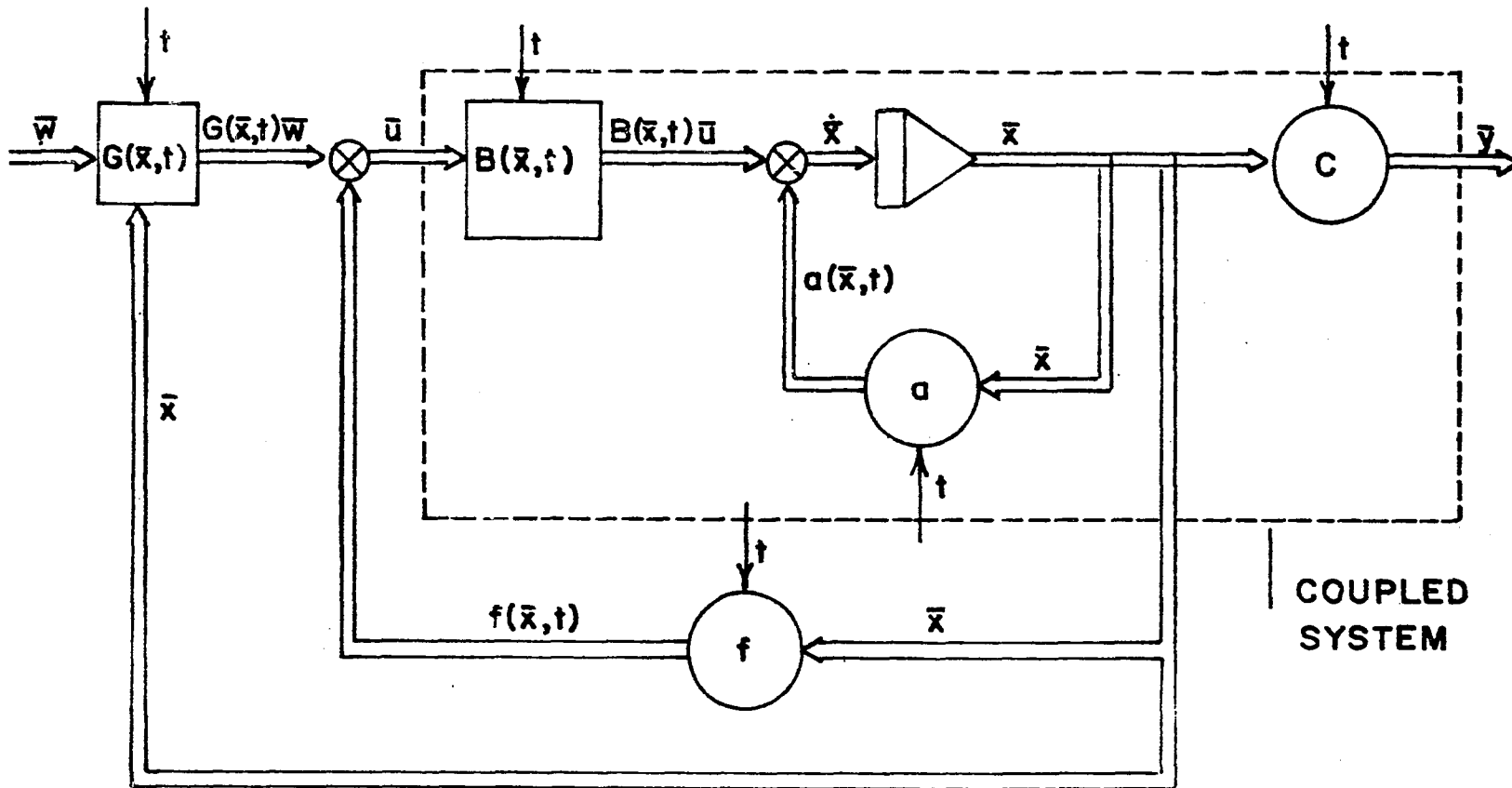
Figure 5 Representation of a Class 1 Nonlinear Decoupled System

It is the objective of the subsequent theory to develop
a procedure for specifying the entries of $f(\bar{x},t)$ and $G(\bar{x},t)$ which
decouple the system. To aid in the theoretical development, a
decoupled system is mathematically defined.

Definition 1

The system of (2.3) is said to be decoupled if the i'th
output y_i is only a function of the initial state $\bar{x}^0$ and has a
nonzero correspondence with the i'th input w_i. Thus it is invariant
with respect to the inputs $w_1, w_2, \ldots, w_{(i-1)}, w_{(i+1)}, \ldots, w_m$.

Conditions for decoupling the system will be derived
through a process involving differentiation of the i'th output
variable y_i. From (2.3), the i'th output y_i is a function of $\bar{x}$
and t.

$$y_i = c_i(\bar{x},t) \tag{2.4}$$

To make y_i a function of the input w_i and thus be in a
position to decouple the system according to Definition 1, it is
logical to assume that we need an equation functionally relating
y_i and w_i. Since y_i is a function of $\bar{x}$, which by (2.3) is a function
of $\bar{w}$ containing w_i, the necessary equation can be obtained by dif-
ferentiating y_i in (2.4) giving

$$\frac{Dy_i}{Dt} = \nabla c_i(\bar{x},t)\dot{\bar{x}} + \frac{\partial c_i(\bar{x},t)}{\partial t} \tag{2.5}$$

where ∇ = Gradient = $\left[\dfrac{\partial}{\partial x_1}, \dfrac{\partial}{\partial x_2}, \ldots\ldots, \dfrac{\partial}{\partial x_n} \right]_{1 \times n}$

Equation (2.3) containing $\bar{w}$ can be substituted for $\dot{\bar{x}}$ to give

$$\frac{Dy_i}{Dt} = \nabla c_i(\bar{x},t) \left[a(\bar{x},t) + B(\bar{x},t)f(\bar{x},t) + B(\bar{x},t)G(\bar{x},t)\bar{w} \right] + \frac{\partial c_i(\bar{x},t)}{\partial t}$$

$$(2.6)$$

If $\nabla c_i(\bar{x},t)B(\bar{x},t) = 0$, then the first derivative of y_i will not contain $\bar{w}$ and it will be necessary to differentiate again. The following definition is introduced to generalize this process.

Definition 2

Let the integer constants $\rho_1, \rho_2, \ldots\ldots, \rho_m$ be given by ρ_i = smallest α such that

$$\nabla y_i^{(\alpha-1)} B(\bar{x},t) \neq 0, \quad \alpha = 1, 2, \ldots, n \text{ and } \rho_i = n$$

if $\nabla y_i^{(\alpha-1)} B(\bar{x},t) = 0$ for all α

and $y_i^{(\alpha-1)}$ is the $(\alpha-1)$'th total derivative with respect to time of the i'th component of $\bar{y}$.

2-B.2 The Decoupling Procedure - Class 1

Repeated differentiation up to the ρ_i'th derivative of the i'th output variable y_i and application of Definition 2 yields

$$y_i = c_i(\bar{x}, t)$$

$$y_i^{(1)} = \nabla c_i(\bar{x}, t)\dot{\bar{x}} + \frac{\partial c_i(\bar{x}, t)}{\partial t}$$

$$= \nabla y_i a(\bar{x}, t) + \nabla y_i B(\bar{x}, t) f(\bar{x}, t) + \nabla y_i B(\bar{x}, t) G(\bar{x}, t)\bar{w} + \frac{\partial y_i}{\partial t}$$

$$y_i^{(1)} = \nabla y_i a(\bar{x}, t) + \frac{\partial y_i}{\partial t}$$

$$y_i^{(2)} = \nabla y_i^{(1)} a(\bar{x}, t) + \frac{\partial y_i^{(1)}}{\partial t}$$

$$\vdots \qquad \vdots \qquad \vdots$$

$$y_i^{(\rho_i - 1)} = \nabla y_i^{(\rho_i - 2)} a(\bar{x}, t) + \frac{\partial y_i^{(\rho_i - 2)}}{\partial t}$$

$$y_i^{(\rho_i)} = \nabla y_i^{(\rho_i - 1)} a(\bar{x}, t) + \nabla y_i^{(\rho_i - 1)} B(\bar{x}, t) f(\bar{x}, t)$$

$$+ \nabla y_i^{(\rho_i - 1)} B(\bar{x}, t) G(\bar{x}, t)\bar{w} + \frac{\partial y_i^{(\rho_i - 1)}}{\partial t}$$

$$(2.7)$$

Note that $y_i^{(\rho_i)}$ is the lowest order derivative which involves $\bar{w}$.

These derivatives of y_i for $i = 1, \ldots, m$ can be collected and written in vector-matrix form as

$$
\begin{bmatrix}
y_1^{\rho_1} \\
y_2^{\rho_2} \\
\cdot \\
\cdot \\
\cdot \\
\cdot \\
y_m^{\rho_m}
\end{bmatrix}
=
\begin{bmatrix}
\nabla y_1^{(\rho_1 - 1)} a(\bar{x}, t) + \partial y_1^{(\rho_1 - 1)} / \partial t \\
\nabla y_2^{(\rho_2 - 1)} a(\bar{x}, t) + \partial y_2^{(\rho_2 - 1)} / \partial t \\
\cdot \\
\cdot \\
\cdot \\
\cdot \\
\nabla y_m^{(\rho_m - 1)} a(\bar{x}, t) + \partial y_m^{(\rho_m - 1)} / \partial t
\end{bmatrix}
+
\begin{bmatrix}
\nabla y_1^{(\rho_1 - 1)} B(\bar{x}, t) \\
\nabla y_2^{(\rho_2 - 1)} B(\bar{x}, t) \\
\cdot \\
\cdot \\
\cdot \\
\cdot \\
\nabla y_m^{(\rho_m - 1)} B(\bar{x}, t)
\end{bmatrix}
G(\bar{x}, t)
\begin{bmatrix}
w_1 \\
w_2 \\
\cdot \\
\cdot \\
\cdot \\
\cdot \\
w_m
\end{bmatrix}
$$

$$
+
\begin{bmatrix}
\nabla y_1^{(\rho_1 - 1)} B(\bar{x}, t) \\
\nabla y_2^{(\rho_2 - 1)} B(\bar{x}, t) \\
\cdot \\
\cdot \\
\cdot \\
\cdot \\
\nabla y_m^{(\rho_m - 1)} B(\bar{x}, t)
\end{bmatrix}
f(\bar{x}, t)
\qquad (2.8)
$$

Inspection of (2.8) provides most of the insight necessary to select an $f(\bar{x}, t)$ and $G(\bar{x}, t)$ which will decouple the system. It should be apparent that if $G(\bar{x}, t)$ is chosen to be inverse of the

matrix premultiplying it in the second term on the RHS of (2.8), then the product of these two matrices will be the identity matrix with the result that this term will contain only the input vector $\bar{w}$. Similarly, if $f(\bar{x},t)$ is made equal to the product of $G(\bar{x},t)$ and a column matrix whose rows are chosen to cancel the rows of the first term in (2.8), then $y_i^{(\rho_i)}$ will depend only on w_i and the system will be decoupled according to Definition 1. This motivates the following theorem.

Theorem 1

There exists an m dimensional vector $f^*(\bar{x},t) = f(\bar{x},t)$ and an mxm matrix $G^*(\bar{x},t) = G(\bar{x},t)$ which decouple the system of (2.3) on a space H, which is a subspace of the state space $\bar{x}$, if and only if det $D^*(\bar{x},t) \neq 0$ on H. Thus H is the set of points for which det $D^*(\bar{x},t) \neq 0$ over the time interval $(t_o \leq t \leq t_f)$.

$$\text{where } D^*(\bar{x},t) = \begin{bmatrix} \nabla y_1^{(\rho_1-1)} B(\bar{x},t) \\ \nabla y_2^{(\rho_2-1)} B(\bar{x},t) \\ \vdots \\ \nabla y_m^{(\rho_m-1)} B(\bar{x},t) \end{bmatrix}_{mxm} \qquad (2.9)$$

It is claimed that the pair $\left[f^*(\bar{x},t), G^*(\bar{x},t)\right]$ are given by

$$G^*(\bar{x},t) = D^{*-1}(\bar{x},t) \qquad (2.10)$$

and $f^*(\bar{x},t) = -D^{*-1}(\bar{x},t)a^*(\bar{x},t) \qquad (2.11)$

$$\text{where } a^*(\bar{x},t) = \begin{bmatrix} \nabla y_1^{(\rho_1-1)} a(\bar{x},t) + \dfrac{\partial y_1^{(\rho_1-1)}}{\partial t} \\[2ex] \nabla y_2^{(\rho_2-1)} a(\bar{x},t) + \dfrac{\partial y_2^{(\rho_2-1)}}{\partial t} \\[2ex] \vdots \qquad\qquad \vdots \\[2ex] \nabla y_m^{(\rho_m-1)} a(\bar{x},t) + \dfrac{\partial y_m^{(\rho_m-1)}}{\partial t} \end{bmatrix}_{m\times 1} \qquad (2.12)$$

Proof of Sufficiency

Substituting $f(\bar{x},t) = f^*(\bar{x},t)$ and $G(\bar{x},t) = G^*(\bar{x},t)$ into the ρ_i'th derivative of y_i in (2.7) and making use of (2.9) -(2.12) results in the following

$$y_i^{(\rho_i)} = \nabla y_i^{(\rho_i-1)} a(\bar{x},t) - \nabla y_i^{(\rho_i-1)} B(\bar{x},t) D^{*-1}(\bar{x},t) a^*(\bar{x},t)$$

$$+ \nabla y_i^{(\rho_i-1)} B(\bar{x},t) D^{*-1}(\bar{x},t) \bar{w} + \frac{\partial y_i^{(\rho_i-1)}}{\partial t}$$

$$= \nabla y_i^{(\rho_i-1)} a(\bar{x},t) - D_i^*(\bar{x},t) D^{*-1}(\bar{x},t) a^*(\bar{x},t) + D_i^*(\bar{x},t) D^{*-1}(\bar{x},t) \bar{w}$$

$$+ \frac{\partial y_i^{(\rho_i-1)}}{\partial t}$$

$$y_i^{(\rho_i)} = \nabla y_i^{(\rho_i-1)} a(\bar{x},t) + \frac{\partial y_i^{(\rho_i-1)}}{\partial t} - a_i^*(\bar{x},t) + w_i$$

$$y_i^{(\rho_i)} = w_i \text{ for } i = 1, 2, \ldots, m \tag{2.13}$$

and the system is decoupled by Definition 1. Thus $f(\bar{x},t) = f^*(\bar{x},t)$ and $G(\bar{x},t) = G^*(\bar{x},t)$ decouple the system in (2.3).

Proof of Necessity

Suppose that there exists an $f^*(\bar{x},t)$ and $G^*(\bar{x},t)$ that decouple (2.3) on a set of points $\bar{x}$, over the interval $(t_o \leq t \leq t_f)$. To be decoupled the last term in $y_i^{(\rho_i)}$ must depend only on w_i, that is

$$\nabla y_i^{(\rho_i-1)} B(\bar{x},t) G(\bar{x},t) \bar{w} = w_i$$

which is by (2.9)

$$D_i^*(\bar{x},t) G(\bar{x},t) \bar{w} = w_i$$

Thus $\quad D_i^*(\bar{x},t) G(\bar{x},t) = e_i$

where $e_i = \begin{bmatrix} 00\ldots010\ldots00 \end{bmatrix}$

the "1" being in the i'th column.

Suppose $D^*(\bar{x},t)$ is singular for some $\bar{x} \in H$ over $(t_o \le t \le t_f)$ then either

$$D_i^*(\bar{x},t) = \sum_{i \ne j} d_j D_j^*(\bar{x},t) \text{ for some } i, \; i=1,\ldots, m, \qquad (2.14)$$
$$\text{not all } j$$

or $D_i^*(\bar{x},t) = 0$ for some i, $i=1,\ldots, m$ \qquad (2.15)

If (2.14) is true then

$$D_i^*(\bar{x},t)G(\bar{x},t)\bar{w} = \sum_{i \ne j} d_j D_j^*(\bar{x},t)G(\bar{x},t)\bar{w}$$

$$= \sum_{i \ne j} d_j w_j \ne w_i$$

and y_i does not depend on w_i alone so the system is not decoupled; a contradiction.

If (2.15) is true then

$$D_i^*(\bar{x},t)G(\bar{x},t)\bar{w} = 0$$

and y_i has no dependence on w_i so the system is not decoupled; a contradiction.

Therefore, $D^*(\bar{x},t)$ must be nonsingular everywhere on H. The space H over which the system (2.3) can be decoupled is uniquely defined as those values of the state vector $\bar{x}$ and time t for which $\det D^*(\bar{x},t) \ne 0$. If $\det D^*(x,t)=0$, then the entries of $G(\bar{x},t)$ become infinite requiring infinite values for the inputs $\bar{u}$ in Equation (2.2)

From (2.9), it is apparent that $D^*(\bar{x},t)$ is not a function of the feedback vector $f(\bar{x},t)$ making the region in the state space H over which the system can be decoupled $f(\bar{x},t)$ invariant. Thus it may be possible to choose entries of $f(\bar{x},t)$ to obtain a desired set of closed loop system dynamics.

2-B.3 A Synthesis Procedure - Class 1

Procedures for decoupling the system and specifying the system closed loop dynamics are developed. Using these procedures the system may be made to exhibit input-output transfer relationships which are linear or nonlinear depending on the choice of feedback.

We can generalize (2.10) by letting

$$G(\bar{x},t) = \Lambda D^{*-1}(\bar{x},t) \qquad (2.16)$$

where Λ is a matrix of gain constants acting on the input vector $\bar{w}$ and is given by

$$\Lambda = \begin{bmatrix} \zeta_1 & & & \\ & \zeta_2 & & O \\ & & \ddots & \\ O & & & \zeta_m \end{bmatrix}_{m \times m} \qquad (2.17)$$

$$(2.17)$$

Since Λ is diagonal and nonsingular (2.16) still decouples the system by making each output component y_i depend on $\zeta_i w_i$.

Similarly we can generalize (2.11) to give

$$f(\bar{x},t) = D^{*^{-1}}(\bar{x},t)\left[r(\bar{x},t) - a^*(\bar{x},t)\right] \qquad (2.18)$$

where $r(\bar{x},t)$ is an mx1 vector function of $\bar{x}$ and t.

From the previous proof of sufficiency, we know that $f(\bar{x},t)$ given by (2.18) will map in the i'th rows of $r(\bar{x},t)$ and $a^*(\bar{x},t)$. The entries of $a^*(\bar{x},t)$ have already been chosen to decouple the system. Now the row entries of $r(\bar{x},t)$ can be chosen to specify the system closed loop dynamics. One possibility is to choose the i'th row of $r(\bar{x},t)$ so that it contains, in linear progression, each of the derivatives of the i'th output variable y_i up to the ρ_i'th derivative. This would result in linear input-output transfer relationships. The following equation illustrates this choice:

$$r_i(\bar{x},t) = m_{io}c_i(\bar{x},t) + \sum_{v=1}^{(\rho_i-1)} m_{iv}\left[\nabla y_i^{(v-1)} a(\bar{x},t) + \frac{\partial y_i^{(v-1)}}{\partial t}\right]$$

$$\text{for } i = 1, 2, \ldots, m \qquad (2.19)$$

where the m's are suitably chosen constants. By definition the series shall terminate if the lower index is greater than the upper one. Note from (2.7) that each term in the series represents a derivative of y_i. Combining (2.7), (2.17) and (2.19) gives for the ρ_i'th derivative of y_i

$$y_i^{(\rho_i)} = m_{io}y_i + m_{i1}y_i^{(1)} + \ldots + m_{i(\rho_{i-1})}y_i^{(\rho_i-1)} + \zeta_i w_i$$

$$\text{for } i = 1, 2, \ldots, m \qquad (2.20)$$

thus $f(\bar{x},t)$ and $G(\bar{x},t)$ decouple the system of (2.3) and $\sum_{i=1}^{m}\rho_i$ of the system closed loop poles can be specified.

It is apparent from (2.20) that $r(\bar{x},t)$ as given by (2.19) and Λ by (2.17) result in linear input-output transfer relationships. A more general form would be

$$r_i(\bar{x},t) = g(y_i, y_i^{(1)}, \ldots, y_i^{(\rho_i-1)}) \qquad (2.21)$$

$$\text{for } i = 1, 2, \ldots, m$$

and

$$\Lambda(\bar{x},\bar{w},t) = \text{diag}\left[\zeta_1(y_1, \ldots, y_1^{(\rho_1-1)} w_1, t), \ldots, \zeta_m(y_m, \ldots, y_m^{(\rho_m-1)} w_m \right.$$

$$(2.22)$$

which, depending on the choice of r_i and ζ_i, would make the system have a specified nonlinear relationship between the input w_i and output y_i.

These results for Class 1 systems are equally appliable to linear systems with constant and time-varying coefficients.

A word of caution should be injected here concerning system realizability. Equation (2.20) does not completely represent

the decoupled system but only the input-output relationships. Since the output function $\bar{y}$ is a function of the state $\bar{x}$, then in general the closed loop equation for $\bar{x}$ in (2.3) must be examined for stability and controllability before the input-output relationships of (2.20) can be guaranteed. This will be discussed in more detail later in the thesis.

A numerical example of the decoupling procedure for a Class 1 system is given in Appendix B. It serves to illustrate the details of applying the decoupling and synthesis procedures. Note that in this example even though the closed loop decoupled system input-output relationships are linear, the input-state relationships are not.

2-C   Class 2 Systems

This class of systems is similar to Class 1 except that the terms in the differential equations involving the forcing functions or input vector $\bar{u}$ are nonlinear.

2-C.1   Definitions and Notations - Class 2

This class of systems can be represented as

$$\dot{\bar{x}} = a(\bar{x},t) + b(\bar{x},\bar{u},t)$$

$$\bar{y} = c(\bar{x},t) \qquad\qquad (2.23)$$

where $b(\bar{x},\bar{u},t)$ is an n vector function of $\bar{x},\bar{u}$ and t. All other quantities are as defined for Class 1 systems.

The system of (2.23) will decouple by solving for all the components of the input vector $\bar{u}$ in the following general vector feedback equation:

$$d(\bar{x},\bar{u},t) = f(\bar{x},t) + \bar{w} \qquad (2.24)$$

where $d(\bar{x},\bar{u},t)$ is an m vector function of $\bar{x},\bar{u}$ and t, $f(\bar{x},t)$ is an m vector function of $\bar{x}$ and t and $\bar{w}$ is the new input vector as in (2.3). In general the terms in $d(\bar{x},\bar{u},t)$ containing the components of $\bar{u}$ will be nonlinear.

Unlike Class 1 systems, we cannot directly combine (2.23) and (2.24) to eliminate $\bar{u}$ and obtain an expression for the closed loop system similar to (2.3). The reason for expressing the feedback equation by (2.24) is that we want to decouple the system by state variable feedback thus eliminating $\bar{u}$ completely from the equations for the closed loop system response. It should be pointed out that another approach is possible.

If $b(\bar{x},\bar{u},t)$ was written instead as $B(\bar{x},\bar{u},t)\,\bar{u}$ in (2.23) and if the feedback equation of (2.24) was written as

$$\bar{u} = f(\bar{x},\bar{u},t) + G(\bar{x},\bar{u},t)\bar{w} \qquad (2.25)$$

then the equations could be combined, as for Class 1 systems to obtain the equations for the closed loop system. Conditions for

decoupling could then be developed in almost exactly the same manner as they were for Class 1 systems.

The main reason for not adopting this approach is that by this approach we introduce a set of hidden variables, the $u_i \epsilon \bar{u}$, into the internal dynamics of the closed loop system. This introduces further complications in terms of the stability of the decoupled system.

The procedure to determine the entries of $d(\bar{x}, \bar{u}, t)$ and $f(\bar{x}, t)$ which will decouple the system of (2.23) follows along somewhat the same lines as for Class 1 systems. The i'th output variable y_i is differentiated until the input vector $\bar{u}$ is introduced. A definition similar to Definition 2 is given to generalize the differentiation process.

Definition 3

Let $\rho_1, \rho_2, \ldots, \rho_m$ be given by

$$\rho_i = \text{smallest } \alpha \text{ such that } \nabla y_i^{(\alpha-1)} b(\bar{x}, \bar{u}, t) \neq 0$$

$$\text{for } \alpha = 1, 2, \ldots, n$$

$$\rho_i = n \text{ if } \nabla y_i^{(\alpha-1)} b(\bar{x}, \bar{u}, t) = 0 \text{ for all}$$
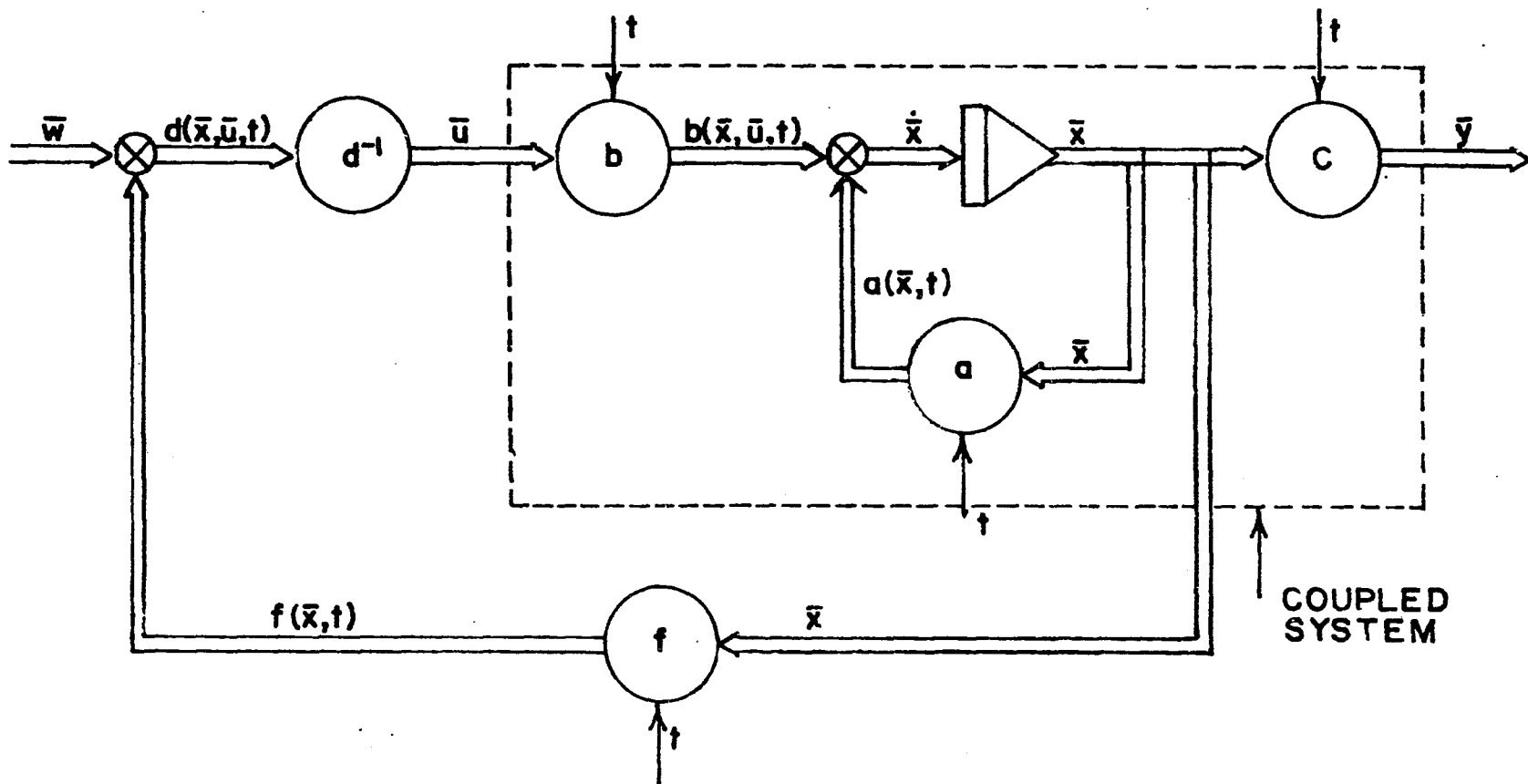
Figure 6   Representation of a Class 2 Nonlinear Decoupled System

2-C.2 Decoupling Procedure - Class 2

Differentiating the i'th output y_i of the system of (2.23) gives

$$y_i = c_i(\bar{x},t)$$

$$y_i^{(1)} = \nabla y_i \dot{\bar{x}} + \frac{\partial y_i}{\partial t} = \nabla y_i [a(\bar{x},t) + b(\bar{x},\bar{u},t)] + \frac{\partial y_i}{\partial t}$$

$$y_i^{(1)} = \nabla y_i a(\bar{x},t) + \frac{\partial y_i}{\partial t}$$

$$y_i^{(2)} = \nabla y_i^{(1)} a(\bar{x},t) + \frac{\partial y_i^{(1)}}{\partial t}$$

$$\vdots \qquad \vdots \qquad \vdots$$

$$y_i^{(\rho_i-1)} = \nabla y_i^{(\rho_i-2)} a(\bar{x},t) + \frac{\partial y_i^{(\rho_i-2)}}{\partial t}$$

$$y_i^{(\rho_i)} = \nabla y_i^{(\rho_i-1)} a(\bar{x},t) + \nabla y_i^{(\rho_i-1)} b(\bar{x},\bar{u},t) + \frac{\partial y_i^{(\rho_i-1)}}{\partial t}$$

$$(2.26)$$

Insight into the choice of $d(\bar{x},\bar{u},t)$ and $f(\bar{x},t)$ to achieve decoupling is obtained by inspection of the ρ_i'th derivative of y_i in (2.26). If the i'th row of $d(\bar{x},\bar{u},t)$ is chosen to be the term containing $\bar{u}$ and if the i'th row of $f(\bar{x},t)$ is chosen to cancel the remaining terms then the result should be an equation relating the i'th output y_i to the i'th input, w_i. This motivates the following theorem.

Theorem 2

There exist m dimensional vectors $d^*(\bar{x},\bar{u},t) = d(\bar{x},\bar{u},t)$ and $f^*(\bar{x},t) = f(\bar{x},t)$ which decouple the system of (2.24) by state variable feedback if the Jacobian $J_d(\bar{x},\bar{u},t) \neq o$ on a space H. The space H is the set of points $\bar{x}$ and $\bar{u}$ over time interval $(t_o < t \leq t_f)$ for which $J_d(\bar{x},\bar{u},t) \neq o$.

$$\text{where} \quad J_d(\bar{x},\bar{u},t) = \begin{vmatrix} \dfrac{\partial d_1(\bar{x},\bar{u},t)}{\partial u_1} & \cdots & \dfrac{\partial d_1(\bar{x},\bar{u},t)}{\partial u_m} \\ \vdots & & \vdots \\ \dfrac{\partial d_m(\bar{x},\bar{u},t)}{\partial u_1} & \cdots & \dfrac{\partial d_m(\bar{x},\bar{u},t)}{\partial u_m} \end{vmatrix}$$

(2.27)

To decouple the system, $d^*(\bar{x},\bar{u},t)$ and $f^*(\bar{x},t)$ are

$$d^*(\bar{x},\bar{u},t) = \begin{bmatrix} \nabla y_1^{(\rho_1 - 1)} b(\bar{x},\bar{u},t) \\ \nabla y_2^{(\rho_2 - 1)} b(\bar{x},\bar{u},t) \\ \vdots \\ \nabla y_m^{(\rho_m - 1)} b(\bar{x},\bar{u},t) \end{bmatrix}$$

mx1   (2.28)

and $f^*(\bar{x},t) = -a^*(\bar{x},t) = $

$$\begin{bmatrix} -\nabla y_1^{(\rho_1-1)} a(\bar{x},t) & - & \dfrac{\partial y_1^{(\rho_1-1)}}{\partial t} \\[2em] -\nabla y_2^{(\rho_2-1)} a(\bar{x},t) & - & \dfrac{\partial y_2^{(\rho_2-1)}}{\partial t} \\[1em] \vdots & & \\[1em] -\nabla y_m^{(\rho_m-1)} a(\bar{x},t) & - & \dfrac{\partial y_m^{(\rho_m-1)}}{\partial t} \end{bmatrix}_{m\times 1}$$

(2.29)

Proof:

With $d^*(\bar{x},\bar{u},t) = d(\bar{x},\bar{u},t)$ and $f^*(\bar{x},t) = f(\bar{x},t)$ and using (2.28) and (2.29), the i'th component of (2.24) can be written as

$$\nabla y_i^{(\rho_i-1)} b(\bar{x},\bar{u},t) = -\nabla y_i^{(\rho_i-1)} a(\bar{x},t) - \frac{\partial y_i^{(\rho_i-1)}}{\partial t} + w_i$$

(2.30)

Combining (2.30) and the equation for the ρ_i'th derivative of y_i in (2.26) gives

$$y_i^{(\rho_i)} = w_i \quad \text{for } i=1, 2,\ldots, m$$

(2.31)

Thus $d(\bar{x},\bar{u},t)$ and $f(\bar{x},t)$ as given by (2.27) and (2.28) are sufficient to decouple the system of (2.23).

The vector feedback equation of (2.24) constitutes a set of m nonlinear algebraic equations. To decouple the system by nonlinear state variable feedback it is necessary to solve (2.24) for all the components of $\bar{u}$. A sufficient condition for a solution set to exist is that $J_d(\bar{x},\bar{u},t) \neq o$.[40]

The condition $J_d(\bar{x},\bar{u},t) \neq o$ is sufficient only for the existence of a set of solutions. Since decoupling in the practical sense can only be achieved if the solutions to (2.24) for all the components of $\bar{u}$ are real and finite, the space H is redefined to be

$$H = \left[\bar{x}: \; J_d(\bar{x},\bar{u},t) \neq o, \; t_o \leqslant t \leqslant t_f, \; \bar{u} \in R^m, \; |\bar{u}| < \infty \right] \qquad (2.32)$$

where R^m is the real m space.

Note that Class 2 systems contain Class 1 systems and linear time-invariant systems since $J_d(\bar{x},\bar{u},t) = \det D^*(\bar{x},t)$ and $J_d(\bar{x},\bar{u},t) = \det B^*$ where B^* is defined in Reference 9.

2-C.3 Synthesis Procedure - Class 2

The synthesis procedure for Class 2 systems is similar to that for Class 1 systems. Let

$$f(\bar{x},t) = r(\bar{x},t) - a^*(\bar{x},t) \qquad (2.33)$$

and the input vector $\bar{w}$ in (2.24) be premultiplied by the diagonal

matrix Λ . Thus for linear decoupling the vector feedback equation
which must be solved for all the components of $\bar{u}$ becomes

$$d(\bar{x},\bar{u},t) = r(\bar{x},t) - a^*(\bar{x},t) + \Lambda \bar{w} \tag{2.34}$$

Since (2.34) is nonlinear in $\bar{u}$, the space H is not necessarily
invariant with respect to $f(\bar{x},t)$ implying that, unlike Class 1
systems, the region over which the system can be decoupled is
influenced by the entries of $f(\bar{x},t)$. Thus a choice of $r(\bar{x},t)$ in
(2.33) to achieve good dynamic response could greatly reduce the
region of effectiveness of the control law.

For a nonlinear decoupled system, the matrices in the
synthesis procedure would be given by (2.21) and (2.22).

A numerical example illustrating the details in apply-
ing the decoupling and synthesis procedures to a Class 2 system
are contained in Appendix B.

2-D Extension and Modification of the Theory

In this section feedback control laws are derived for
the self-regulation of nonlinear time-varying systems. This is
accomplished by a direct extension of the results of the previous
two sections. In addition, alterations of the theory to include
practical considerations such as system stability and saturation
of inputs are discussed.

2-D.1 Regulatory Feedback Control

Considering first the Class 1 systems defined previously in Section 2 -B and given by

$$\dot{\bar{x}} = a(\bar{x},t) + B(\bar{x},t)\bar{u}$$

$$\bar{y} = c(\bar{x},t)$$

It is desired to develop a feedback control law which will automatically regulate the output $\bar{y}$, to some prescribed values, $\bar{y}_d$, where $\bar{y}_d$ is an m dimensional vector whose entries must be continuously differentiable functions of time. This regulatory control will be achieved using state variable feedback of the form

$$\bar{u} = f(\bar{x},\bar{y}_d,t) \tag{2.35}$$

which combined with the equations for the Class 1 systems results in the closed loop system

$$\dot{\bar{x}} = a(\bar{x},t) + B(\bar{x},t)f(\bar{x},\bar{y}_d,t)$$

$$\bar{y} = c(\bar{x},t) \tag{2.36}$$

Define as an error vector the difference between the actual and desired system outputs due to a disturbance in the states of the system

$$\bar{e} = \bar{y} - \bar{y}_d \tag{2.37}$$

Applying Definition 2, the i'th component of the error is differentiated as before up to the ρ_i'th derivative

$$e_i = c_i(\bar{x}, t) - y_{di}$$

$$e_i^{(1)} = \nabla y_i a(\bar{x}, t) + \nabla y_i B(\bar{x}, t) f(\bar{x}, t) + \frac{\partial y_i}{\partial t} - y_{di}^{(1)}$$

$$= \nabla y_i a(\bar{x}, t) + \frac{\partial y_i}{\partial t} - y_{di}^{(1)} = y_i^{(1)} - y_{di}^{(1)}$$

$$e_i^{(2)} = \nabla y_i^{(1)} a(\bar{x}, t) + \frac{\partial y_i^{(1)}}{\partial t} - y_{di}^{(2)}$$

$$\vdots \qquad \vdots \qquad \vdots \qquad \vdots$$

$$e_i^{(\rho_i - 1)} = \nabla y_i^{(\rho_i - 2)} a(\bar{x}, t) + \frac{\partial y_i^{(\rho_i - 1)}}{\partial t} - y_{di}^{(\rho_i - 1)}$$

$$e_i^{(\rho_i)} = \nabla y_i^{(\rho_i - 1)} a(\bar{x}, t) + \frac{\partial y_i^{(\rho_i - 1)}}{\partial t} - y_{di}^{(\rho_i)} + \nabla y_i^{(\rho_i - 1)} B(\bar{x}, t) f(\bar{x}, \bar{y}$$

$$(2.38)$$

It is desired to choose an $f(\bar{x}, \bar{y}_d, t)$ so that the error vector will converge to zero from any initial state driving the system to the desired output levels. One possibility is to choose a form of feedback which would make each of the error terms behave as a linear stable homogeneous differential equation. This can be achieved by the following choice for $f(\bar{x}, \bar{y}_d, t)$ based on Theorem 1 and the synthesis procedure for Class 1 systems:

$$f(\bar{x}, \bar{y}_d, t) = D^*(\bar{x}, t) \left[r(\bar{x}, t) - a^*(\bar{x}, t) \right] \qquad (2.39)$$

where $D^*(\bar{x},t)$ and $a^*(\bar{x},t)$ are given by (2.9) and (2.12) and the i'th component of $r(\bar{x},t)$ is given by

$$r_i(\bar{x},t) = m_{io}\left[c_i(\bar{x},t) - y_{di}\right] + \sum_{v=1}^{(\rho_i-1)}\left[m_{iv} \nabla y_i^{(v-1)} a(\bar{x},t) - y_{di}^v\right] + y_{d_i}^{(\rho_i)}$$

$$\text{for } i = 1, 2, \ldots, m \qquad (2.40)$$

This results in the following

$$e_i^{(\rho_i)} = m_{io}e_i + m_{i1}e_i^{(1)} + \ldots\ldots + m_{i(\rho_i-1)}e_i^{(\rho_i-1)}$$

$$(2.41)$$

By choosing the m's < 0 in (2.41), the feedback control will tend to drive the error to zero. The rate at which this occurs will depend on the choice of m's. Note that for the error to converge the rate of variation in $\bar{y}_d$ would have to be small compared to the system dynamics. The procedure was applied to develop a control policy for the regulation of nonlinear population dynamics.[4] Development of a regulatory feedback control law for Class 2 system would proceed along similar lines according to the results of Section 2-C. A regulated Class 1 system is depicted in Figure 7.

2-D.2 Stability of Decoupled Systems

From the synthesis procedure given in Section 2-B.3 it
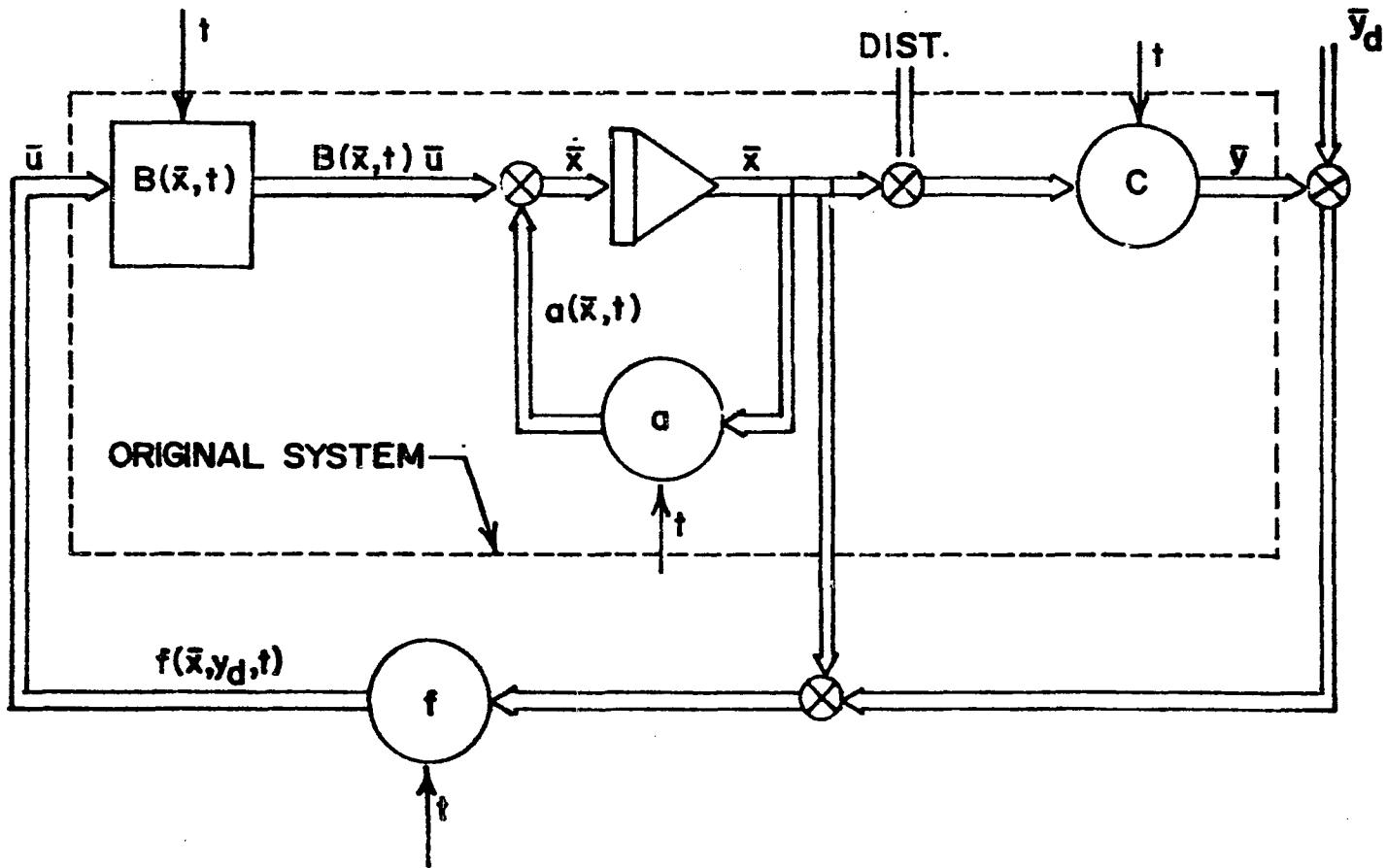
Figure 7   Representation of a Nonlinear Regulated System

is apparent that the decoupled system input-output relationships
can be made linear by proper choice of m's. This is particularly
evident in Equation (2.20). As previously mentioned, these results
are somewhat misleading. The output vector $\bar{y}$ is some combination
of the internal states $\bar{x}$ of the system. The states are in turn
affected by $\bar{w}$ and there is no guarantee that these closed loop
input-state relationships will be stable. A similar problem was
encountered in the decoupling of linear systems. It was shown
that if, and only if the open loop system was both controllable
and observable could the system be decoupled and the input-output
dynamics realized independent of the input-state relationships.[42-44]

A system is said to be controllable if all the states
$\bar{x}$ of the system can be transferred from any initial state $\bar{x}^o$ to
any final state $\bar{x}^f$ in a finite time by some control input $\bar{u}$. In
other words, the control input must affect each state variable.
A system is said to be observable if every state $\bar{x}^o$ can be deter-
mined from measurements of the output vector $\bar{y}$ over a finite time
interval.[45]

Conditions enabling the determination of controllability
and observability of nonlinear systems are scarce and those that
do exist are cumbersome to apply.[46-50] This lack of generality is
not overly restrictive but requires, as with linear systems which
are not controllable and observable, that the input-state closed
loop dynamics and stability be investigated as a special case for
each system. For Class 1 systems this means examining the expres-

sion for $\dot{x}$ in (2.3). For Class 2 systems, the expression for $\dot{x}$ given in (2.19) is examined after the elimination of $\bar{u}$ by solving the vector feedback equation. If the closed loop input-state relationships are linear, as in Example 2, Appendix B, then the well known techniques for determining the stability of linear multivariable systems can be used.[45-51] On the other hand, if as in Example 1, Appendix B, the input-state relations are nonlinear and the system is not controllable, then determining the closed loop system dynamics and stability will be more difficult. Fortunately the DSRV decoupled system dynamics are both linear and controllable.

It should be pointed out that to ensure system input-state stability, it could be necessary to place restrictions on the m's chosen in the synthesis procedure.

2-D.3 Other Constraints

The decoupling theory defines regions in the state space where the system cannot be decoupled using the procedures outlined. The reason is that some of the inputs u_i required to ensure decoupling are infinite and/or are not real (contained in a complex subspace). In the development of the theory the input vector $\bar{u}$ was assumed unbounded as long as it remained finite. In practice, the system inputs or forcing functions have bounded magnitudes considerably less than infinity. Therefore the actual region over which decoupling is possible in the practical sense may be substantually

reduced over that defined by the theory.

The above considerations, together with the stability considerations of the previous section, can be formulated as a set of constraint relationships. These serve to define the physically realizable region in the state space over which the decoupling control law applies. The constraint relationships are as follows:

The preceeding decoupling theory gives the feedback control law which decouples the system. It can be expressed generally as

$$\bar{u} = g(\bar{x}, \bar{w}, M, t) \tag{2.42}$$

where M is the set of coefficients (m's) which determine the decoupled system dynamics as given in the synthesis procedure.

The region over which a system can be decoupled is constrained by the theory to the space H which is defined by the set of $\bar{x}$ and t for which det $D^*(\bar{x}, t) \neq 0$ for Class 1 systems and by (2.32) for Class 2 systems.

As indicated previously in this section, the space H may be further constrainted by physically bounded input magnitudes which can be written as

$$K_v \leq \bar{u} \leq K_u \tag{2.43}$$

where K_v and K_u are m dimensional vectors whose entries are constants representing the lower and upper bounds respectively of the set of acceptable or physically realizable inputs.

To implement the preceeding, a set of m's would have to
be selected to give the desired input-output response characteris-
tics while simultaneously satisfying the stability constraints of
Section 2-D.2. A numerical search routine would then be employed,
varying $\bar{x}$, $\bar{w}$ and t over the range of interest, to determine the
region in the state space over which the feedback control law appli
It may be necessary to relax or reduce the closed loop system speed
of response by choosing different m's thus increasing the region
H over which the decoupling control law is effective.

2-D Summary

Conditions for decoupling two classes of nonlinear sys-
tems have been developed. Necessary and sufficient conditions for
decoupling a class of nonlinear time-varying systems in which the
forcing functions appeared linearly were developed (Class 1). Suf-
ficient conditions were derived for decoupling a larger class of
systems in which the inputs appeared nonlinearly (Class 2). Decoup-
ling in each class was achieved by nonlinear feedback of the states
$\bar{x}$ of the system. For both classes of systems a synthesis procedure
was provided for the specification of the system closed loop dyn-
amics. The results were extended to develop feedback control laws
for the regulatory control of these nonlinear systems.

The theory was derived using basic principles of dif-
ferentiation and matrix manipulations. The ability to decouple
Class 1 systems was shown to depend on the invertibility of a matrix

$D^*(\bar{x},t)$. For the inverse of this matrix to exist, the determinant must be nonzero. Values of the system states $\bar{x}$ over time t where this condition is not met serve to define regions in the state space where the system cannot be decoupled. In an analagous fashion, the decoupling of Class 2 systems by state variable feedback was shown to depend on the ability to solve a set of nonlinear algebraic equations for all the components of $\bar{u}$. Decoupling is theoretically possible where these solutions are real and finite. The conditions for decoupling developed herein contain the previously developed results for linear systems, indicating they are a valid extension of the linear theory.

Two factors which could reduce the regions of applicability of the decoupling control laws were discussed. The first deals with system stability and realizability. It is emphasized that the system closed loop input-output dynamics given by the synthesis procedure do not completely describe the decoupled system. It is necessary to investigate the stability and controllability of the input-state relationships before definitive claims can be made concerning the input-output dynamics.

The second factor is the effect on the decoupled system of the potential saturation of the inputs $\bar{u}$. The theory delineates those regions where the inputs become infinite. In practice, saturation of the inputs would occur at values considerably less than infinity. This will act to further reduce the system realizability. The system inputs defined by the decoupling feedback control law

are functions of several variables $(\bar{x},\ m\text{'s},\ \bar{w})$. For complex higher order systems, a numerical search routine would have to be employed to ensure that the region of operation of these variables did not result in input saturation. Both of these aspects are potential areas of future research.

CHAPTER III

DECOUPLING THE MOTIONS OF A SUBMERSIBLE

3-A   General

In this Chapter the theory developed in Chapter II for decoupling nonlinear systems is applied to decouple the motions of the DSRV. The theory is first applied to decouple the roll-surge equations to which linear theory has been applied.[21] The saturation of inputs such as mercury pump rates is shown to adversely affect the decoupled system response. Methods for resolving these difficulties are provided. Using the theory, a set of general feedback equations are derived for complete decoupling of the dynamic motion in all six degrees of freedom.

The dynamic equations considered necessary for adequately describing the motion of a submersible, such as the DSRV, are a complex set of nonlinear differential equations.[35] The equations of motion in all six degrees of freedom for the DSRV relative to an axis system located in the vehicle center of gravity are given in Appendix A. The numerical values of the various parameters and constants in these equations are also given in Appendix A.

3-B   Decoupling the Roll and Surge Motions

One of the prime motivating factors in developing a theory for decoupling nonlinear systems was the failure of the

linear theory to decouple a reduced or simplified set of roll-surge equations. The nonlinear theory of Chapter II is applied to those same equations in this section.

A number of assumptions are used to simplify Equations A.1 and A.2 of Appendix A which describe the roll and surge motions respectively. These assumptions are listed below:

1. The vehicle is restricted to motion in the roll and surge directions. Thus the terms for motion in all other degrees of freedom are zero.

2. Only _forward_ motion in the surge direction is considered. Describing reverse motion requires changing some of the coefficients in the equations according to Table 9 in Appendix A.

3. The propeller is constrained to rotate in only the direction which produces a forward surge motion of the submersible. Thus the propeller force X_p in Equations A.1 and A.2 are given by Equation A.16 . A different equation would be necessary to predict the force resulting from rotation in the opposite direction. This assumption and the preceeding one are not particularly restrictive since the feedback control laws could be adapted to take into account these changes in the mathematical model.

4. The mercury roll control pump and main propeller dynamics are not included in the equations. The speed of response of the propeller and mercury shift system to input commands

are assumed very fast compared to the vehicle dynamics.

5. Mercury roll weight and main propeller speed are assumed to have unbounded magnitudes.

Assumptions 4 and 5 are not completely valid for all maneuvers. These assumptions will be considered in detail later in this chapter.

Under these assumptions, the roll-surge dynamic equations of motion can be written in state vector form as a Class 2 system

$$
\begin{bmatrix} \dot{x}_1 \\ \dot{x}_2 \\ \dot{x}_3 \end{bmatrix} = \begin{bmatrix} -4.55(10)^{-3}x_1^2 \\ x_3 \\ -.444 \sin x_2 - .0443 x_1 x_3 - .781 x_3\,x_3 - .958(10)^{-4}x_1^2 \end{bmatrix}
$$

$$
+ \begin{bmatrix} -.0129 x_1 u_1 + .168 u_1^2 \\ 0 \\ -1.54(10)^{-4}x_1 u_1 + .0125 u_1^2 + 1.05(10)^{-4}\cos x_2 u_2 \end{bmatrix}
$$

$$(3.1)$$

where x_1 = surge velocity (ft/sec)

x_2 = roll angle (radians)

x_3 = roll rate (radians/sec)

u_1 = main propeller speed (revs/sec)

u_2 = moment due to displaced weight of mercury (ft - lbs)

The outputs of interest are surge velocity and roll angle.

$$\begin{bmatrix} y_1 \\ y_2 \end{bmatrix} = \begin{bmatrix} x_1 \\ x_2 \end{bmatrix} \qquad (3.2)$$

The next step is to apply the decoupling theory for Class 2 systems derived in Chapter II to the roll-surge equations. A representative example illustrating how the theory is applied to Class 2 systems is contained in Appendix B. Application of the theory to the roll-surge equations closely parallels this example. The objective is to generate the components of a vector feedback equation

$$d(\bar{x},\bar{u},t) = r(\bar{x},t) - a^*(\bar{x},t) + \Lambda \bar{w} \qquad (3.3)$$

and to solve this equation for all the components of $\bar{u}$.

Using these solutions for $\bar{u}$ as inputs results in a decoupled system and enable the closed loop input-output dynamics to be specified.

According to the theory, the components of $a^*(\bar{x},t)$ and $d(\bar{x},\bar{u},t)$ are obtained by differentiating the outputs y_1 and y_2. This gives

$$d(\bar{x},\bar{u},t) = \begin{bmatrix} -.0129x_1u_1 + .168u_1^2 \\ \\ -1.54(10)^{-4}x_1u_1 + .0125u_1^2 + 1.05(10)^{-4}\cos x_2u_2 \end{bmatrix}$$

and

$$a^*(\bar{x},t) = -\begin{bmatrix} 4.55(10)^{-3}x_1^2 \\ \\ .444 \sin x_2 + .0443x_1 x_3 + .781x_3 \, x_3 + .958(10)^{-4}x_1^2 \end{bmatrix}$$

(3.5)

To be able to solve (3.3) for the components of $\bar{u}$, it is a sufficient condition that the Jacobian $J_d(\bar{x},\bar{u},t) \neq 0$

$$J_d(\bar{x},\bar{u},t) = \begin{vmatrix} .336u_1 + .0129x_1 & 0 \\ \\ .025u_1 - 1.54(10)^{-4}x_1 & 1.05(10)^{-4}\cos x_2 \end{vmatrix} \neq 0$$

Therefore a solution to the vector feedback equation exists.

The components for the feedback matrices $r(\bar{x},t)$ and which specify the form of the closed loop transfer function are chosen to give linear input-output transfer relationships according to the synthesis procedure of Chapter II. This gives

$$r(\bar{x},t) = \begin{bmatrix} m_{10}x_1 \\ \\ m_{20}x_2 + m_{21}x_3 \end{bmatrix}$$

(3.6)

and

$$\Lambda = \begin{bmatrix} \zeta_1 & 0 \\ 0 & \zeta_2 \end{bmatrix}$$

(3.7)

Without affecting the results, the constants ζ_1 and ζ_2 can be set equal to unity.

Equations (3.4) to (3.7) give the following two non-linear algebraic equations for the components of the vector feedback equation (3.3):

$$-.0129x_1u_1 + .168u_1^2 = m_{10}x_1 + 4.55(10)^{-3}x_1^2 + w_1$$

$$\text{(3.8)}$$

$$-1.54(10)^{-4}x_1u_1 + .0125u_1^2 + 1.05(10)^{-4}\cos x_2 u_2 = m_{20}x_2 + m_{21}x_3$$

$$+ .444 \sin x_2 + .0443x_1x_3 + .781x_3 x_3 + .948(10)^{-4}x_1^2 + w_2$$

To decouple the roll-surge system using only measurements of surge velocity x_1, roll angle x_2 and roll rate x_3, (3.8) must be solved for the main propeller speed u_1 and mercury moment u_2. The solution for u_1 is given

$$u_1 = \frac{.0129x_1 \pm \sqrt{(.0129x_1)^2 + .672(m_{10}x_1 + 4.55(10)^{-3}x_1^2 + w_1)}}{.336}$$

$$\text{(3.9)}$$

This result can be substituted into (3.8) to give a solution for u_2.

Note that the input u_1 must be real to have any physical meaning and therefore decouple the system. This requires the

quantity under square root sign in (3.9) to be equal to a greater than zero.

Examination of (3.9) also reveals that there are two possible roots for u_1. Since the main propeller is restricted to rotation in the positive direction by a previous assumption, the positive root is chosen. Note, however, that there will be two positive roots if the quantity under the square root (3.9) is less than $.0129x_1$, thus generating two possible values for propeller speed u_1.

This apparent anomally is due to an inaccuracy in Equatio: (A.16) for the main propeller force X_p given by

$$X_p = 775u_1^2 - 58x_1u_1 - 3.8x_1^2 \tag{3.10}$$

This equation has a minimum which is a function of x_1 and u_1 shown in Figure 8. Because this minimum does not lie along the x_1 axis, a region exists where the propeller force is bivalued indicating that there are two propeller speeds which will produce the same propeller force. This is a situation which physically cannot exist and is therefore due to an inaccuracy in the describing equation (3.10) at very low propeller speeds. For these speeds the largest positive root is used.

The system closed loop input-state relationships are obtained by substituting the solutions for u_1 and u_2 into (3.1)
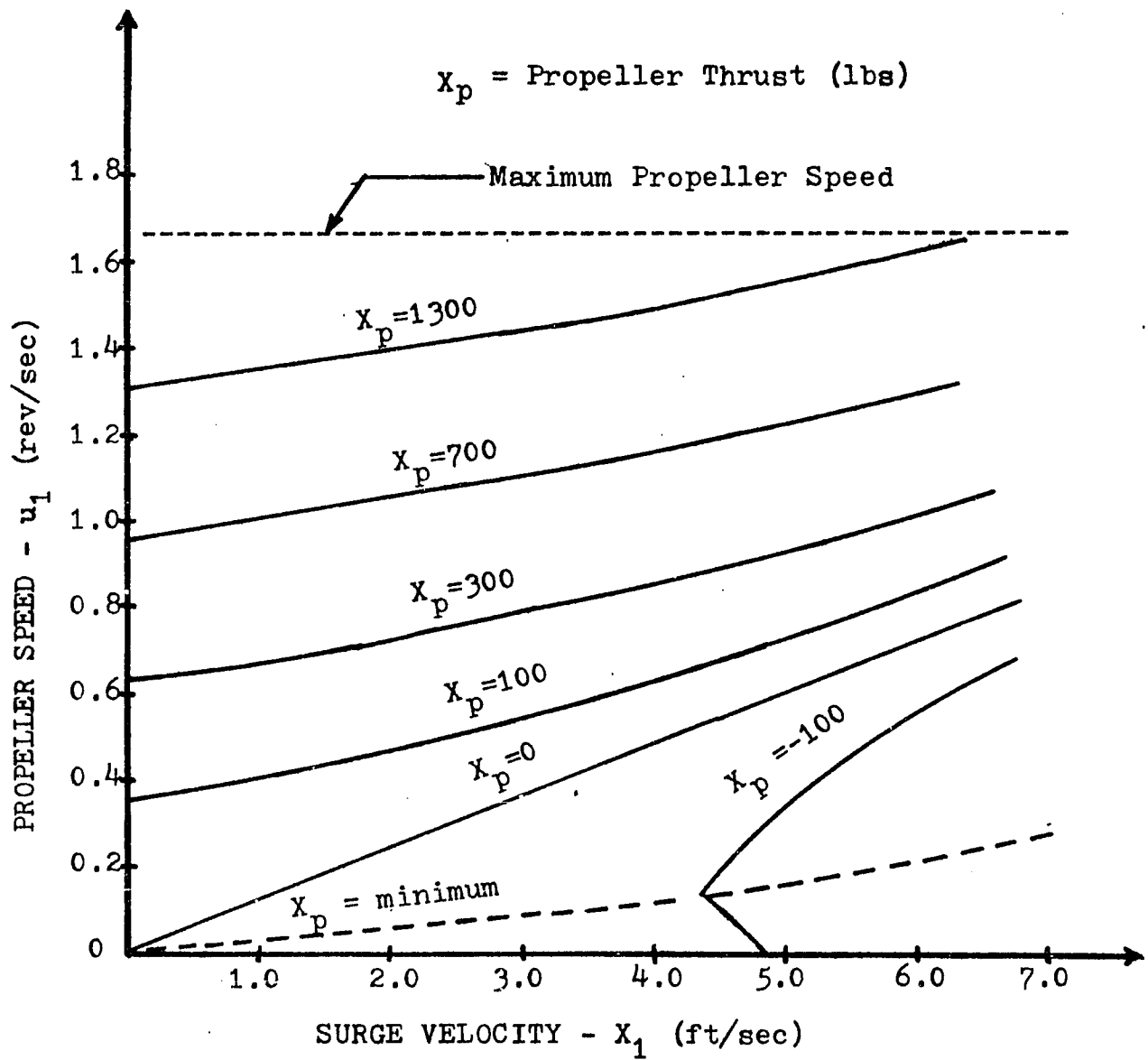
Figure 8   Propeller Force Versus Propeller Speed and
Surge Velocity

giving

$$\dot{x}_1 = m_{10}x_1 + w_1$$

$$\dot{x}_2 = x_3 \qquad\qquad (3.11)$$

$$\dot{x}_3 = m_{20}x_2 + m_{21}x_3 + w_2$$

and the input-output transfer relations from the decoupling theory are

$$\dot{y}_1 = m_{10}y_1 + w_1$$

$$\ddot{y}_2 = m_{20}y_2 + m_{21}\dot{y}_2 + w_2 \qquad\qquad (3.12)$$

The closed loop system is obviously linear and choosing the m's ≤ 0 in (3.11) and (3.12) give a stable system which is completely controllable and observable.

Simulations were conducted on the digital computer using the IBM Continuous System Modelling Program[52] to verify the preceeding conclusions. Printouts of all the computer programs are contained in Appendix C. The decoupling feedback control law was applied to the roll-surge system described by (3.1). The submersible was accelerated from rest a number of times using different step inputs to the surge command w_1. This type of maneuver produces the maximum amount of surge to roll coupling in the open loop system.

The results of these simulations are shown in Figures 9 and 10. The open loop or coupled system response to surge input

is shown for comparison. Also shown is the system response using
feedback control laws based on the linear theory. The nonlinear
theory exactly decoupled the system, as predicted, compared with
the linear theory which showed only a marginal improvement over
the original coupled system response.(See Figure 10). The m's
used in the simulation were selected to give closed loop dynamics
approximately equivalent to the coupled system. This is evident
in comparing the rise time of the surge velocity of the coupled
system and decoupled system in Figure 9. It should be noted that
input u_1 was at all times real valued.

3-C Input Constraints

Two assumptions were made in the previous section con-
cerning the input vector $\bar{u}$. Briefly restated, these were:

1) The input dynamics have a negligible effect and can there-
   fore be ignored.

2) The input magnitudes are unbounded.

In this section the validity of these two assumptions
is examined for both the roll and surge inputs. Methods are pre-
sented for modifying the feedback control laws to resolve any
adverse effects on the decoupled system. Computer simulations
were conducted to determine the decoupling effectiveness of the
modified feedback control laws with the input dynamics and bounds
on inputs included.
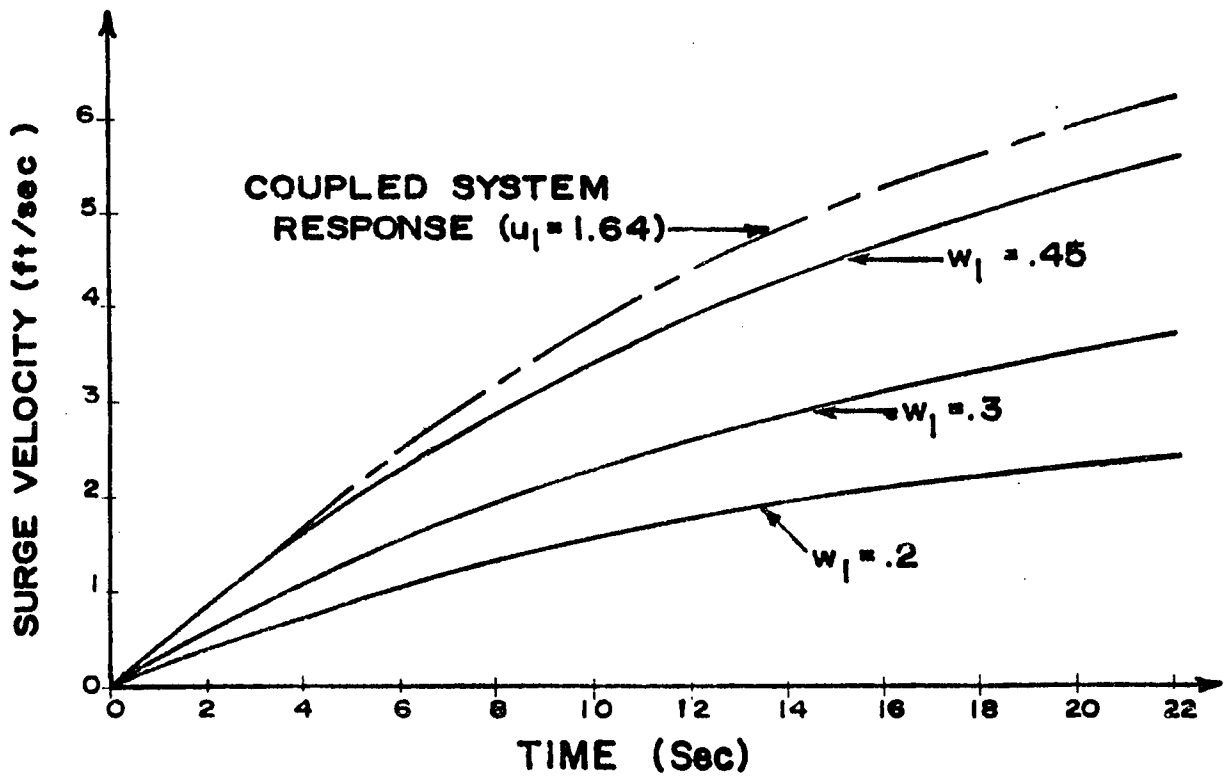
Figure 9 Surge Response
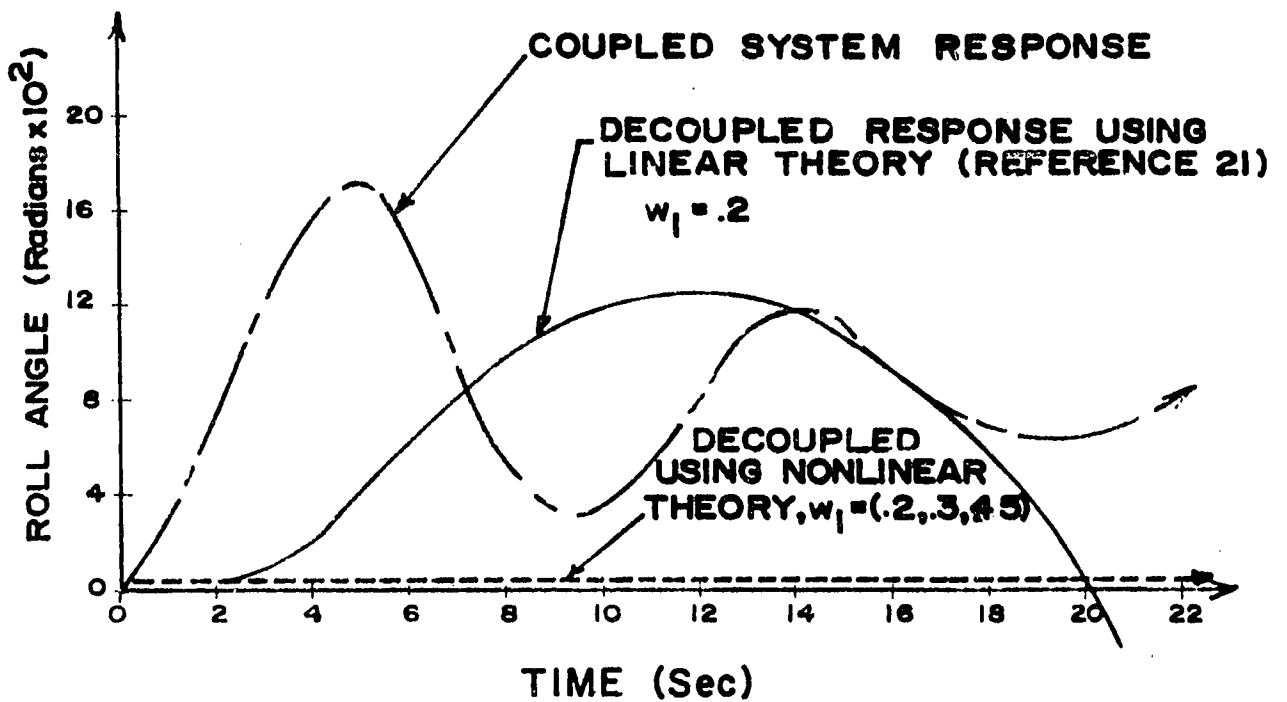
Figure 10 Roll Response

3-C.1   The Surge Input

3-C.1.1   Surge Input Dynamic Constraints

For input u_1 corresponding to the main propeller speed, the assumption was that the input dynamics had only a small effect on the total system dynamics and therefore could be ignored. In effect, this is saying that the rise time of the propeller speed to a command input is much faster than the rise time of surge velocity to a change in propeller speed. The transfer function for the propeller speed is given as

$$u_1(s) = \frac{(1 + .49s)u_{1c}(s)}{(1 + .7s)(1 + .245s)} \tag{3.13}$$

where s = Laplace operator

u_{1c} = command propeller speed

The rise time associated with this transfer function is small ($\approx .5$ sec) compared with the rise time of the surge velocity (≈ 17 sec) to a step change in propeller speed. Therefore, ignoring surge dynamics should not have an appreciable effect on the validity of the feedback control laws.

3-C.1.2   Surge Input Magnitude Constraints

Some of the constraints on main propeller speed u_1 were

derived previously, such as the requirement that the positive root to Equation (3.9) be chosen to ensure the values for u_1 are always positive. Another constraint is the physical limitation on the maximum speed of rotation of the main propeller to 1.64 rev/sec. Thus the positive root in Equation (3.9) becomes a constraint equation by setting $u_1 = 1.64$ giving

$$\frac{.0129x_1 + \sqrt{(.0129x_1)^2 + .672(m_{10}x_1 + 4.55(10)^{-3}x_1^2 + w_1)}}{.336} \leq 1.64$$

(3.14)

Also the input u_1 is required to be real valued to have any physical significance. This restricts the magnitude of the quantity under the square root sign to

$$(.0129x_1)^2 + .672(m_{10}x_1 + 4.55(10)^{-3}x_1^2 + w_1) \geq 0 \qquad (3.15)$$

The closed loop surge time constant m_{10} in (3.14) and (3.15) can be chosen to give a rise time approximately equal to the open loop system as was done for the simulations in Section 2-B ($m_{10} = -.059$). Constraint Equations (3.14) and (3.15) can then be used to map out the region of acceptable values of the new system input w_1 as a function of surge velocity x_1. This region is shown in Figure 11.

The upper boundary, described by setting $u_1 = 1.64$ in (3.14) is not restrictive in terms of desired system behavior
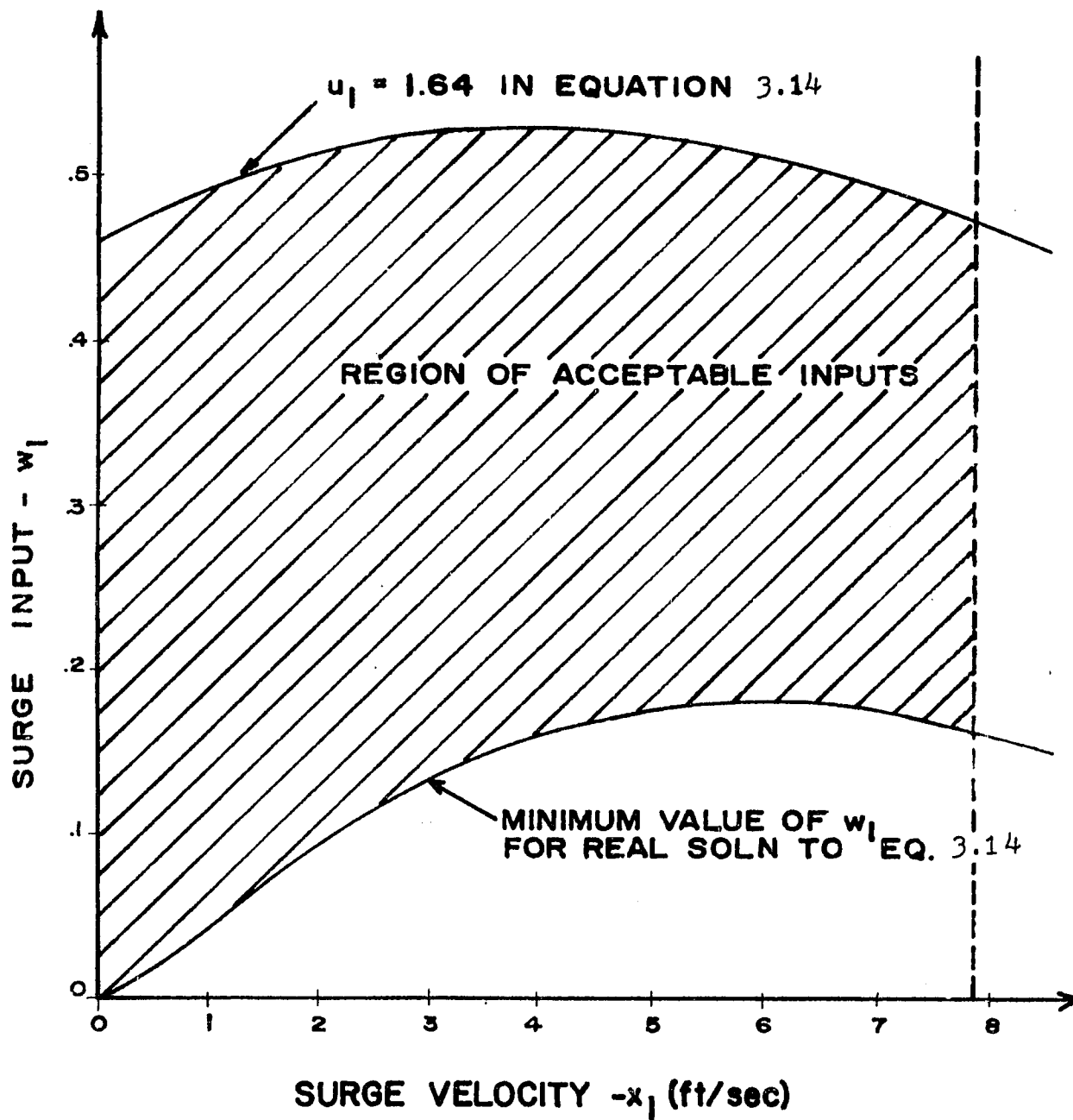
Figure 11   Decoupled System Surge Input as a Function of

Surge Velocity

since w_1 = .47 gives the same maximum surge velocity as the open loop system. The lower bounds are described by setting the quantity on the LHS of (3.15) equal to zero. The positive values of w_1 reflect in part the inaccuracy of the equation describing propeller force X_p discussed in Section 3-B since positive values of u_1 produce minimum propeller force. The values are also influenced by the choice of m_{10} as indicated in (3.15). Thus choosing w_1 within the limits indicated by Figure 11 should satisfy all constraints thus yielding an acceptable decoupled linear system response.

3-C.2   The Roll Input

3-C.2.1   Roll Input Dynamic Constraints

The input u_2 in the roll-surge equation (3.1) represents the displaced weight of mercury causing a roll moment. Since this mercury is controlled by pumping it from tank to tank, the actual system input is the pumprate W_p. The transfer function defining the dynamic relationship between u_2 and W_p is given by[20]

$$u_2(s) = \frac{W_p(s)}{s(1 + .083s)} \tag{3.16}$$

The pole at s = -12 represents the time constant of the pump and reflects the pump inertia. As with the main propeller dynamics, it can be ignored without significantly affecting vehicle response characteristics and (3.16) becomes

$$u_2 = \int_0^t W_p \, dt \qquad (3.17)$$

The decoupling theory gives the equation for the roll weight of mercury u_2 to dynamically decouple the system. As evident in (3.17) it will be necessary to differentiate the equatiion for u_2 to obtain the pumprate. Since u_2 is a function of $\bar{x}$ and $\bar{w}$ this becomes

$$W_p = \frac{Du_2}{Dt} = \nabla u_2 \dot{\bar{x}} + \nabla_w u_2 \dot{\bar{w}} \qquad (3.18)$$

where $\qquad \nabla_w = \left[\dfrac{\partial}{\partial w_1}, \dfrac{\partial}{\partial w_2}; \ldots, \dfrac{\partial}{\partial w_m} \right]_{1 \times m}$

and ∇ has been defined previously.

The value for u_2 obtained by substituting the solution for u_1 into (3.8) is rather lengthy. The operations on u_2 described by (3.18) make it even more cumbersome. As a result these equations will not be written here.

3-C.2.2 Roll Input Magnitude Constraints

As indicated in (3.18), the equation for the pumprate W_p will contain derivatives of the input vector $\bar{w}$. Thus rapid or

step changes in the inputs will have extremely large derivatives calling for large magnitudes of the pumprate. Since the pumprate is limited to 56.4 lbs/sec, saturation will likely occur reducing the effect of the decoupling feedback. This can be offset by limiting the rate change of the inputs $\bar{w}$ using first order filters. A block diagram representation is shown in Figure 12.

$$w_{1c} \longrightarrow \boxed{\dfrac{1}{t_{c1}s + 1}} \longrightarrow w_1$$

$$w_{2c} \longrightarrow \boxed{\dfrac{1}{t_{c2}s + 1}} \longrightarrow w_2$$
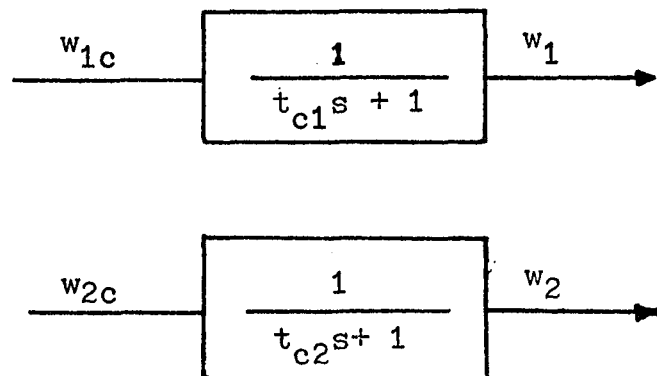
Figure 12   Block Diagram Representation of Input Rate
Limiting Filters

3-C.3 Simulations

The roll-surge equations including all the input dynamics and bounds on the input magnitudes were programmed on the digital computer. The roll feedback was modified according to Equation (3.18). Simulations were conducted both with and without first order filters to compensate the inputs $\bar{w}$. The time constants t_{c1} and t_{c2} of the first order filters for the compensated case were set equal to 1.5.

The results for the surge and roll responses are shown in Figures 13 and 14. The maximum amount of coupling was reduced by about half for the uncompensated case as evident in comparing the roll response for this case with the coupled system response. By compensating the inputs, the amount of cross-coupling was practically eliminated. However, the use of input compensation causes a more sluggish response in the surge velocity to an input command as shown in Figure 13. Thus a tradeoff exists between minimizing the degree of cross-coupling while maintaining adequate response dynamics.

3-D   Decoupling the Six Degrees of Freedom

In this section the complete set of equations describing submersible motion in all six degrees of freedom are considered. Some simplifying assumptions are made to enable these equations to be written in a general state vector form as a Class 2 system. The feedback control laws for decoupling the motions of the submersible during hovering are derived with the terms appearing as general functions.

Although the decoupling problem can be approached in degree of freedom pairs such as roll-surge, this method is satisfactory only for maneuvers involving those two degrees of freedom. Where much of the submersible motion involves only the pair and and a relatively high degree of coupling exists, as in the roll-
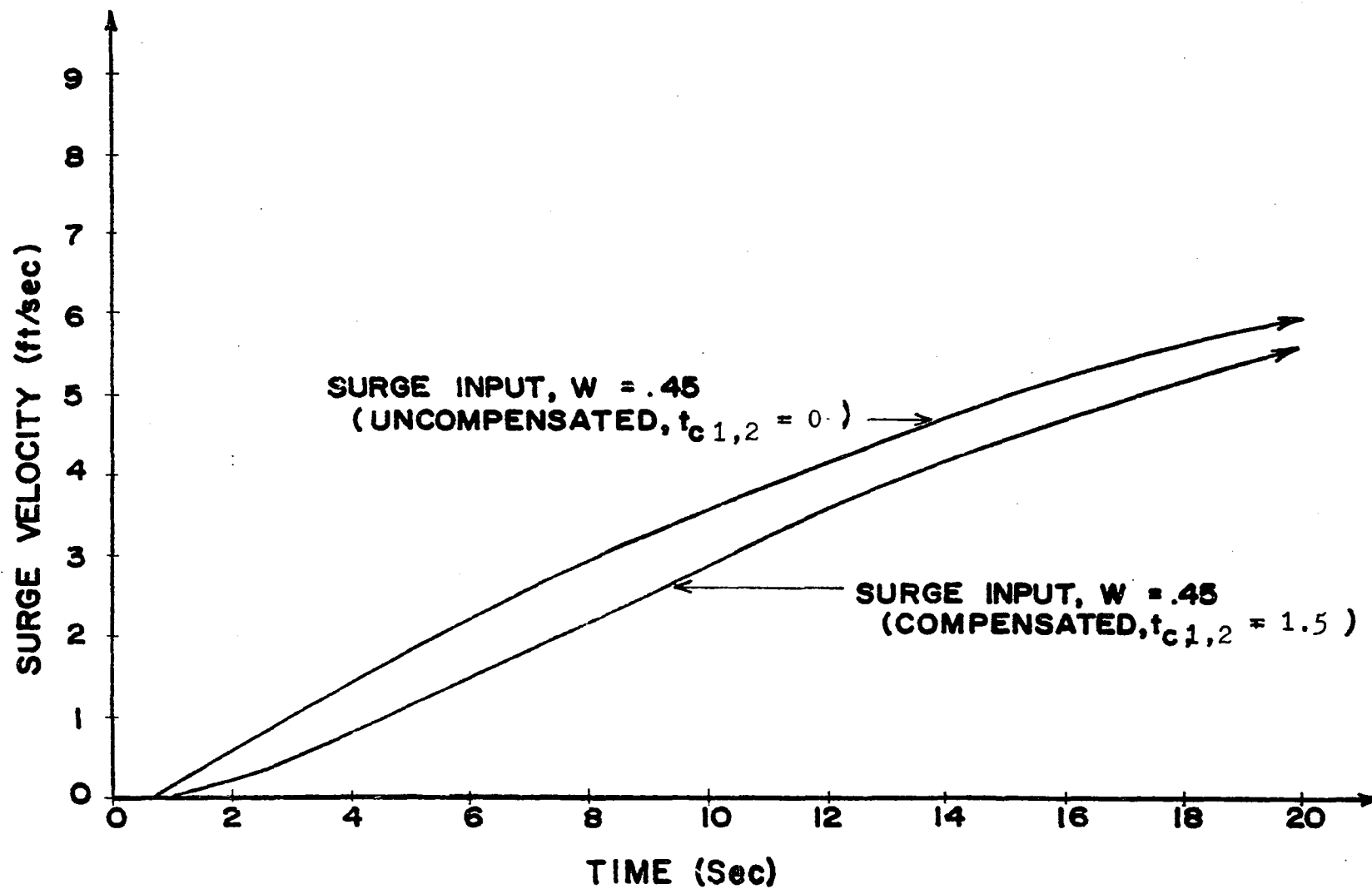
Figure 13   Surge Response - System Input Constraints Included
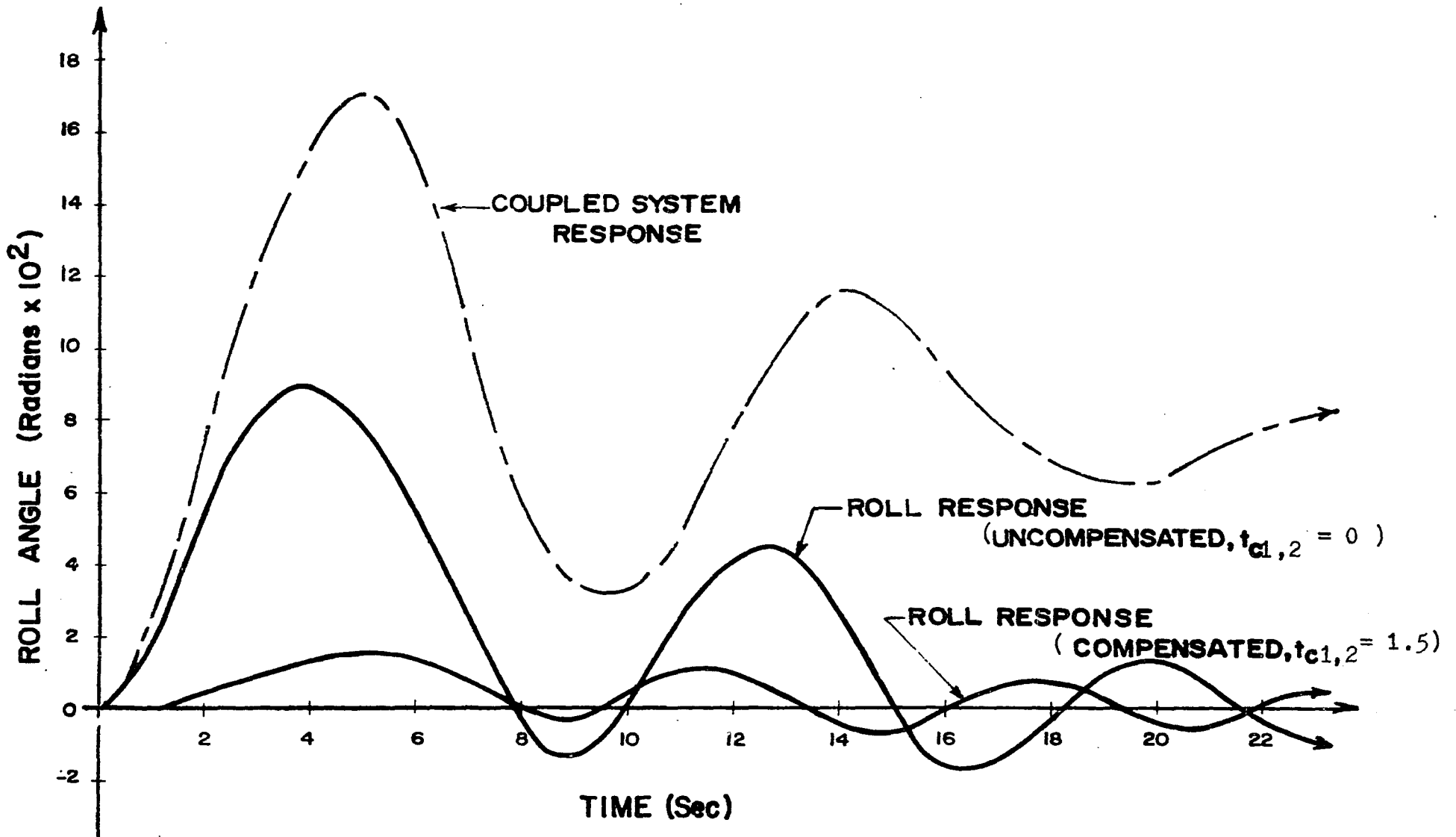
Figure 14   Roll Response - System Input Constraints Included

surge motions, the approach is justified. For the case of "in-tight" hovering maneuvers where positioning accuracy is desired, dynamic motion in several degrees of freedom may be required. In this instance, simultaneous decoupling between all six degrees of freedom is required to ensure complete single degree of freedom control.

3-D.1   The Simplified Equations

A set of coupled nonlinear equations describing the DSRV motion in the six degrees of freedom is given in Appendix A. These equations can be simplified by dropping the acceleration terms contributing to the coupling in each degree of freedom. Although not strictly necessary, this eliminates the excessive algebraic manipulations otherwise required to express each equation in terms of only one derivative for state variable representation. The error introduced by dropping these terms is given in Table 1 as a maximum percentage of the principal control thrust or moment in each degree of freedom. The errors are small and could be represented as disturbance inputs.

By dropping the acceleration terms it is possible to write the equations of Appendix A directly in state variable form as a Class 2 system:

TABLE 1

MAGNITUDE OF ACCELERATION CROSS-COUPLING FORCES

AS A PERCENTAGE OF MAIN CONTROL FORCE

Degree of Freedom	Acceleration Coupling Terms Percentage of Control Force	
Surge	$my_G\dot{r}$	$mz_G\dot{q}$
	.023%	0.53%
Sway	$(mz_G + Y_{\dot{p}})\dot{p}$	$(mx_G - Y_{\dot{r}})\dot{r}$
	1.26%	1.71%
Heave	$(mx_G + Z_{\dot{q}})\dot{q}$	$my_G\dot{p}$
	1.49%	1.53%
Yaw	$my_G\dot{u}$	$(mx_G - N_{\dot{v}})\dot{v}$
	0.43%	0.47%
Roll	$my_G\dot{w}$	$(mz_G + K_{\dot{v}})\dot{v}$
	0.35%	2.81%
Pitch	$mz_G\dot{u}$	$(mx_G + M_{\dot{w}})\dot{w}$
	1.53%	0.52%

$$
\begin{bmatrix} \dot{x}_1 \\ \dot{x}_2 \\ \dot{x}_3 \\ \dot{x}_4 \\ \dot{x}_5 \\ \dot{x}_6 \\ \dot{x}_7 \\ \dot{x}_8 \\ \dot{x}_9 \end{bmatrix} = \begin{bmatrix} h_1(\bar{x}) \\ h_2(\bar{x}) \\ h_3(\bar{x}) \\ x_5 \\ h_4(\bar{x}) \\ x_7 \\ h_5(\bar{x}) \\ x_9 \\ h_6(\bar{x}) \end{bmatrix} + \begin{bmatrix} X \\ Y \\ Z \\ 0 \\ N \\ 0 \\ K \\ 0 \\ M \end{bmatrix} \qquad (3.19)
$$

where

x_1 = u (surge velocity), x_2 = v (sway velocity), x_3 = w (heave velocity)

x_4 = θ (roll angle), x_5 = p (roll rate), x_6 = θ (pitch angle)

x_7 = q (pitch rate), x_8 = Ψ (yaw angle), x_9 = r (yaw rate)

and

$(h_1(\bar{x}), h_2(\bar{x}), \ldots, h_6(\bar{x}))$ - represent all the terms involving only velocities and displacements in Equations (A.1) to (A.6) respectively.

(X,Y,Z) - represent the terms containing the control forces or inputs in Equations (A.1) to (A.3)

(N,K,M)   — represent the terms containing control

                moments in Equations (A.4) and (A.6).

    The outputs we want to control independently are the
surge, sway and heave velocities and the roll, pitch and yaw
angles. Therefore the output vector $\bar{y}$ is given by

$$
\begin{bmatrix} y_1 \\ y_2 \\ y_3 \\ y_4 \\ y_5 \\ y_6 \end{bmatrix} = \begin{bmatrix} x_1 \\ x_2 \\ x_3 \\ x_4 \\ x_5 \\ x_6 \end{bmatrix} \qquad\qquad (3.20)
$$

3-D.2   Application of the Decoupling Theory

    Leaving the input vector in the form of (3.19) and again
applying the decoupling procedure for Class 2 systems as was done
previously for the roll-surge equations, the following matrices
are generated:

$$d(\bar{x}, \bar{u}) = \begin{bmatrix} X \\ Y \\ Z \\ N \\ K \\ M \end{bmatrix} \quad , \qquad a^*(\bar{x}) = \begin{bmatrix} h_1(\bar{x}) \\ h_2(\bar{x}) \\ h_3(\bar{x}) \\ h_4(\bar{x}) \\ h_5(\bar{x}) \\ h_6(\bar{x}) \end{bmatrix}$$

For a linear decoupled system:

$$r(\bar{x}) = \begin{bmatrix} m_{10}x_1 \\ m_{20}x_2 \\ m_{30}x_3 \\ m_{40}x_4 + m_{41}x_5 \\ m_{50}x_6 + m_{51}x_7 \\ m_{60}x_8 + m_{61}x_9 \end{bmatrix} \qquad \text{and} \quad \Lambda = I \text{ (Identity Matrix)}$$

This gives the following equations for the decoupling vector feedback equation (3.3)

$$X = m_{10}x_1 - h_1(\bar{x}) + w_1$$

$$Y = m_{20}x_2 - h_2(\bar{x}) + w_2$$

$$Z = m_{30}x_3 - h_3(\bar{x}) + w_3$$

$$N = m_{40}x_4 + m_{41}x_5 - h_4(\bar{x}) + w_4$$

$$K = m_{50}x_6 + m_{51}x_7 - h_5(\bar{x}) + w_5$$

$$M = m_{60}x_8 + m_{61}x_9 - h_6(\bar{x}) + w_6$$

(3.21)

To decouple in all six degrees of freedom by state feedback, it is necessary to solve for the control force inputs $\bar{u}$, such as propeller speeds and pumprates, that make up the terms on the LHS of (3.21). These are lengthy nonlinear equations. Typical of these is the equation for the control force in the surge direction (X)[20],

For $u_1 \geqq 0$, $x_1 \geqq 0$

$$X = .168u_1^2 - 1.54(10)^{-4} x_1 u_1 + g_1(x_2,x_3,x_7,x_9)u_1 + g_2(x_1)u_2^2$$

$$+ g_3(x_1)u_3^2 + g_4(x_1)u_4^2 + g_5(x_1)u_5^2$$

$$(3.22)$$

where u_1 = main propeller rotational speed.

u_2 = forward horizontal ducted thruster rotational speed.

u_3 = forward vertical ducted thruster rotational speed.

u_4 = aft horizontal ducted thruster rotational speed.

u_5 = aft vertical ducted thruster rotational speed.

and the g's are nonlinear functions of the velocities.

A simplification of the terms on the LHS of (3.21) is possible if decoupling of the motions in only the hovering mode is considered. Hovering maneuvers for a submersible such as the DSRV, require a high degree of accuracy, particularly for rescue and recovery operations. It is during these types of maneuvers

that a decoupling control stategy would be of most benefit to the operator.

Since the hovering mode is essentially dynamic positioning in a very localized region, it is reasonable to assume that the velocities attained in any of the degrees of freedom will be quite small. This particularly is true for the translational velocities. On the other hand, the initial control forces and moments used during this type of maneuvering are usually quite large, requiring high speed rotation of the propellers.[3] In view of these considerations, the thrust deduction terms[*] in the forcing function equations such as (3.22) will be small compared to the velocity squared terms and can be ignored. The terms on the LHS of (3.21) then become

$$X = \begin{cases} -.0812u_1^2 & (u_1 < 0) \\ .168u_1^2 & (u_1 \geqq 0) \end{cases}$$

$$Y = 5.5(10)^{-4}u_2|u_2| + 5.5(10)^{-4}u_4|u_4|$$

$$Z = 5.95(10)^{-4}u_3|u_3| + 5.95(10)^{-4}u_5|u_5| \qquad (3.23)$$

$$N = 1.06(10)^{-4}u_2|u_2| - 1.0(10)^{-4}u_4|u_4|$$

$$K = \begin{cases} -.0111u_1^2 + 1.05(10)^{-4}\cos x_2 u_6 & (u_1 < 0) \\ .0125u_1^2 + 1.05(10)^{-4}\cos x_2 u_6 & (u_1 \geqq 0) \end{cases}$$

$$M = 1.14(10)^{-4}u_3|u_3| - 1.08(10)^{-4}u_5|u_5|$$

---

[*] These terms appear in the propeller force equations to account for the loss in propeller thrust with speed of advance through the fluid (53). These terms usually appear as first order cross products $(x_i u_i)$.

Equation (3.23) can be combined with (3.22) to give the components of the vector feedback equation which must be solved for all the u's to decouple the system.

$$\left.\begin{array}{c} -.0812u_1^2 \\ .168u_1^2 \end{array}\right\} = m_{10}x_1 - h_1(\bar{x}) + w_1$$

$$5.5(10)^{-4}(u_2|u_2| + u_4|u_4|) = m_{20}x_2 - h_2(\bar{x}) + w_2$$

$$5.95(10)^{-4}(u_3|u_3| + u_5|u_5|) = m_{30}x_3 - h_3(\bar{x}) + w_3$$

$$\left.\begin{array}{c} -.0111u_1^2 \\ .0125u_1^2 \end{array}\right\} + 1.05(10)^{-4} \cos x_4 u_6 = m_{40}x_4 + m_{41}x_5 - h_4(\bar{x}) + w_4$$

$$1.14(10)^{-4} u_3|u_3| - 1.08(10)^{-4} u_5|u_5| = m_{50}x_6 + m_{51}x_7 - h_5(\bar{x}) + w_5$$

$$1.06(10)^{-4} u_2|u_2| - 1.0(10)^{-4} u_4|u_4| = m_{60}x_8 + m_{61}x_9 - h_6(\bar{x}) + w_6$$

$$(3.24)$$

A solution to this set exists since $J_d(\bar{x}, \bar{u}, t) = 0$ for (3.24). The absolute value signs indicate the directional characteristics of the propeller forces and serve to distinguish between the two roots that exist when (3.24) is solved for each propeller speed. The h's in (3.24) could likely be simplified according to the previous assumption concerning the thrust deduction terms. Once again the set of all $(\bar{x}, \bar{w})$ would have to be examined to

determine input constraints. Since the solutions for the u's will likely be much more lengthy than those for the roll-surge problem, numerical search routines would have to be used. With the exception of roll pump rate, input dynamics in each degree of freedom can likely be ignored without appreciably affecting system response

The detailed development of the feedback control laws by solving (3.24) for all the u's and taking into account input constraints will not be pursued. The procedure, although very lengthy, would be fairly mechanistic from here on in. The development would follow along lines similar to that used for the roll-surge equation

3-E Summary

The nonlinear decoupling theory developed in Chapter II was applied to the equations describing the motion of the DSRV.

The theory was first applied to exactly decouple a reduce form of the roll-surge equations. The use of linear theory had previously failed to satisfactorily decouple the system. Including the input dynamics and limitations on input magnitudes in the equations required modification of the theory to decouple the system. Although successful, some of these modifications were arrived at in a somewhat heuristic manner. Further development of the decoupling theory to more completely take into account input constraints would be useful. One approach might be to formulate the decoupling

problem as a type of mathematical programming problem. The input dynamics, input magnitudes and feedback control laws would act as system constraint equations and an objective function would be formulated. This function could serve to enlarge the decoupled space and response characteristics by selecting optimal values of $f(\bar{x},t)$ and Λ in the synthesis procedure.

Decoupling the complete six degrees of freedom was also investigated. By considering only hovering maneuvers, the equations of motion were simplified and the feedback equations necessary to decouple the motions were developed. A method of obtaining explicit solutions to these equations, subject to input constraints, was outlined.

The decoupling strategies investigated require the manipulation of lengthy nonlinear equations and therefore could not be easily implemented using analog controllers. This means that an onboard digital computer is required. In addition, sensors would be required to provide continuous measurement of the velocities and angular displacements. The potential application to actual submersible operation of the control laws developed in this chapter is good. Although the DSRV is one of the few submersibles to currently possess the above mentioned capabilities, this is likely to change. The recent technological advances in dedicated computers coupled with new and improved sensors of all types are now beginning to place submersible control strategies, such as those developed in this chapter, well within the realm of the practical.

CHAPTER IV

THE WAKE STEERING NOZZLE - STATIC PERFORMANCE

4-A General

The wake steering nozzle (WSN) is a new method of developing propulsion and steering forces for submersibles. It has the potential advantages over conventional systems of increasing vessel geometric symmetry and reducing the number of thrusters. (See Figure 4, Chapter 1).

Most submersibles require precise control at very low forward speeds. This control is not easily achieved using conventional movable surfaces such as rudders. Thus, one of the prime advantages of the WSN over the movable surfaces is its ability to develop steering forces at zero forward velocity.

This chapter deals with the experimental investigation of a number of geometric parameters of the WSN at zero forward velocity or _static_ operation. The experimental facility constructed for testing the WSN is described. Several nondimensional numbers are developed to enable a reduction of the data for comparison of the axial thrust characteristics of the WSN with those of conventional shrouded propellers.[24-25] A preliminary series of exploratory tests were run. These served to define a number of important parameters of shroud geometry which were investigated in a more extensive set of tests. Mathematical modelling of the observed flow field used as an aid in guiding the experimental effort is also discussed.

4-B   The WSN Test Facility

4-B.1   The Measurement System

In the experimental system used by Wozniak, the axial
and radial forces produced by a WSN were determined indirectly,
using measurements of the pressure on the inside shroud surface.[29]
These pressure measurements were converted to forces using a
computer program which took into account shroud shape. This method
was time consuming and cumbersome. Our first task therefore was to
develop a means for direct measurement of the forces being produced
by a WSN.

To this end, a five component dynamic force balance or
dynamometer was designed and constructed.[31] It essentially consists
of a vertical beam instrumented with strain gages. (See Figure 15).
The gages and associated instruments allow the axial force and the
horizontal component of radial force to be measured and recorded
as functions of time on an oscillograph. To completely specify the
radial force, another component must be measured. This other com-
ponent is obtained by repeating the test run and opening a port
located at 90° from the first port. The two components are then
added vectorially to determine the radial force magnitude and direc-
tion. In addition, the system can also measure and record all three
moments. The beam is damped in the horizontal plane by two mechanical
dampers, manufactured by Airpot Corporation, mounted along axes
orthogonal to each other. The WSN to be tested were mounted on the
end of the beam and emmersed in a tank 3.0 feet by 8.0 feet with
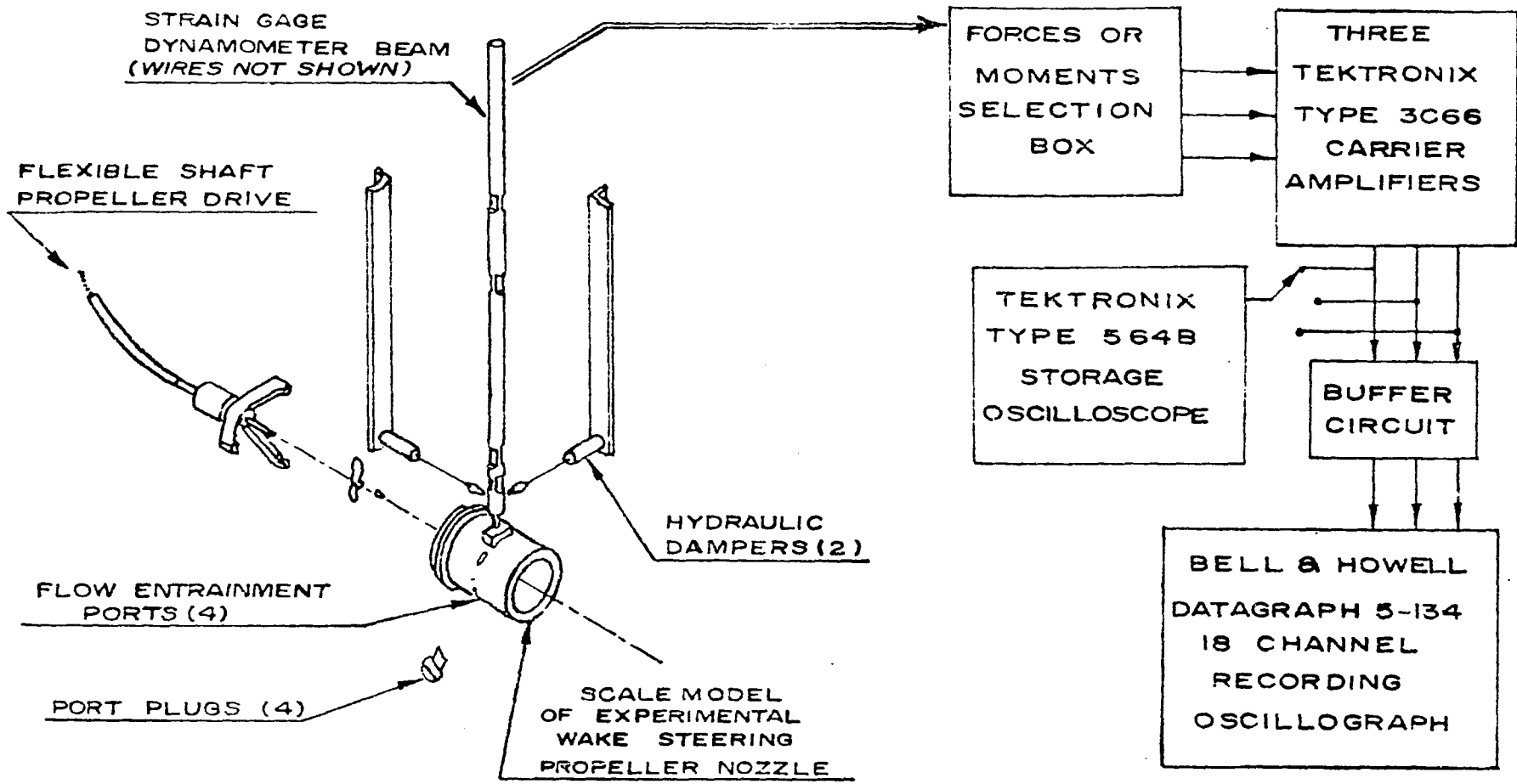
Figure 15 Nozzle Force and Moment Measurement System

the water depth kept at about 2.0 feet. The tank was baffled to reduce recirculation eddies in the region of the shroud occurring as a result of the pumping action of the propeller and the constriction imposed by the tank.

The propeller is driven by a DC motor through a flexible shaft. Propeller torque is measured by measuring and recording armature current and propeller torque. Motor speed was controlled by varying the armature current with speed measured by a tachometer. A schematic of the motor control circuit is shown in Figure 16.

Pressures inside the aluminum shrouds were measured by means of a manometer bank connected to the shroud by tubing through the tank.

The aluminum shrouds were time consuming to make and difficult to machine. As a result, a special shroud holder was designed and constructed by Clark which enabled the shroud shape to be easily and rapidly changed. The shroud holder was mounted on the same dynamometers used for testing the aluminum shrouds. The system is shown in Figure 17. The shroud holder has a cylindrical inner surface of fixed diameter in the region of the control port. This ring contains a port valve assembly which is rotatable. This valve is actuated by means of an air cylinder. The shroud surface fore and aft of the holder can be changed by switching inserts. These inserts are machined out of wax stiffened by a section of aluminum pipe. The machining of the wax was done on a lathe using a forming tool constructed from heavy gage metal cut to the desired nozzle shape.
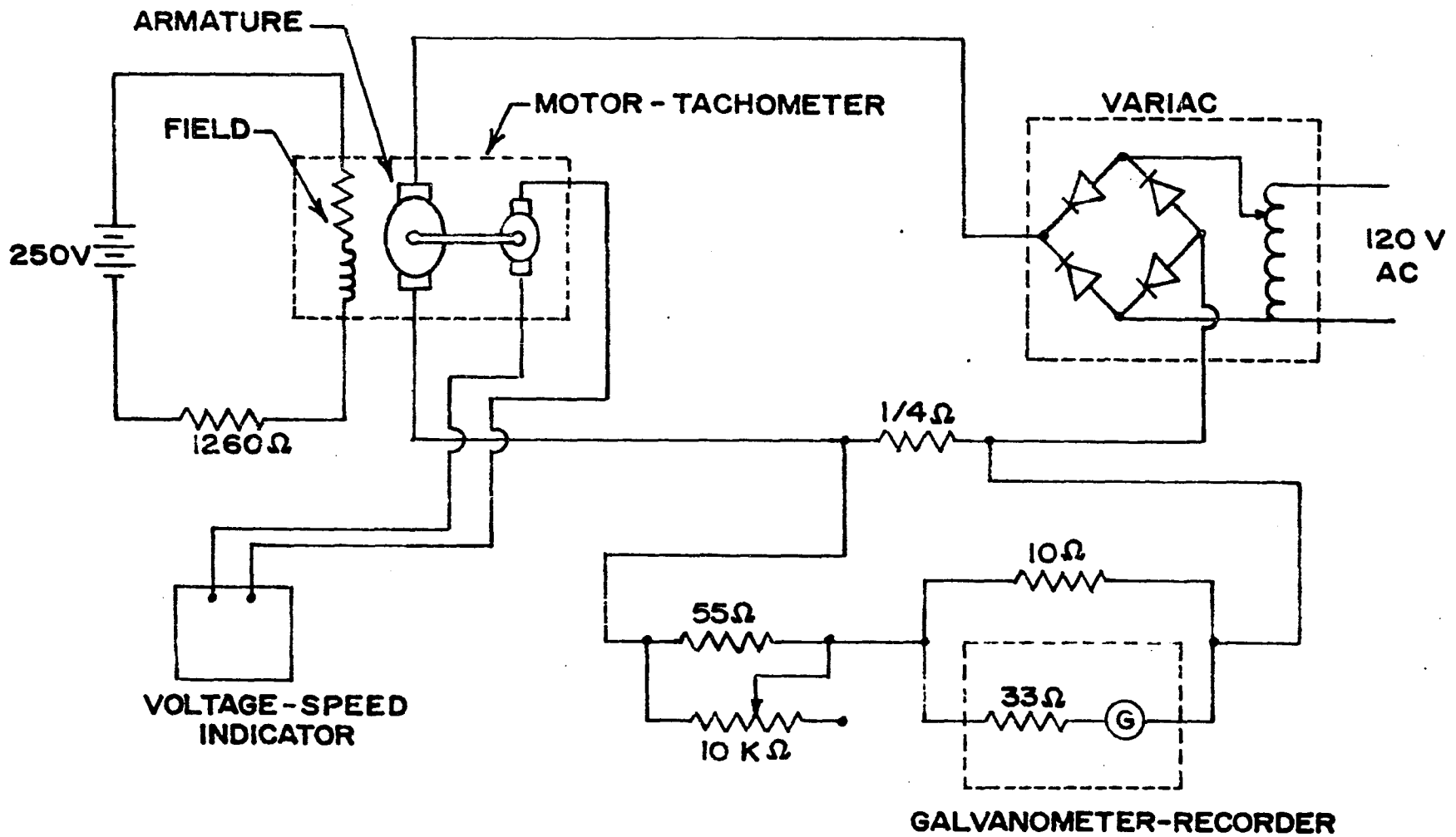
Figure 16   Motor Control Circuit

EXISTING FLEXIBLE SHAFT
FOR PROPELLER DRIVE

FLEXIBLE SHAFT
FOR NOZZLE
ROTATION

EXISTING STRAIN
GAGE DYNAMOMETER

AIR CYLINDER TO
ACTUATE FLAPPER
VALVE ON PORT

PROPELLER AXIAL
POSITION ADJUSTMENT

FWD NOZZLE INSERT

AFT NOZZLE INSERT
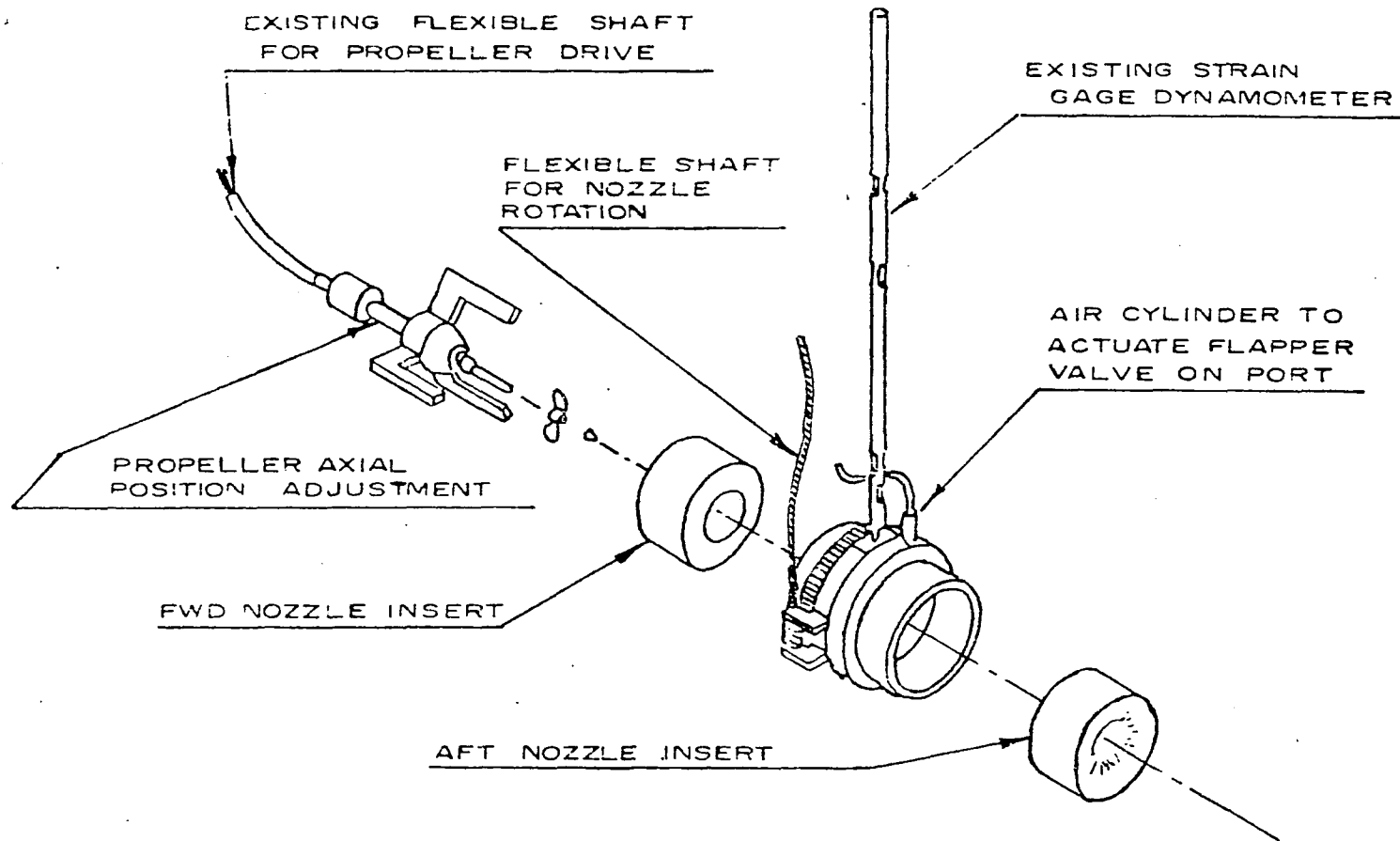
Figure 17   Nozzle Variation System

4-B.2   Propellers and Nozzles

A series of two bladed propellers were used. The prin-
ciple difference between the propellers is in their pitch to
diameter ratios which varied from 1.24 to 2.06 (measured at 7/10
the radius). The propellers also differed in blade length L_p,
blade thickness t_p and propeller diameter D. The dimensions of the
six propellers used in the tests are given in Table 2. Drawings
showing the profiles of each of the propellers are contained in
Reference 32.

The two aluminum nozzles tested, designated No.1 and
No.2, are shown to full scale in Figures 18(a) and 18(b) respec-
tively. The inside shape of nozzle No.1 is based on nozzle No.32
developed by the Netherlands Ship Model Basin[24] and nozzle No.2
has the inside shape of an NACA-16-021 airfoil at zero angle of
attack.[53]

Two series of wax nozzles were developed for extensive
testing. Figure 19 identifies the parameters varied in this series
of nozzles. This series utilized the shroud variation system and
was therefore made up of fore and aft inserts machined from wax.
Both series used the same fore insert having a length of 2.0 inches
and the same inside profile as aluminum nozzle No.2. The rear inserts
of both series were varied as shown in Table 3. Series A was gene-
rated by varying the radius of curvature R_c and Series B by varying
the length of the aft section L_a.

TABLE 2

PROPELLER DIMENSIONS

Propellers	$2r_p/D$	L_p/D	t_p/D	P in.
Prop. No.1 D = 1.74 in. r_h = 0.37 in. P/D= 1.24	.930 .818 .702 .585 .468 .351	.374 .496 .609 .620 .541 .397	.014 .022 .034 .040 .041 .039	2.10 2.17 2.17 2.17 2.17 2.13
Prop. No.2 D = 1.74 in. r_h = 0.39 in. P/D= 1.41	.936 .818 .702 .585 .468 .351	.316 .487 .607 .620 .541 .458	.007 .015 .017 .028 .031 .024	2.96 2.61 2.45 2.30 2.28 2.29
Prop. No.3 D = 1.70 in. r_h = 0.41 in. P/D= 1.64	.936 .818 .702 .585 .468 .351	.468 .594 .629 .577 .495 .419	.022 .032 .029 .043 .043 .049	2.79 2.82 2.78 2.80 2.79 2.61
Prop. No.4 D = 1.74 in. r_h = 0.41 in. P/D= 1.73	.936 .818 .702 .585 .468 .351	.346 .462 .475 .449 .402 .348	.010 .014 .024 .076 .034 .043	3.47 3.18 3.00 2.86 2.79 2.61
Prop. No.5 D = 1.72 in. r_h = 0.40 in. P/D= 1.97	.936 .818 .702 .585 .468 .351	.488 .540 .514 .480 .428 .376	.020 .034 .036 .036 .052 .051	3.45 3.38 3.29 3.20 3.42 3.25
Prop. No.6 D = 1.74 in. r_h = 0.42 in. P/D= 2.06	.936 .818 .702 .585 .468 .354	.316 .445 .513 .474 .439 .372	.011 .016 .026 .030 .036 .037	3.65 3.53 3.59 3.46 3.49 3.41

a) ⊄

a)   Nozzle No. 1

b) ⊄

b)   Nozzle No. 2

Figure 18   Cross Sections of Aluminum Nozzles
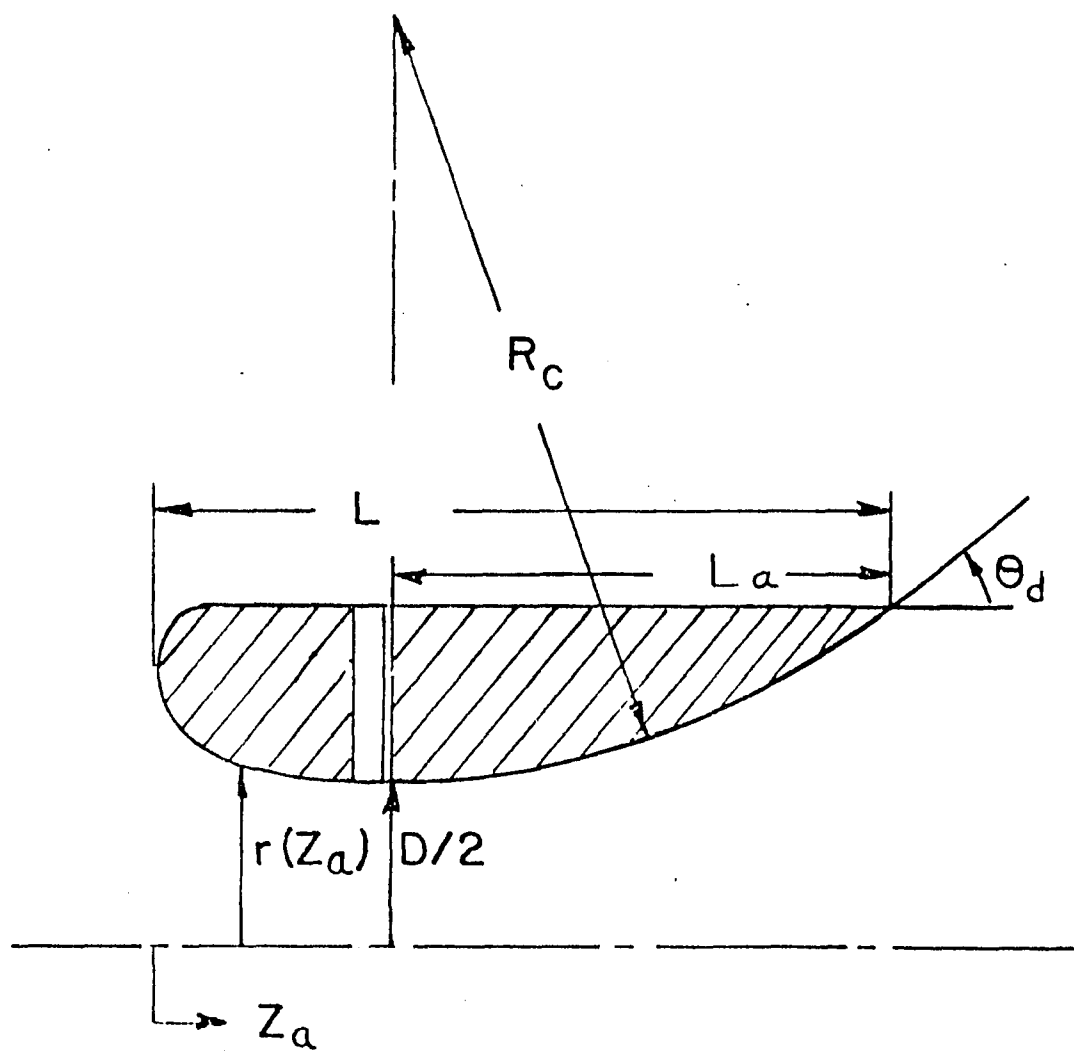
Figure 19   Identification of Nozzle Geometric Parameters

TABLE 3

DESCRIPTION OF WAX NOZZLES

Nozzle Numbers	θ_d (Degrees)	R_c/D	L_a/D
Series A			
A1	12.5	5.28	1.14
A2	19.4	3.43	1.14
A3	22.9	2.93	1.14
A4	28.1	2.43	1.14
A5	31.5	2.19	1.14
Series B			
B1	12.5	2.19	0.47
B2	19.4	2.19	0.72
B3	22.9	2.19	0.85
B4	28.1	2.19	1.02
B5	31.5	2.19	1.14

D = 1.75 inches

4-C Dimensionless Numbers

To reduce the number of parameters to be varied in
the testing and nondimensionalize the data, some dimensionless
numbers are developed in this section.

For a given propeller and nozzle design, it can be shown
that the thrust, torque and pressure difference between the inside
and outside shroud surfaces of the nozzle are a function of the

velocity of the nozzle relative to the fluid.

That is:

Thrust $= F = g_1(V,n,D,\rho,\mu)$

Torque $= Q = g_2(V,n,D,\rho,\mu)$

$P_s - P_a = P = g_3(V,n,D,\rho,\mu,Z_a,\theta)$

where V = velocity of nozzle relative to fluid.

n = propeller rotational speed (rev/sec).

ρ = density of the fluid.

μ = viscosity of the fluid.

P_s = pressure at any point (Z_a,θ) inside the shroud.

P_a = ambient pressure of the fluid outside the shroud.

Z_a = distance from the shroud entrance.

θ = angle measured ccw from the control port.

A dimensional analysis yields:

$F/\rho n^2 D^4 = \phi_1(V/nD, \rho nD^2/\mu)$

$Q/\rho n^2 D^5 = \phi_2(V/nD, \rho nD^2/\mu)$

$P/\rho n^2 D^2 = \phi_3(V/nD, \rho nD^2/\mu, Z_a/D, \theta)$

This is one set of dimensionless numbers; others are also possible.

In most submersible and ship designs, Reynolds number is very high so that the flow is essentially turbulent and independent of Reynolds number. In the testing program, Reynolds number based on tip speed $= \rho nD^2/\mu$, varied from $1.00(10)^5$ to $3.75(10)^5$ over the range of propeller speeds of interest indicating operation in a turbulent regime. In addition, the cavitation number based on tip speed $= 2(P_a - P_v)/(\rho n^2 D^2)$, where P_v

is the fluid vapor pressure, has a minimum value of 1.63 which is large enough to ensure that propeller cavitation is not occurring in the tests. Hence, the dimensionless equations can be simplified to

$$F/\rho n^2 D^4 = \emptyset_1 (V/nD) \tag{4.1}$$

$$Q/\rho n^2 D^5 = \emptyset_2 (V/nD) \tag{4.2}$$

$$P/\rho n^2 D^2 = \emptyset_3 (V/nD, Z_a/D, \theta) \tag{4.3}$$

where $F/\rho n^2 D^4$ = coefficient of thrust, K_T

$Q/\rho n^2 D^5$ = coefficient of torque, K_Q

$P/\rho n^2 D^2$ = coefficient of pressure, K_p

V/nD = coefficient of advance, J

as defined by previous researchers on nozzled propellers. [23-28]

The ratio of the radial (K_{TR}) to axial (K_{TA}) coefficients of thrust is a measure of the ability of the WSN to produce steering moments on a vessel and will be defined as the steering ratio

$$K_{TR}/K_{TA} = \text{steering ratio, } K_{TR-A}$$

In practice, we would want this ratio to be as large as possible. The radial thrust obtained from the WSN is dependent on the axial thrust developed. Therefore, by maximizing this ratio, we minimize the space required for a submersible to turn thus increasing its maneuverability.

Another parameter of equal importance is the thrusting efficiency η of the WSN. This can be expressed in terms of the nondimensional coefficients as

$$\eta = \frac{J\, K_{TA}}{2\pi K_Q} \tag{4.4}$$

Since in this chapter we are concerned only with tests on the WSN at zero forward velocity, the advance coefficient was zero throughout. Thus the thrust coefficient and pressure coefficient distribution along the nozzle inside surface characterize the static performance of a given WSN.

4-D Preliminary Experimental Investigation

The axial and radial thrusts of aluminum nozzles No.1 and No.2 using propeller No.2, were measured with a control port open and closed. Analysis of the thrust data reveal that the thrust very nearly varies with the square of propeller speed as was expected from the dimensional analysis. This is evident in Figure 20. The results also revealed that an angular displacement θ_r of the radial thrust vector relative to the open port occurs. The rotation occurs in the direction of propeller rotation according to Figure 21.
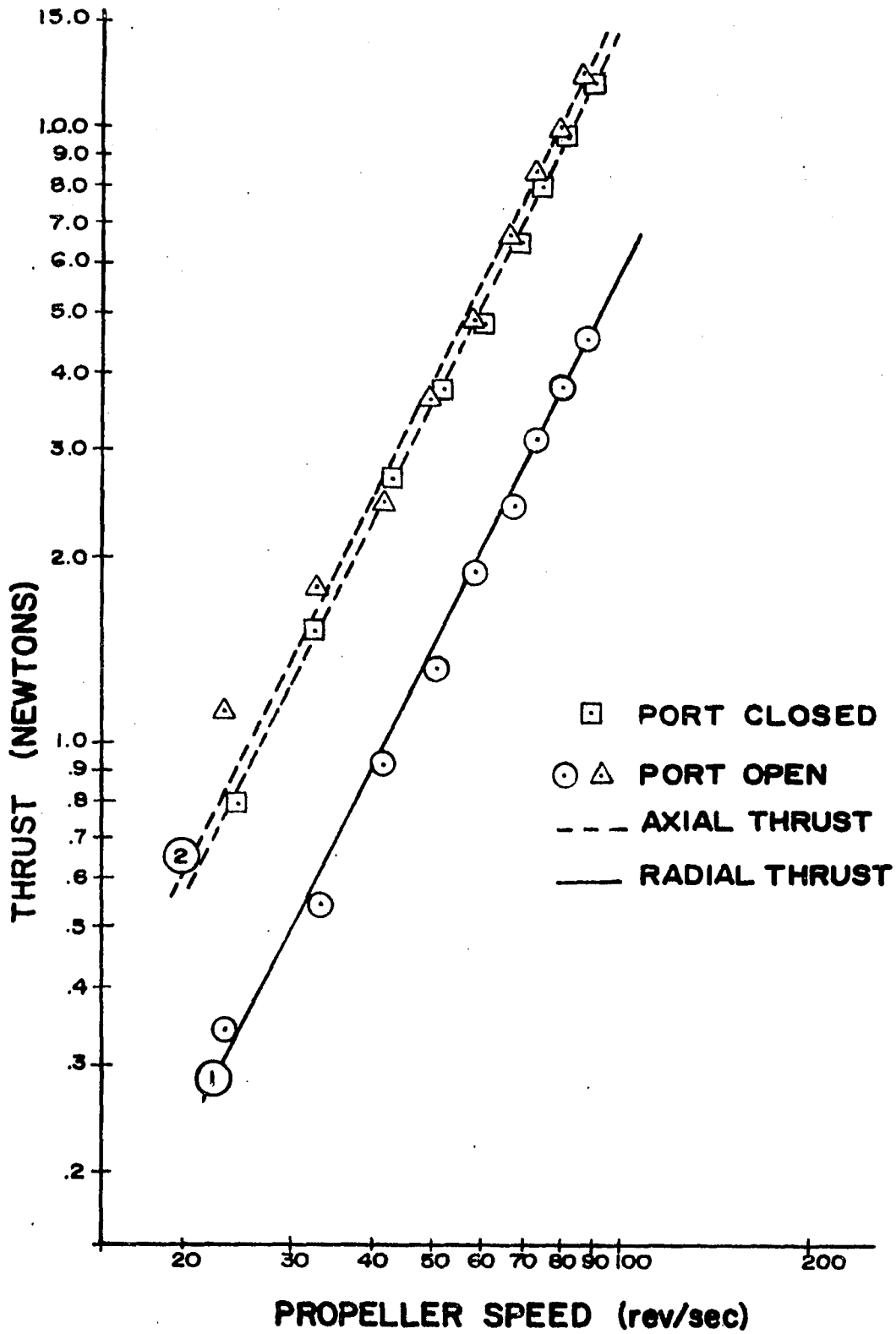
Figure 20 Thrust Versus Propeller Speed for Nozzle No.2
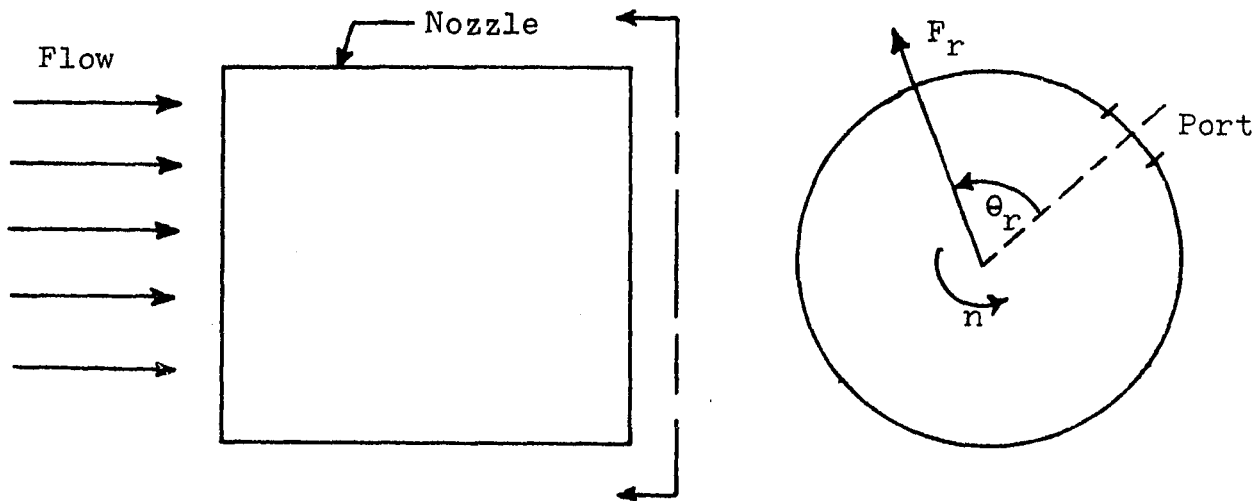
Figure 21   Rotation of the Thrust Vector

The relative angle of the thrust vector decreases only slightly with propeller speed. The results are summarized in Table 4.

TABLE 4

THRUST COEFFICIENTS FOR NOZZLE NO.1 AND NO.2

Nozzle	K_{TA}	K_{TR}	K_{TR-A}	θ_r	
				25 rev/sec	90 rev/sec
No.1	.71	.38	.54	22.4	18.0
No.2	.79	.28	.36	35.2	33.5

Moments about the three mutually perpendicular axes
of nozzle No.2 were measured. These were found to be small and
insignificant when compared with vessel turning moments produced
by nozzle radial thrust and propeller torque. The measurement of
the moments revealed that the point of location of the thrust
vector was inside the aft section of the nozzle at Za/L = .84
and that the variation in location of this vector was less than
$\pm$ 3.8% over the full range of propeller speed. (See Reference 32).
Hence, the errors in vessel turning moments which occur due to
variation in the location of the radial thrust vector will be
small. In view of this, it was decided to discontinue making
moment measurements.

A set of circumferential pressure taps at each of
five axial locations along the inside surface of nozzle No.1
enabled the pressure to be measured during operation. Measure-
ments were made for both the port closed and port open modes of
operation. The pressure coefficient K_p was computed and plotted
versus angular position with respect to the control port for
each normalized axial location Z/L. The plots for the port closed
and port open cases are shown in Figures 22 and 23 respectively.
The port is located at an axial position Z/L of .39 to .45. The
axial location of the propeller is such that the trailing edge
of the propeller is flush with the leading edge of the port. It
is apparent from Figure 22, in which the values of K_p at each axial
location do not change with angular position, that the wake flow
is symmetric with respect to the propeller axis. Thus, no radial
force is being produced. Opening the port results in separation

of the wake downstream of the port, producing a radial thrust
in the approximate direction of the port. This is evident by
comparatively higher (near zero) values of K_p in Figure 23. Note
that the pressures ahead of the propeller plane (Za/L = .12) and
in the vicinity of the propeller plane (Za/L = .31) are not ap-
preciably affected. The slight antisymmetrical distribution in
the pressure coefficient about the port in Figure 23 is attributed
to the rotational motion imparted to the fluid by the propeller.
This accounts for the measured rotation of the radial thrust
vector for nozzles No.1 and No.2 given in Table 4.

From the data on WSN No.1 and No.2 in Table 4, nozzle
No.1 appears to be the best choice as a propulsion-steering
device since it has an appreciably higher steering ratio while
producing almost the same axial thrust. However, there is ano-
ther important factor to be taken into consideration.

Observation of separation and reattachment of the
wake from inside nozzle No.1 and No.2 revealed an inconsistancy
in the behavior pattern of the wake. The wake from nozzle No.2
remained attached to the inside surface except when a port was
opened, at which time it would switch, producing a radial force.
The wake would reattach when the port was closed. Nozzle No.1
followed the same pattern except that the wake would not reattach
after the port was closed. Instead the wake from nozzle No.1
would remain separated and oscillate in an erratic manner and
would not reattach unless the propeller speed was reduced. This
necessitated a means for interpreting the reliability of the WSN.
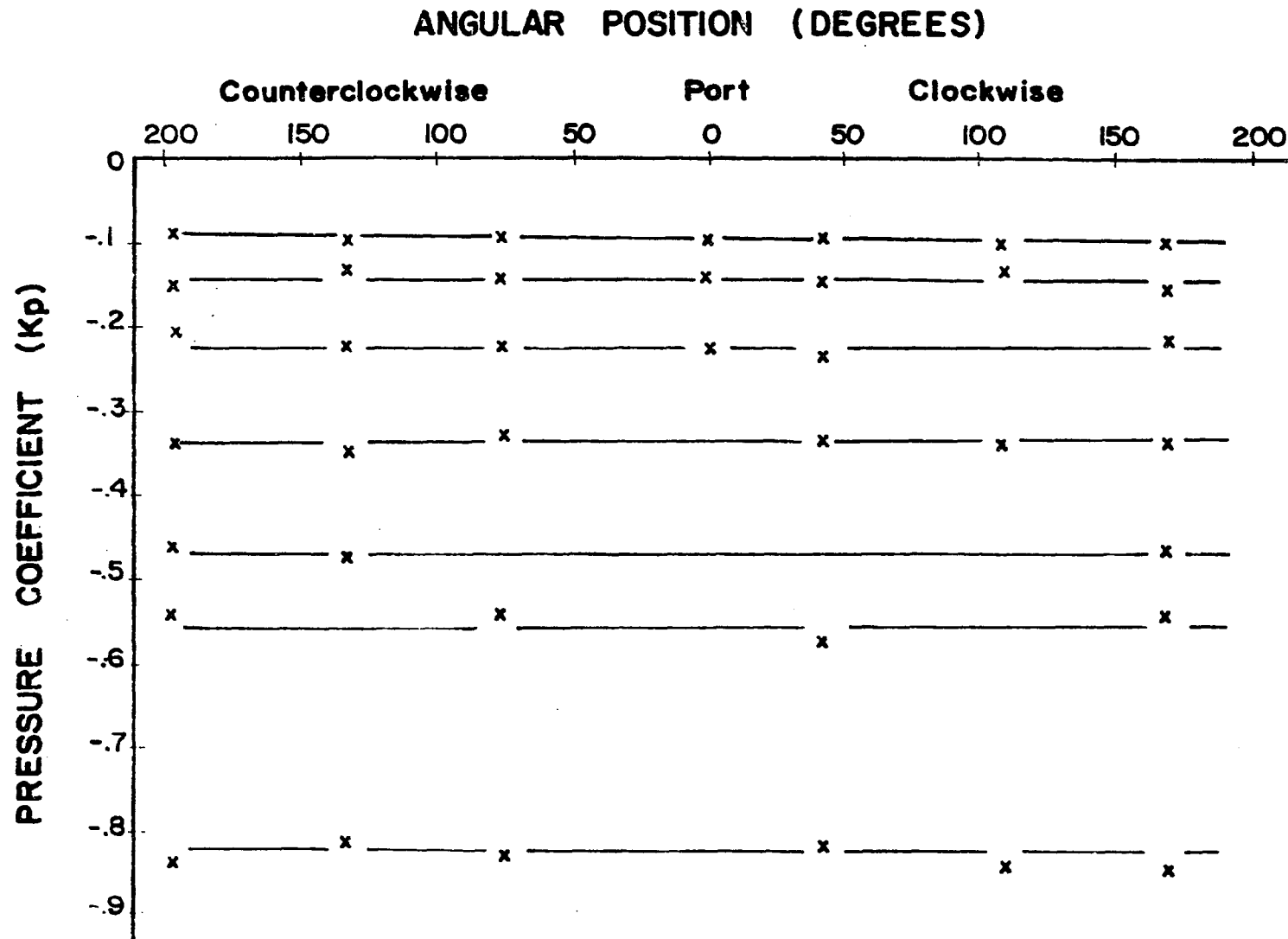
Figure 22   Closed Port Pressure Distribution for Nozzle No.2

ANGULAR POSITION (DEGREES)
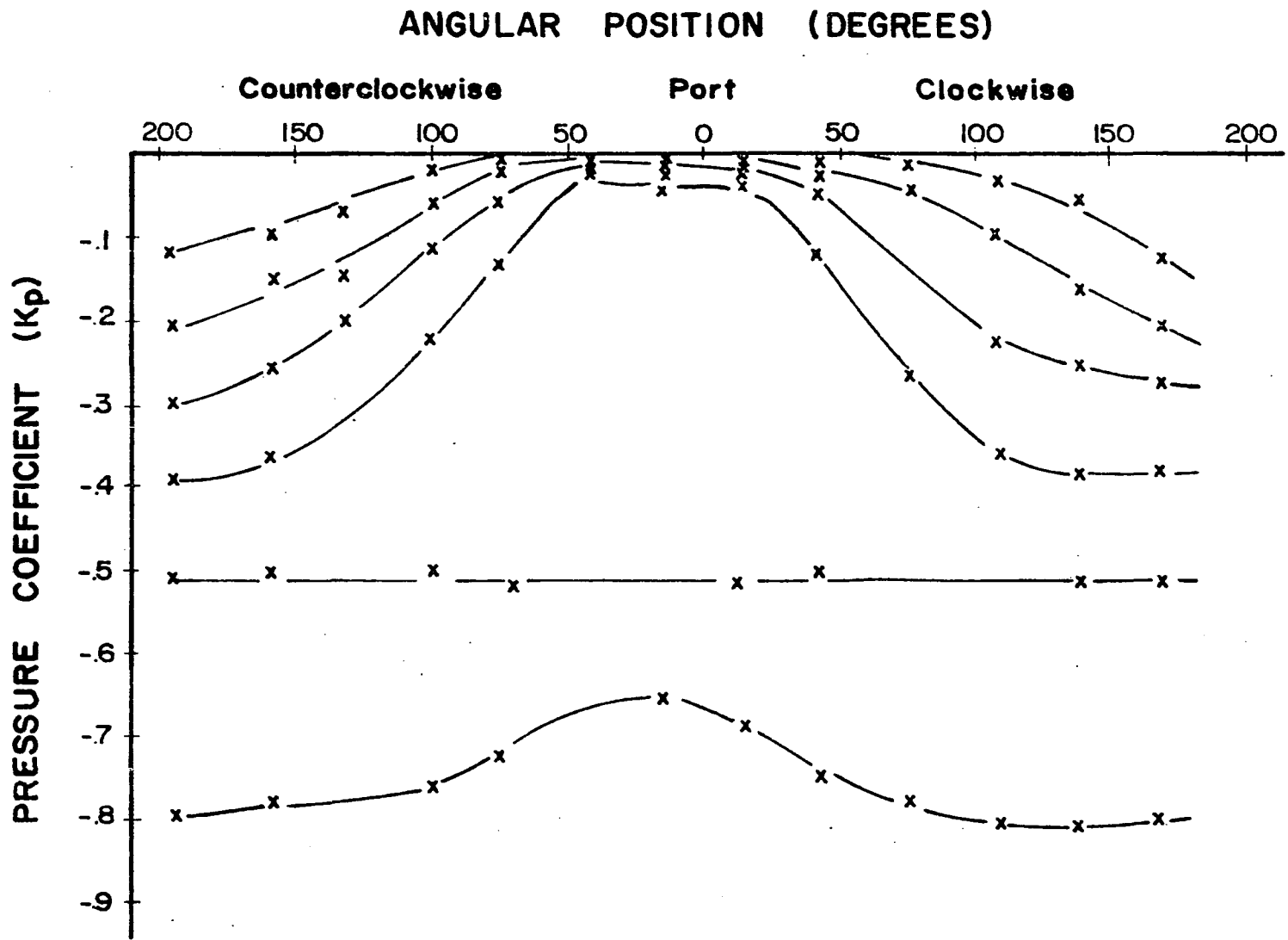
Figure 23 Open Port Pressure Distribution for Nozzle No.2

To be reliable, a WSN must develop a radial force when
a control port is open. This force must disappear when the port
is closed. Allowances are made for the transition time or time for
the flow field to re-establish after a port has been opened then
closed. A WSN is defined as reliable if the transition time is
less than 3 seconds, marginally reliable if it is greater than 3
seconds and unreliable if the time is greater than 15 seconds or
if the wake separates when the port is not opened.

It should also be pointed out that some circumferential
separation of the flow at the trailing edge of both nozzles was
observed using flow visualization techniques. This separation was
much more pronounced in nozzle No.1 than for nozzle No.2. In pre-
liminary tests on nozzle A3, a long streamlined hub was added. It
was found that the addition of this hub created or promoted sepa-
ration of the flow at the trailing edge to the point where the
shroud operated unreliably.[33] Two models were sketched from obser-
vations of the flow field using air bubbles and streamers entrained
in the flow. Figures 24(a) and 24(b) depict the flow field of a
WSN without the hub and with the hub, respectively. One plausible
explanation for this behavior is that the hub provides a smooth
continuous surface for the flow near the propeller axes to follow.
Thus the fluid velocity with the hub is greater along the propeller
axis and lower along the shroud surface. The resulting lower momen-
tum of the fluid at the shroud surface causes separation to occur
earlier in the flow. It was also observed for some nozzles that
increasing vibration by removing the dampers improved nozzle
reliability.[32, 33]

a)   Without Propeller Hub

b) With Propeller Hub
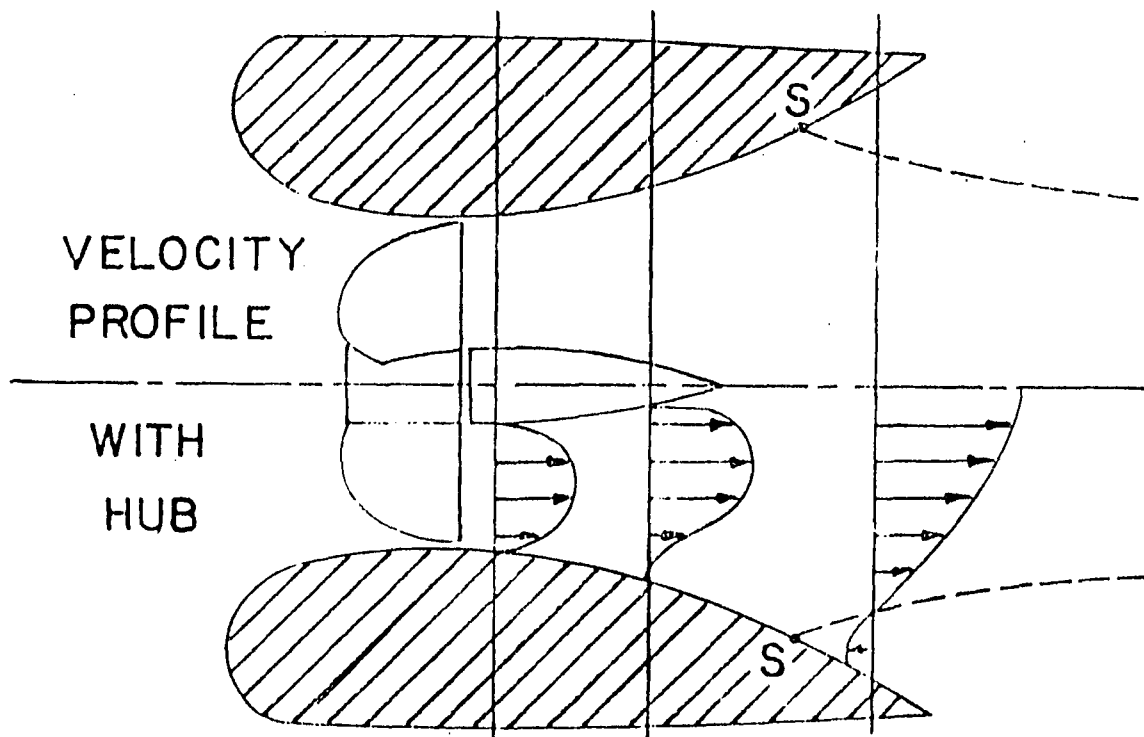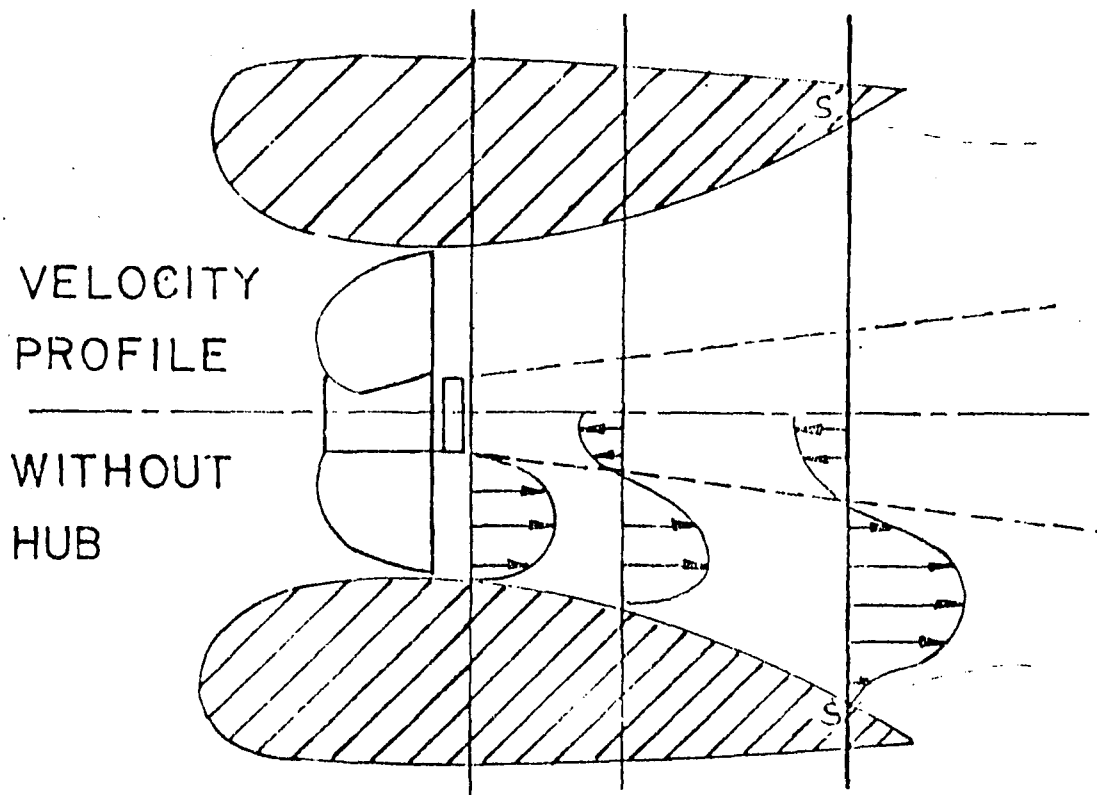
Figure 24   Flow Field of the Wake Steering Nozzle

4-E   Analytical Modelling of the Nozzle Flow Field

The experimental work in the previous section gives
some indication of the complexity of the flow field of the WSN.
To assist us in our investigation of the WSN, the development of
a mathematical model capable of describing the flow field of the
WSN was considered.

The problem of mathematically modelling the flow field
in and around conventional shrouded or nozzled propellers is
difficult. Some hydrodynamic models have been developed but in
spite of their sophistication, agreement with the test results
over a range of operating conditions has only been fair.[26-28] In
addition, these models are valid only for axisymmetric flows and
therefore apply only to the port closed case. Still, the possi-
bility of using these analyses to predict the pressure distribution
along the inside of the of the nozzle surface was considered. By
designing the nozzle shape aft of the propeller plane to have as
negative a pressure distribution as possible, it was felt that a
maximum radial thrust could be produced. According to Figure 23,
the pressure downstream of the port is essentially ambient for the
open port case, thus, by making the pressure distribution as negative
as possible, a large radial thrust should result when the control
port is opened.

In axisymmetric hydrodynamic models developed in the
literature, the approach used is to model the flow by means of a
distribution of ring vortices and ring sources.[26-28] Most of these

models are based on linear theory which means the ring vortices
and sources lie along a cylinder and the model is only valid for
shroud shapes which do not deviate greatly from a cylindrical
shape. It is also assumed that the flow does not separate from
the nozzle.

The preceeding two assumptions limit the applicability
of the models since most of the shrouds investigated herein deviate
substantially from a cylindrical shape and exhibit some separation
along the trailing edge. Aside from these considerations the utility
of the pressure predictions for the closed port case as a means of
maximizing the radial thrust is questionable. This is apparent from
the pressure plots in Figure 25.

Figure 25 is a plot of the pressure coefficients as a
function of axial location for nozzles No.1 and No.2 with all ports
closed. Since the pressure distribution is axisymmetric, the pres-
sure coefficient is a function of axial location alone. Comparing
the two profiles, it is not obvious that the open port radial
thrust of nozzle No.1 would be about 40% greater than for nozzle
No.2 as indicated in Table 4. The length of the shroud aft of the
propeller plane is almost the same for each nozzle: 2.22 inches for
No.1 versus 2.06 inches for No.2. The magnitude of the pressures
in the vicinity of the ports is almost the same while the pressure
downstream of the ports is even more negative for nozzle No.2 than
for No.1, leading one to believe that No.2 would produce a greater
radial thrust. Thus, the port closed pressure distribution is of
little use in predicting WSN radial thrust.
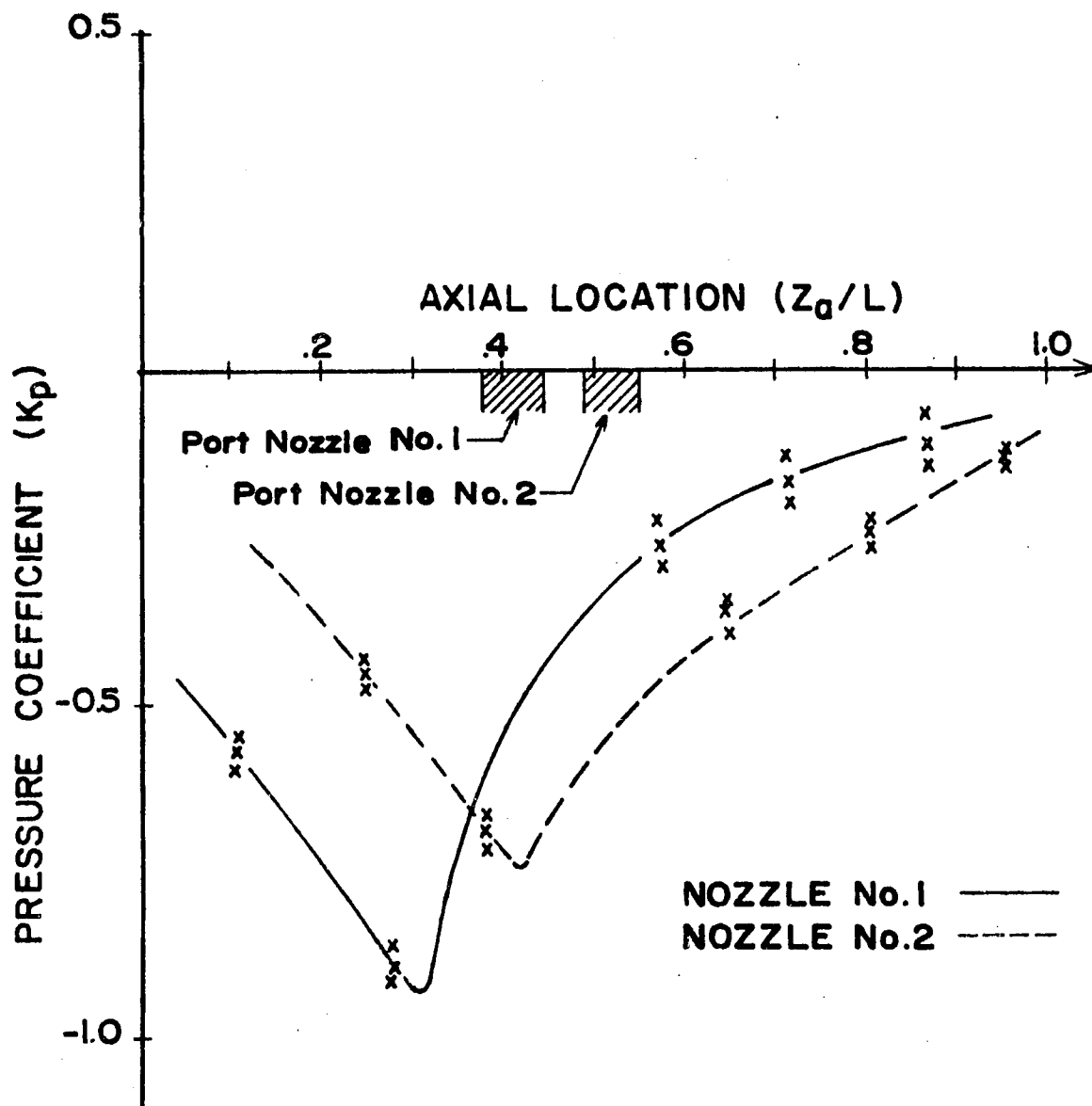
Figure 25   Port Closed Axial Pressure Distribution for

Nozzles No.1 and No.2 with Propeller No.2

It would appear then, that to be of any real benefit, the mathematical model used must be capable of modelling the flow field with the port open. Because of the immense mathematical difficulties posed by the non-symmetric and separated nature of such flow, both within and around the outside of a shroud operating in this mode, it was felt that a useful hydrodynamic model was not within the scope of this project based on the resources and time available. It was therefore decided to concentrate our efforts on experimentally evaluating and developing the wake steering nozzle. Certainly, if the concept proves feasible and highly applicable, then one of the next steps should involve both extensive theoretical and experimental work.

4-F   Experimental Investigation of Major Parameters

The preliminary tests revealed that to develop a high radial thrust requires shrouds of comparatively high divergence. However, separation and thus reliability becomes a problem with the more divergent shrouds. Clearly a trade-off exists between the two conflicting divergence requirements of small divergence for no separation and large divergence for useful deflection of the flow in the steering mode. It was our objective in this set of tests to determine this trade-off and how it is affected by propeller pitch and nozzle length. Previous researchers, principally Van Manen,[24-25] have shown propeller type and nozzle length to be highly significant factors affecting nozzle- propeller performance.

The arc of a circle was chosen to describe the nozzle aft section. The circle was chosen because it is easier to standardize than for example, a parabola. Also it turns out that the arc of a circle is a good approximation for the inside surface of nozzle No.1 and No.2 tested previously. The divergence angle of the nozzles was then varied by simply varying the radius of curvature R_c shown in Figure 19. This generated nozzle series A. Nozzle series B was generated by cutting the most divergent shroud in series A to various lengths to generate the same divergence angles as series A. These two series, described in Table 3, were tested over the complete range of propeller pitch given in Table 2. The data from these tests is presented in Table 5 and Table 6.

The values of K_{TA} in Tables 5 and 6 are based on the axial thrust measured with the port closed and the wake flow symmetrical such that no radial thrust is produced. The absence of measurements of K_{TA} in the tables indicates that this state did not exist. A small decrease between the port open and port closed values of K_{TA} was observed for nozzles which were reliable and marginally reliable (1-5%). For unreliable nozzles where the wake failed to reattach when the port was closed, K_{TA} increased slightly.[32, 33]

TABLE 5

EFFECTS OF MAJOR PARAMETERS ON NOZZLE PERFORMANCE

CHARACTERISTICS — SERIES A

Nozzle	$R_{c/D}$	$L_{a/D}$	$P_{/D}$	K_{TA}	K_{TR}	$K_{TR/A}$	θ_r	Rel*
A1	5.28	1.14	1.24	.417	.053	.127	40.5	R
			1.41	.614	.104	.169	44.9	R
			1.64	.607	.067	.110	47.4	R
			1.73	.807	.092	.114	55.2	R
			1.97	.942	.098	.104	57.0	R
			2.06	.907	.080	.088	61.3	R
A2	3.43		1.24	.380	.070	-	33.8	U
			1.41	.578	.138	.239	37.5	R
			1.64	.566	.133	.235	40.4	R
			1.73	.751	.175	.233	42.4	R
			1.97	.891	.177	.199	55.1	R
			2.06	-	.192	-	48.0	U
A3	2.93		1.24	.352	.101	-	35.5	U
			1.41	.542	.186	.343	35.8	R
			1.64	.498	.168	.337	47.0	M
			1.73	.713	.228	.320	34.7	R
			1.97	.833	.216	-	48.1	U
			2.06	-	.214	-	50.4	U
A4	2.43		1.24	.339	.128	-	33.0	U
			1.41	.518	.193	.373	31.8	M
			1.64	.524	.204	.389	34.6	M
			1.73	.670	.242	.361	34.5	M
			1.97	.733	.236	-	41.1	U
			2.06	-	.247	-	45.9	U
A5	2.19		1.24	.326	.152	-	27.8	U
			1.41	.492	.243	.494	30.7	M
			1.64	.479	.241	.503	33.6	M
			1.73	.619	.312	.504	36.2	R
			1.97	.735	.332	-	41.0	U
			2.06	-	.305	-	42.3	U

*Reliability: R = reliable, M = marginally reliable, U = unreliable

TABLE 6

EFFECTS OF MAJOR PARAMETERS ON NOZZLE PERFORMANCE

CHARACTERISTICS — SERIES B

Nozzle	R_c/D	L_a/D	P/D	K_{TA}	K_{TR}	$K_{TR/A}$	θ_r	Rel*
B1	2.19	0.47	1.24	–	.035	–	27.6	U
			1.41	–	.051	–	28.3	U
			1.64	–	.054	–	26.9	U
			1.73	–	.059	–	27.8	U
			1.97	–	.082	–	33.4	U
			2.06	–	.079	–	33.7	U
B2		0.72	1.24	–	.102	–	25.9	U
			1.41	–	.112	–	27.0	U
			1.64	–	.168	–	29.8	U
			1.73	–	.211	–	31.5	U
			1.97	–	.259	–	32.7	U
			2.06	–	.223	–	36.6	U
B3		0.85	1.24	–	.130	–	28.2	U
			1.41	.599	.183	–	28.0	U
			1.64	.609	.207	–	29.8	U
			1.73	.702	.224	–	31.5	U
			1.97	–	.307	–	32.8	U
			2.06	–	.256	–	36.4	U
B4		1.02	1.24	.351	.144	–	26.5	U
			1.41	.521	.194	.372	31.2	M
			1.64	.524	.216	–	34.1	U
			1.73	.678	.263	.388	35.9	M
			1.97	.802	.307	–	37.6	U
			2.06	–	.274	–	36.7	U
B5		1.14	1.24	.326	.152	–	27.8	U
			1.41	.492	.243	.494	30.7	M
			1.64	.479	.241	.503	33.6	M
			1.73	.619	.312	.504	36.2	R
			1.97	.735	.332	–	41.0	U
			2.06	–	.305	–	42.3	U

*Reliability: R = reliable, M = marginally reliable, U = unreliable

The data in Tables 5 and 6 reveal some general
trends:

Axial thrust   - decreases with nozzle divergence.

                     - decreases with nozzle length.

                     - increases with propeller pitch to diameter ratio.

Radial thrust   - increases with nozzle divergence.

                     - increases with nozzle length.

                     - exhibits a slight maximum when plotted against propeller pitch to diameter ratio.

Steering ratio   - increases with nozzle divergence.

                     - remains almost constant with propeller pitch to diameter ratio.

Thrust angle   - decreases slightly with nozzle divergence.

                     - remains almost constant with nozzle length.

                     - increases with propeller pitch to diameter ratio.

Reliability   - decreases with nozzle divergence.

                     - increases with nozzle length.

                     - appears greatest for propellers which are "mid-range" in terms of pitch to diameter ratio.

4-G Summary

The performance of the WSN at zero forward velocity was investigated. The preliminary tests revealed that the radial thrust of the WSN could be increased by increasing nozzle divergence. However, higher nozzle divergence resulted in an unreliable mode of operation where the wake remains deflected after closing the control port, producing an erratic radial thrust.

A further set of tests were conducted varying nozzle divergence and length and propeller pitch to diameter ratio to determine their effects on the thrusting and steering characteristics of the nozzle. A number of propeller-nozzle combinations were found which exhibited reliable or marginally reliable operation.

This set of shrouds is almost exclusively confined to the longer nozzles of series A. Nozzle A1 was the most reliable over all, as it worked well with all the combinations of propellers. However, for use as a steering device, it is the least desirable since it also produces the smallest steering ratio. According to the combined criteria of large steering ratio and reliable operation, nozzle A5 is the optimum choice.

The best propeller to use would appear to be propeller No.4 with $P_{D} = 1.73$ which operated most reliably. It should be be pointed out that the reliability of all the propellers was sensitive to the axial location of the propeller with the optimum

location of the propeller being at the point where the trailing edge of the propeller was flush with the leading edge of the port. Propeller location became more critical as nozzle divergence was increased. Propellers No.2 and 3 also performed reasonably well. Propeller No.3 operated somewhat less reliably than No.2 and also produced a lower axial thrust. This could be due to the smaller diameter and therefore larger tip clearance of propeller No.3. (D = 1.70 inches versus 1.74 inches). Too large a tip clearance enables backflow around the tips of the propeller blades lowering propeller efficiency.[24]

The static tests have demonstrated that the concept is feasible, but much more information is required to enable an assessment of the potential of the WSN as a submersible propulsion-steering device. Most important is the effect of forward velocity on reliability and steering ratio. In addition, forward velocity data would enable the propulsion efficiency of the WSN to be compared to more conventional nozzled propellers.

CHAPTER V

FORWARD VELOCITY TESTING OF THE WAKE STEERING NOZZLE

5-A General

The previous chapter dealt with the experimental investigation of the static performance of the WSN. One of the prime requirements in evaluating any propulsion-steering system for marine vessels is a knowledge of its behavior over a range of forward velocities. This is true also for rescue submersibles where the typical rescue mission calls for a rapid transport leg between the mother ship and the site of the distressed submarine.

This chapter is concerned with evaluating the effect of forward velocity on the performance characteristics of the WSN identified in Chapter II, particularly the radial steering force, nozzle reliability and an additional performance para- meter, the efficiency of the WSN as a thruster. Two nozzles from the static tests, nozzles A2 and A3, were chosen for evalua- tion with a number of propeller types over a range of forward velocities. These nozzles were chosen because they were about "mid-range" in terms of reliability and steering force in the static tests, thus enabling a shift in either direction in their performance characteristics to be detected. A forward velocity tunnel and measurement system were designed and constructed to enable these tests to be carried out. The shrouds used were manufactured out of aluminum and streamlined to reduce the fluid drag forces. Some preliminary tests were also conducted to

investigate controlling the wake separation to produce a propor-
tionally controlled steering force by locating several ports
axially along the shroud surface downstream of the propeller.

5-B   Forward Velocity Test Facility

To simulate forward velocity, a water tunnel was desig-
ned and constructed by Hudson and Wilson.[34] The tunnel consisted
of an open channel (2 feet high x 1 foot wide). For a water depth
of 1 foot, the system is capable of producing water velocities
of up to 4 feet/second based on a miximum pump capacity of 2000
gallons/minute. Water enters the channel, shown in Figure 26,
through a pipe. To minimize entrance effects and straighten the
flow downstream, a short section at the beginning was fitted with
screens and a honeycomb mesh of small tubing. Preliminary testing
of the water tunnel revealed that the axial flow velocity down-
stream of this section is nearly uniform, varying at most $\pm$ 5%
across the channel, except at points very near the channel walls
and water surface.[34] The sides of the channel were constructed
out of plexiglass to enable the use of flow visualization tech-
niques.

The nozzles tested were constructed out of aluminum
and the outside surface streamlined to minimize drag and inhibit
flow separation. Figure 27 shows the basic WSN configuration used
in forward velocity tests. Three nozzles were constructed having
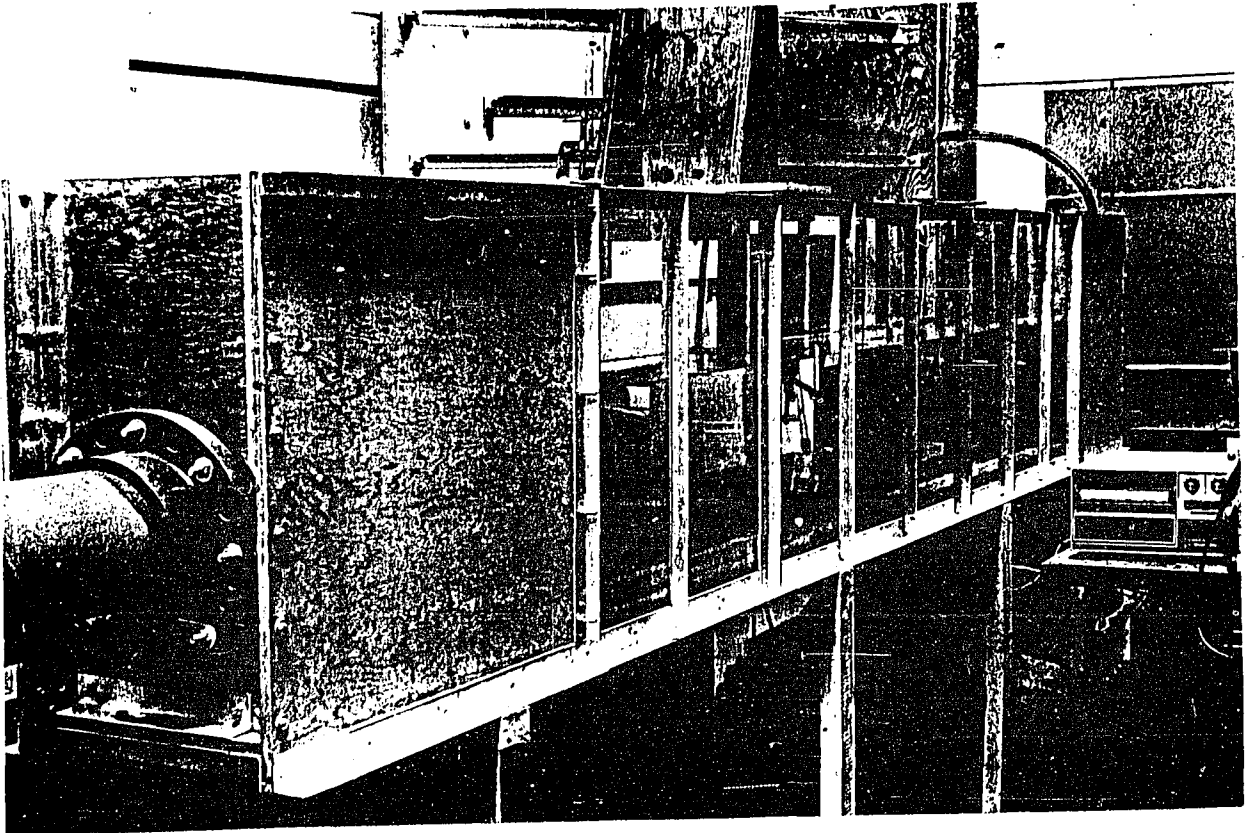
Figure 26   Water Channel Used for Testing Forward Velocity
Nozzles
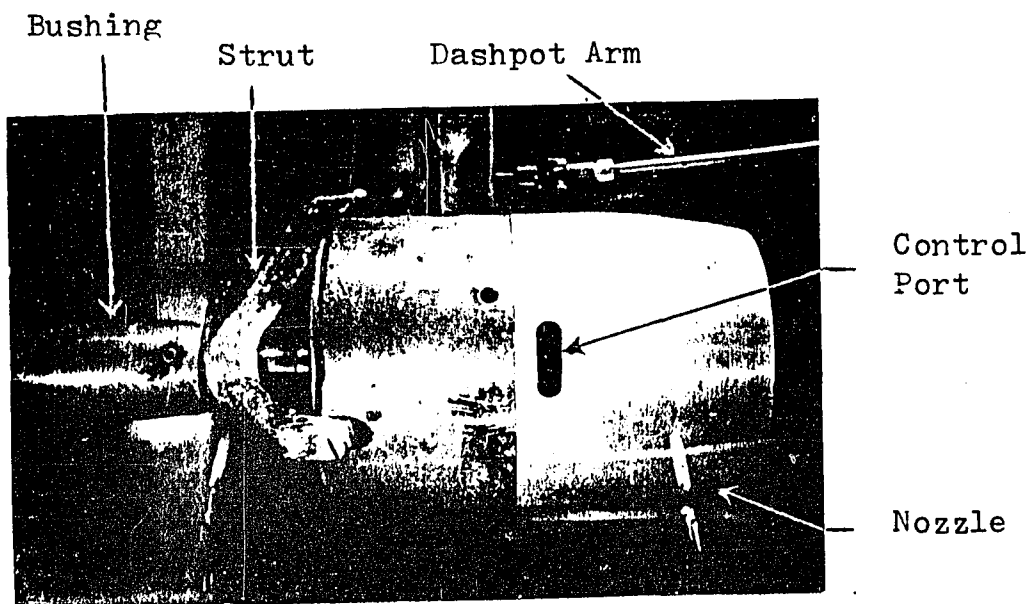
Figure 27 The Basic Configuration of the Wake Steering Nozzles

the same inside shapes as nozzles A2, A3 and A4 used in the static
tests. The front section of these nozzles is the same for all three,
and only the aft sections were varied. This was accomplished by
providing a tongue and groove type of fitting between the front
and aft sections enabling the aft sections to be easily changed
and providing a smooth surface between the two sections. The front
section of the test nozzle is shown to full scale in Figure 28(a).
The outside surface of the nozzle is cylindrical except for the
last 2.0 inches of the aft section which was streamlined by making
it converge. The convergence of the outside surface is described
by the arc of a circle as indicated in the schematic of Figure 28(b).
The numerical values for the geometric parameters describing the
nozzle aft sections are given in Table 7.

The radial and axial thrust, motor speed and propeller
torque were measured using the same basic system as in the static
tests except a streamlined strut was added to the dynamometer to
reduce the drag. The propeller bushings and struts were also stream-
lined.

Nozzle A3 with propeller No.2 is shown in operation
with all ports closed in Figure 29(a). Air bubbles injected up-
stream of the nozzle show that the wake flow is symmetrical about
the propeller axis. Figure 29(b) shows the degree of wake defection
when a port near the top of the shroud is opened.

$\mathcal{C}$

a) Front Section

$\mathcal{C}$

+

R_{co}

R_c

+
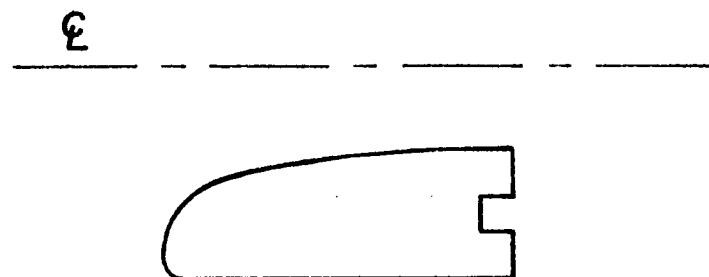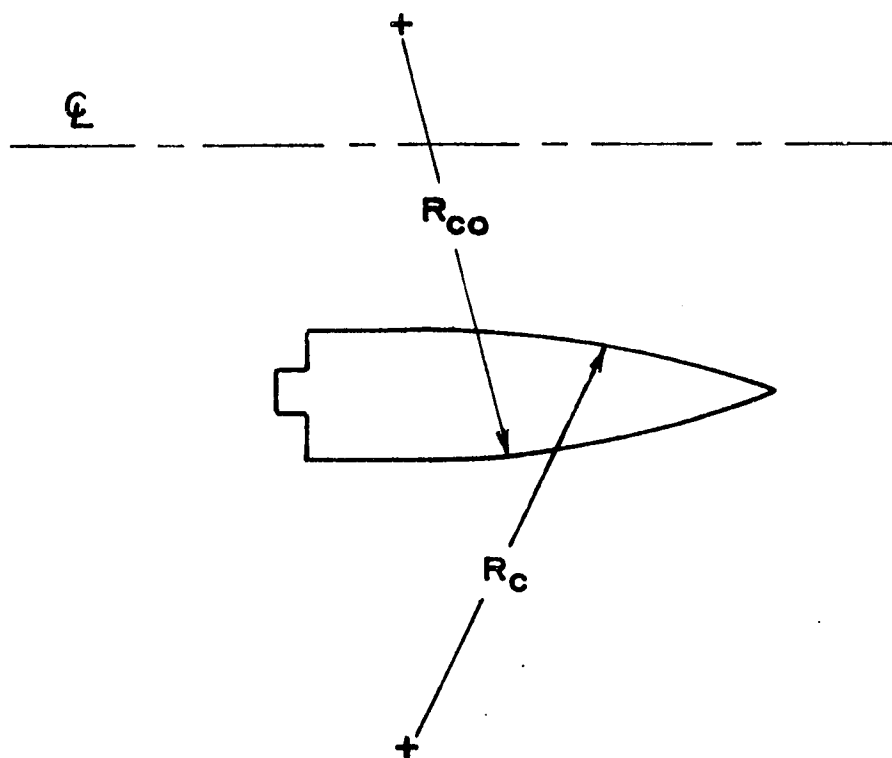
b) Aft Section

Figure 28 Geometric Parameters of the Forward Velocity
Wake Steering Nozzles
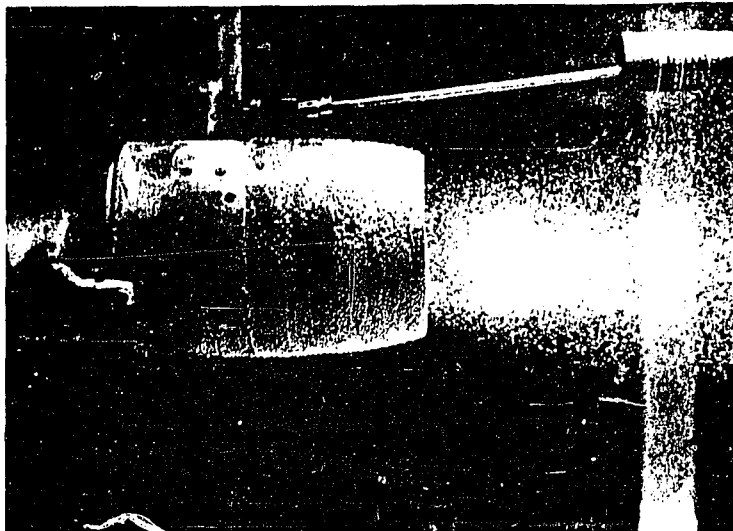
a)   All Ports Closed
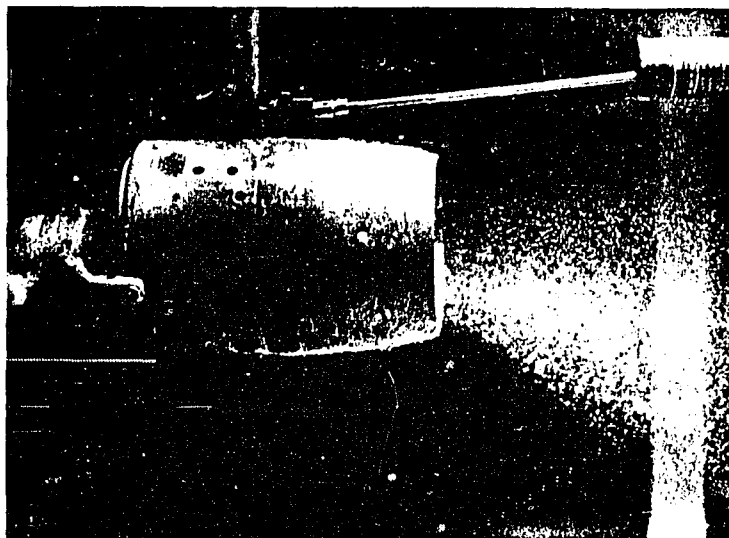
b)   Top Port Closed

Figure 29   Flow Pattern of Nozzle A3 with Propeller
            No. 2

TABLE 7

AFT SECTION SHAPES OF NOZZLES FOR FORWARD VELOCITY TESTING

Nozzles	L_a/D	R_c/D	R_{co}/D
A2	1.43	3.43	3.68
A3	1.43	2.93	4.72
A4	1.43	2.43	4.65

D = 1.75 inches

5-C Effect of Forward Velocity on WSN Performance Characteristics

The previous described test facility was used to evaluate the performance of nozzles A2 and A3 over a range of fluid velocities. Nozzle A4 was used in the investigation of radial force control. A representative variety of propeller types were selected from those used in the static tests. The propellers used for the forward velocity testing were numbers 1, 2, 4 and 5 and are described in Table 2. These two shrouds were tested by Hudson over a range of motor speeds from 23.6 rev/sec to 63.6 rev/sec and at tunnel velocities of from .69 ft/sec to 2.6 ft/sec. The results from the tests are represented in normalized form by plotting the axial thrust coefficient K_{TA}, radial thrust coefficient K_{TR} and efficiency η against the nondimensionalized velocity or advance coefficient J.[24]

Typical curves showing the spread of data points for
one nozzle-propeller combination, nozzle A3 with propeller No.4,
are shown in Figure 30. Figures 31 and 32 summarize the test
results for the complete series of propellers tested with nozzles
A2 and A3, respectively.

It should be pointed out that the values of axial
thrust coefficient are based on the values of system thrust
where the only drag force included is the drag of the shroud.
In other words, the dynamometer and propeller struts and bushing
are not considered part of the basic system and the drag of
these components was subtracted from the axial force before
calculating the axial thrust coefficient and WSN efficiency.
This is the same approach used by Van Manen and other resear-
chers in analyzing the performance of nozzled propellers.[23-25]
No difference between the drag forces of the nozzles could be
detected.[34] The axial thrust coefficient decreases with velo-
city or advance ratio as would be expected from basic propeller
theory.[57] The values of K_{TA} are based on thrust measured with
the control port closed. Axial thrust was observed to increase
slightly when a control port was opened. The increase was grea-
test for those shrouds which operated with a high degree of
circumferential flow separation from the inside shroud surface
at the trailing edge. Except for propeller No.4 operating in
nozzles A2 and A3, all combinations showed some degree of cir-
cumferential separation with all ports closed.

The radial thrust generally exhibits an increase with
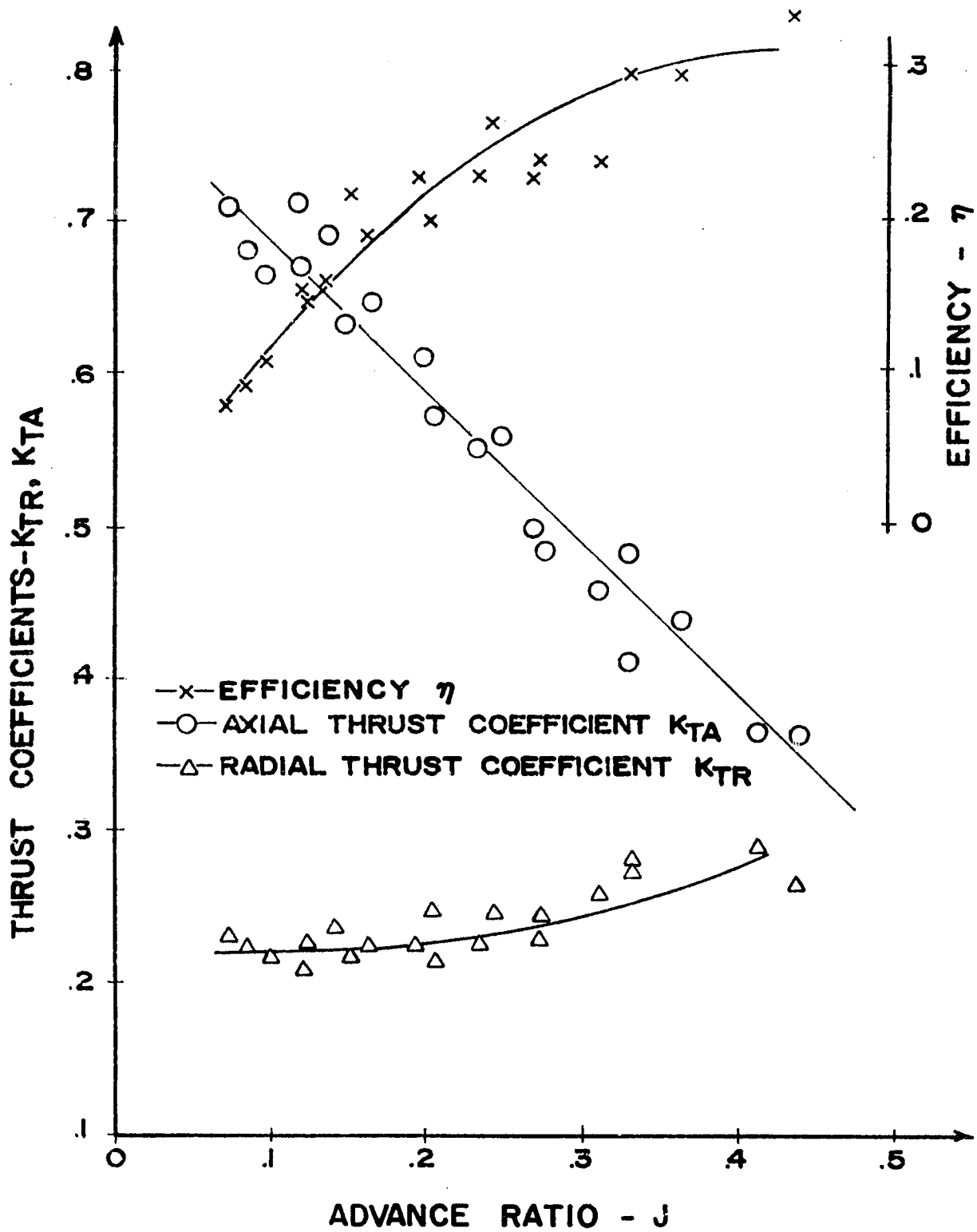
Figure 30   Forward Velocity Test Results for Nozzle A3 with
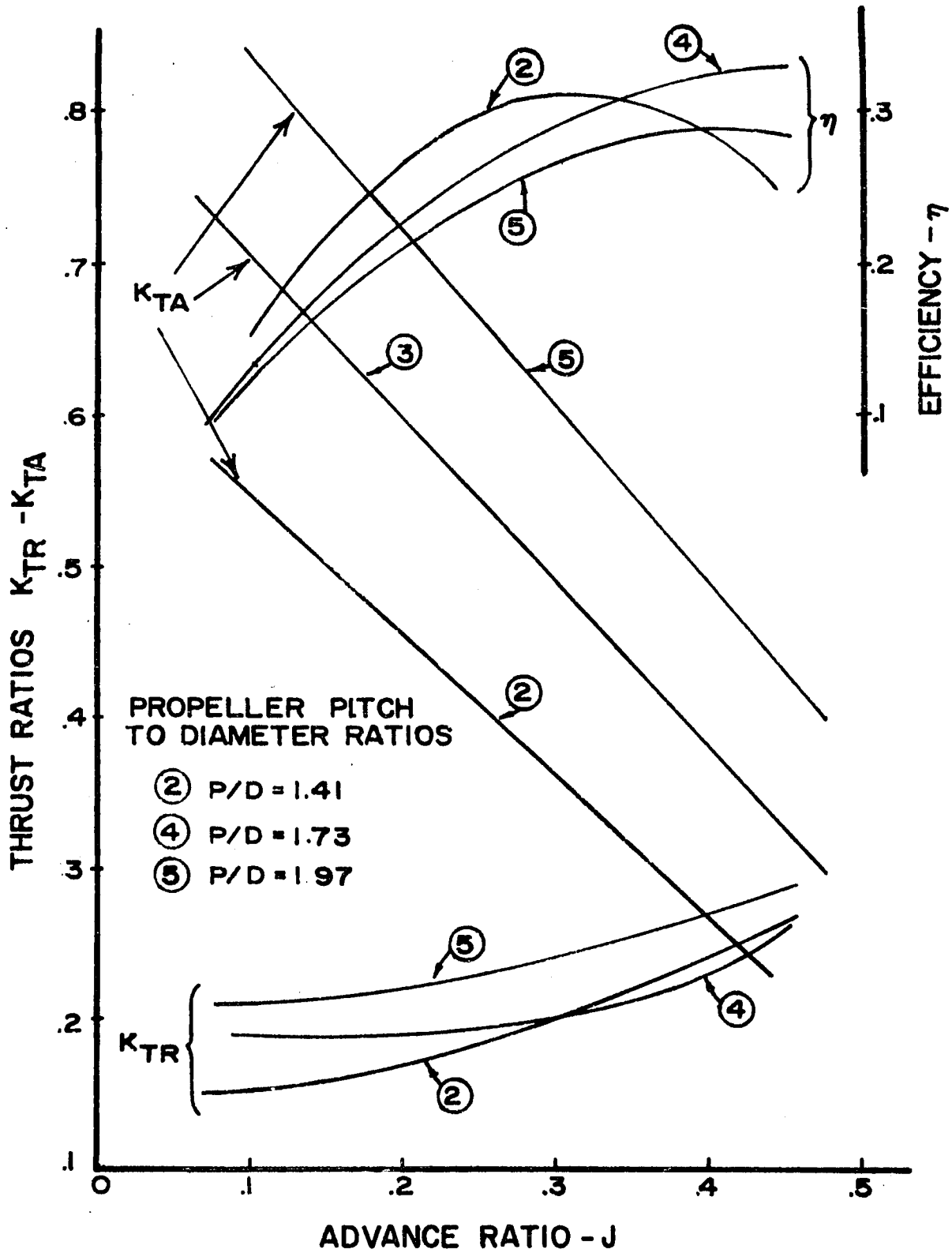
Propeller No.4

Figure 31   Forward Velocity Test Results for Nozzle A2 with
Propeller Nos. 2, 4 and 5
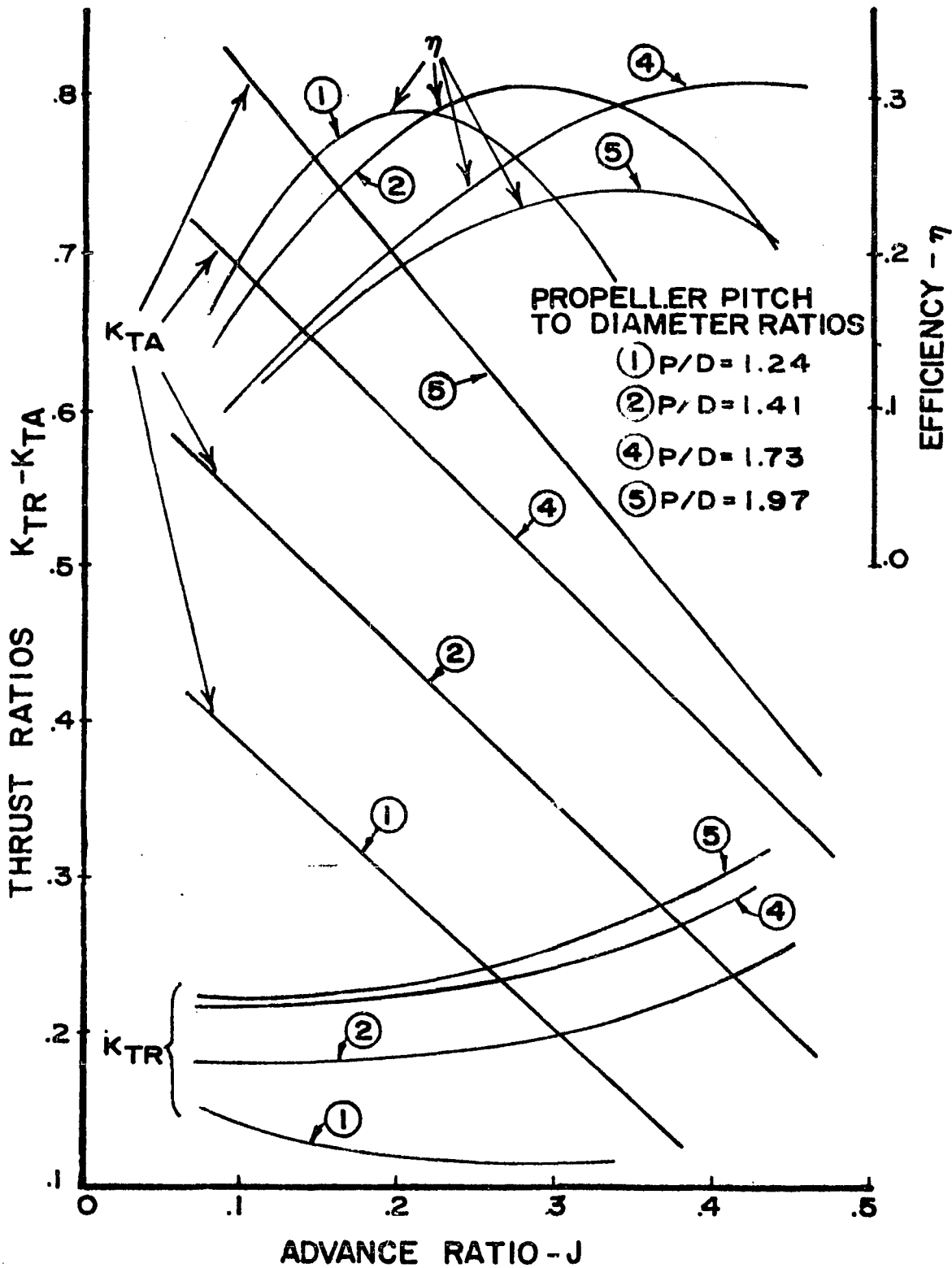
Figure 32   Forward Velocity Test Results for Nozzle A3
with Propeller Nos. 1, 2, 4 and 5

forward velocity as evident in Figures 31 and 32. This increase could be due to the observed rudder-like characteristics of the WSN. Tests conducted over a range of forward velocities on a nozzle without a propeller showed that the nozzle developed a small radial thrust which increased with forward velocity.[34] This increase is due to the fact that when a control port was opened, the flow through the shroud became assymetric causing a radial thrust on the shroud even with no propeller.

The only propeller-nozzle which did not show an increase in radial thrust with advance ratio was propeller No.1 operating in nozzle A3. Flow visualization techniques revealed that this combination was operating with the flow almost fully separated from the inside surface with all ports closed. This was a much higher degree of circumferential separation than was observed for any of the other combinations. This could account for the drop in radial thrust since previous pressure measurements revealed that the pressures were higher for separated flow. The reduced pressures would act to reduce control port flow and thus wake deflection.

All of the propeller-nozzle combinations worked reliably, that is they all produced a radial thrust only when the control port was open and this thrust disappeared in less than three seconds after closing the port. This improvement in reliability over the static tests could be due to two factors. The momentum of the fluid flowing along the outside surface of

the shroud is directed along the propeller axis. This flow would tend to force the deflecting wake to return to an axisymmetric flow after closing the port. Also some leakage was observed to be occurring through the closed port in the static tests which would tend to make nozzle operation less reliable.[32]

Figure 33 is a plot of the steering ratio for nozzles A2 and A3. Taken by themselves, these curves can be somewhat misleading since they would favor operation at a high advance ratio and using propeller No.2. There are other considerations such as efficiency. Propellers No.2 and No.4 are the most efficient as indicated by Figures 20 and 21. From an efficiency standpoint, the choice between propeller No.2 and No.3 would depend on the advance ratio at which the vessel cruises. These aspects of propeller-nozzle selection from the design curves will be covered in more detail in the next section.

5-D Radial Force Control: Preliminary Tests

The tests so far have demonstrated that a number of reliable propeller-nozzle combinations exist which develop radial thrusts of reasonable magnitude. However, for a given control port this radial steering force is single valued, changing only with motor speed. To compete with other steering systems, the WSN should be capable of developing a steering force for which the magnitude can be controlled at any speed. As a result, a preliminary series of tests were conducted on nozzle A4 to inves-
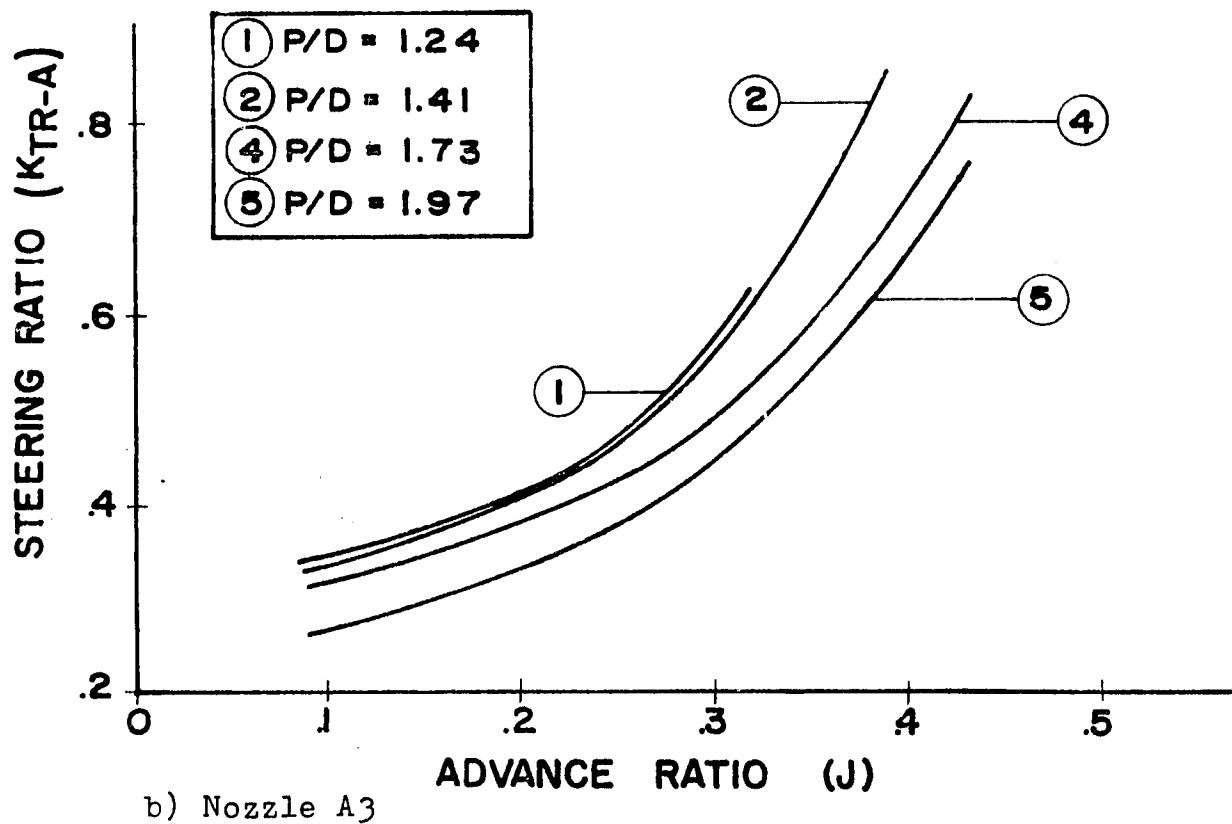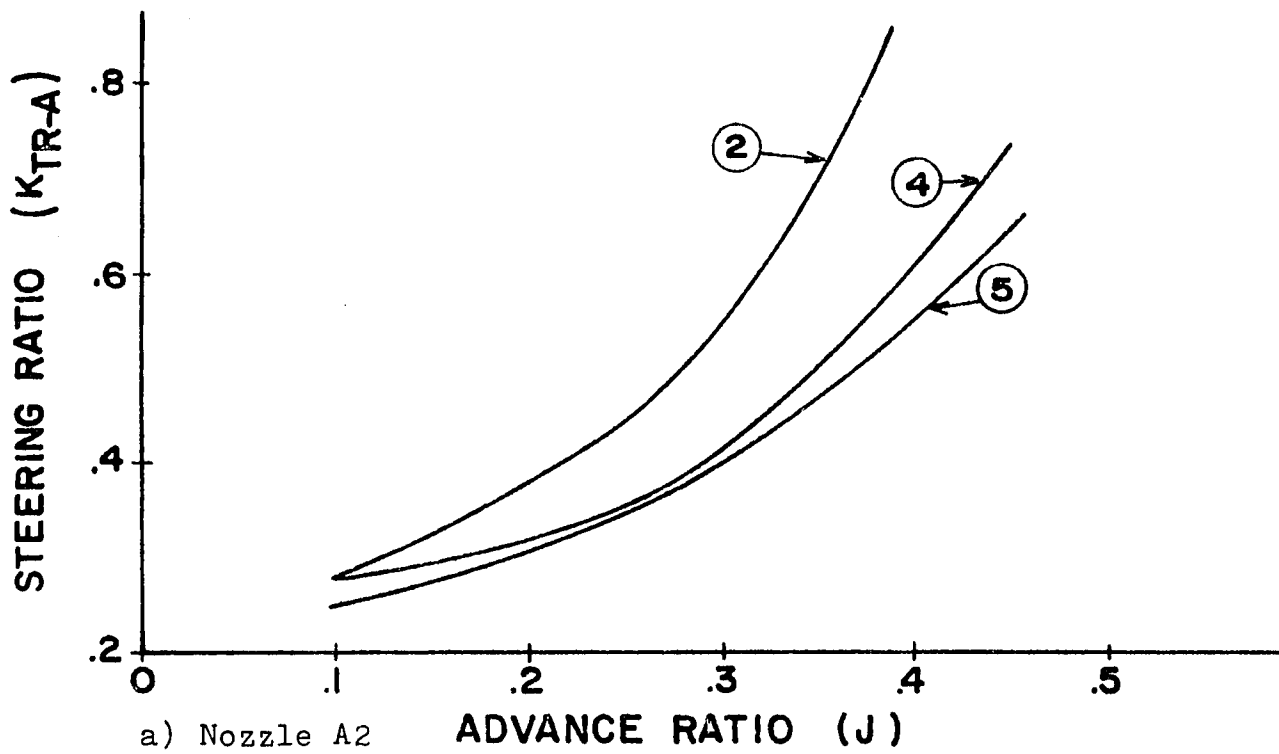
Figure 33 Steering Ratio Versus Advance Ratio for Nozzles
A2 and A3

tigate a method of controlling the magnitude of the radial force.*

A series of ports were placed along the shroud, from just aft of the propeller plane up to the exit plane. It was felt that the magnitude of the radial force could be varied by varying the location at which a control port was opened, based on the assumption that a port near the exit plane would deflect the wake a smaller amount than a port just aft of the propeller plane. To test this out, three slotted ports were drilled to the same dimensions as the ports used in the previous tests(.25 inches x .75 inches).

The nozzle was tested with propeller No.2 over a range of forward velocities. The results are given in Figure 34. As expected, the radial force magnitude decreases with the distance of port location from the propeller plane. Thus, the technique has potential for providing at least some degree of control over the radial force magnitude. Precise control might be possible if a system were designed to provide a control flow at any axial location. Additional test work is required to study the effect of axial port location and shape on the other propeller-nozzle combinations.

5-E   Summary

The results revealed that the reliability of the WSN performance at nonzero forward velocity was improved over the

* This investigation was conducted by Mr.R. Gauthier as part of an Engineering Undergraduate Projects Course at the University of New Hampshire.
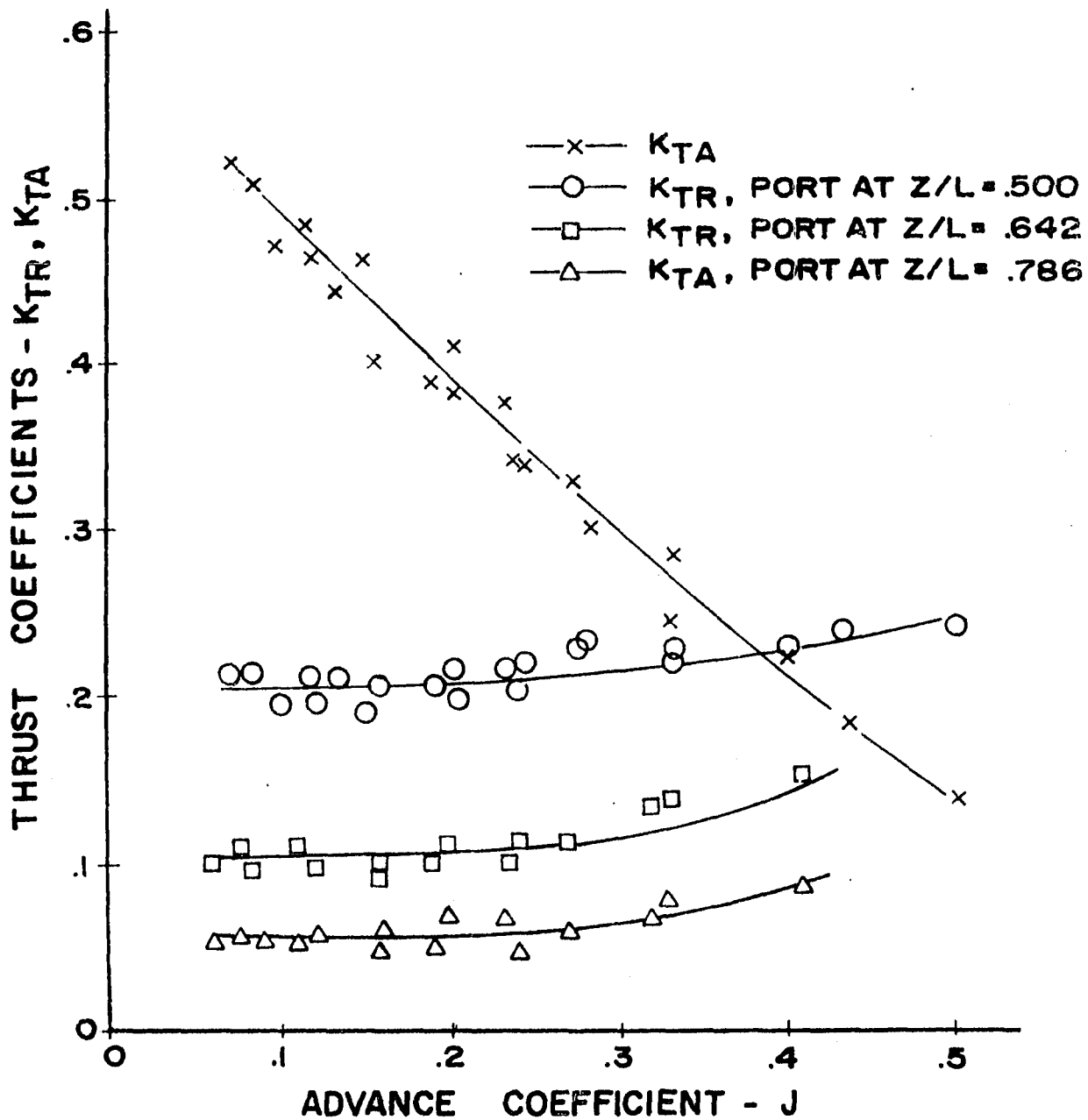
Figure 34   Effect on the Coefficient of Radial Thrust of
Axial Location of the Control Port

static tests. The radial thrust coefficient showed a favorable
increase with advance ratio while the axial thrust decreases as
is the cases with all shrouded propellers. A method was developed
for controlling the radial force magnitude by locating a series
of slots at different axial locations along the aft section of
the shroud.

Additional test work is required to further extend
the set of reliable propeller-nozzle combinatons and to verify
the method of radial force control for other WSN. Development
work is also required to explore such factors as directional
control of radial force. However, before proceeding with more
testwork,an assessment of the potential of the WSN should be
made. The combined static and forward velocity test results
have provided the necessary information. This can be accomplished
by comparing the thrusting and steering characteristics to those
of conventional submersible propulsion-steering systems.

CHAPTER VI

AN EVALUATION OF THE PROPULSION-STEERING CHARACTERISTICS

OF THE WAKE STEERING NOZZLE

6-A   General

The previous two chapters have demonstrated the
feasibility of the wake steering concept. Enough information
on the operating characteristics of the WSN has been obtained
to enable at least a preliminary evaluation of the WSN as a
propulsion-steering device.

In this chapter, the efficiency of the WSN as a
thruster is evaluated by comparing the WSN efficiency to
existing data for nozzled propellers.[23-25] The steering effec-
tiveness of the WSN is investigated for both cruising or
forward velocity mode and hovering mode. The steering effec-
tiveness during cruising is evaluated by comparing the WSN
with a conventional submersible propulsion-steering device,
a propeller surrounded by a tiltable shroud. The comparison is
made by means of computer simulations of the submersible DSRV.
This comparison is based on preliminary forward velocity tests
on a model propeller and nozzle. The capability of the two
WSN, one mounted fore and another aft, as shown in Figure 4, to
provide independent force and moment generation in the various
degrees of freedom during hovering is discussed.

6-B   The Propulsive Efficiency of the WSN

Considerable experimental work on propellered nozzles
has been conducted at the Netherlands Ship Model Basin (NSMB).[23-25]
As a result of these efforts, a number of propellered nozzles
have been developed which are highly efficient thrusters. Some
of the test results showing the axial thrust coefficient and
efficiency plotted as a function of advance ratio for one of the
most efficient nozzles, nozzle 19a taken from Reference 24, Figure
22,are shown in Figure 35. This nozzle was tested with a series
of four bladed propellers ranging in pitch to diameter P/D ratio
from 0.6 to 1.6. The test results for two of the propellers
having P/D ratios of 0.6 and 1.4,are shown in Figure 24 for com-
parison with one of the better performing wake steering nozzles
tested at forward velocity, nozzle A3 with propeller No.2. The
test results for 19a with propeller P/D ratio of 1.4 are used
for comparison with the WSN because propeller No.2 has a nearly
identical P/D ratio of 1.41. The results with the propeller
P/D ratio of 0.6 were chosen because the peak efficiency of
19a with this propeller occurs at very nearly the same advance
ratio as for the WSN.

One deficiency is apparent in comparing the WSN with
nozzle 19a; the efficiency is lower. However, this is to be
expected since nozzle 19a is a highly developed nozzle design
representing the state of the art in conventional non-steering
propellered nozzles, whereas the WSN design has not yet been
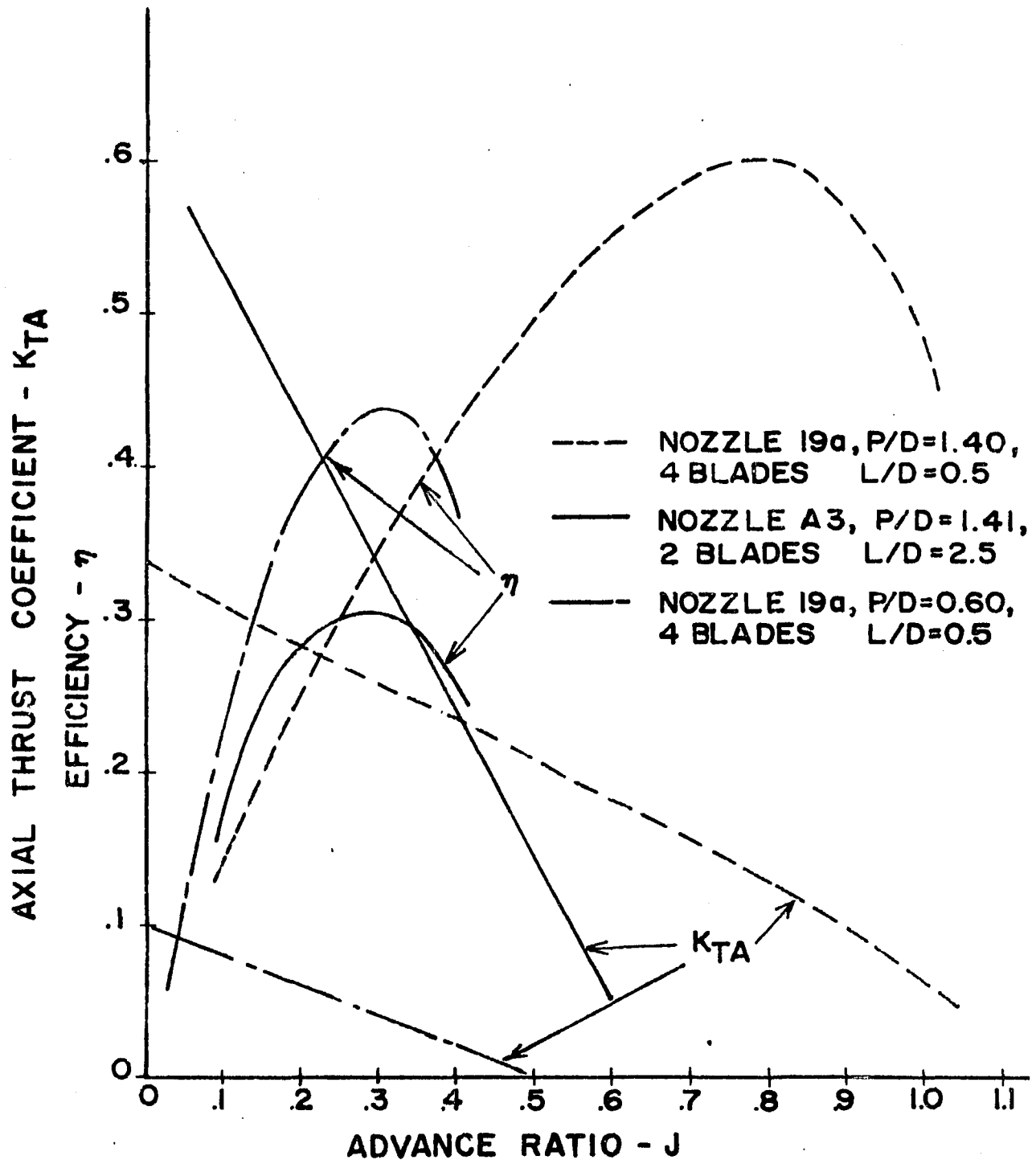
Figure 35   A Comparison of the Axial Thrust Coefficient and
            Efficiency of the Wake Steering Nozzle and Nozzle 19a

optimized. The lower efficiency is also due to limitations in the experimental facility, particularly the propellers which had a blade profile opposite that of most conventional propellers. The blades have a sharp leading edge and blunt trailing edge. The blunt trailing edge would tend to produce a turbulent wake, thus lowering propeller efficiency. Higher efficiencies could probably be obtained by testing larger diameter nozzles where more propeller types are commercially available and manufacturing tolerances can be more easily controlled. In addition, the WSN was tested with a two bladed propeller whereas the propellers used in 19a were four bladed. The four bladed propeller would tend to increase propulsive efficiency by minimizing the unsteady flow. WSN efficiency could also likely be increased by further streamlining the nozzles and supporting struts, thus minimizing the drag forces.

Significant differences in axial thrust coefficient are also apparent in Figure 35. The axial thrust coefficient of the WSN is higher at lower advance ratios but decreases more rapidly with advance ratio than nozzle 19a. The increased axial thrust at low advance ratios could be due to differences in propeller type. Kaplan type propellers which have a wider and flatter blade near the propeller tip were used in 19a. The higher thrust could also be due to the fact that flow through the more divergent WSN tends to separate circumferentially from the inside trailing edge. The resulting high pressure acting on the inside surface of the nozzle aft section would increase the WSN axial thrust coefficient. This separated flow would also increase the

drag force, contributing to the rapid decrease in K_{TA} with advance ratio. Another factor causing the rapid decrease in K_{TA} is the larger length to diameter ratio L/D of the WSN. Van Manen and Oosterveld found that the axial thrust and efficiency of nozzled propellers rapidly decreased with length due to increased nozzle drag.[24] This was particularly evident when the nozzle was lightly loaded (low K_{TA}, high J).

At the present stage of development, it appears that the long highly divergent nozzles are an inherent part of the WSN design required in order to develop large radial thrusts for steering. These same parameters tend to decrease its efficiency and effective range of advance ratios as a forward thruster. Consequently, further development and optimization of the WSN should be directed towards minimizing shroud length and divergence while maintaining comparable steering characteristics.

6-C An Evaluation of the Steering Effectiveness of the WSN

The steering forces developed by movable control surfaces, such as rudders and tiltable shrouds, are usually represented in nondimensional form as lift and drag coefficients by dividing the forces by a term containing rudder area and fluid velocity. The steering characteristics of different control surfaces can then be compared by simply comparing their representative lift and drag coefficients. The WSN steering force,

being a function of propeller thrust, is nondimensionalized by dividing the steering force by a term containing the propeller diameter and rotational speed and therefore a direct comparison is not possible. However, a comparison of the WSN and a conventional control surface is possible for a specific vessel since the propeller thrust and fluid velocity are related through the vehicle dynamics.

The steering characteristics of the WSN are evaluated by comparing it to the tiltable shroud used in the DSRV. This comparison is made by means of computer simulations of the equations of motion of the DSRV given in Appendix A. These were simplified in Appendix D by considering only motion in the horizontal plane. It is, however, assumed that the vehicle is submerged during all maneuvers in the simulation.

Nozzle A3 with propeller No.4 was chosen on the basis of maximum steering ratio K_{TR}/K_{TA} subject to the constraints of efficiency, size and propeller speed. The WSN used in the simulation had a diameter D of 2.7 feet and length to diameter ratio L/D of 2.5 giving it a greater area overall than the tiltable shroud which has a diameter of 6.06 feet and L/D ratio of 0.31. The procedure in selecting this particular WSN is contained in Appendix D. The DSRV equations, together with the equations for tiltable shroud propeller and WSN given in Appendix D were programmed on the IBM System 360 computer using CSMP[52] The computer programs are contained in Appendix C.

Three types of maneuvers were simulated; a full 360°
turn, a 90° accelerating turn and a 90° decelerating turn. The
results of the 360° turn are shown in Figure 36. The 360° turn or
turning circle maneuver is a standard comparative maneuver for
marine vessels and is a steady state or constant velocity maneu-
ver.[57] The tiltable shroud was deflected a maximum amount
which is also standard for this maneuver. The accelerating and
decelerating turns are not standard maneuvers. They were chosen
because they are considered to reflect the dynamic maneuvering
characteristics of the steering devices. In the accelerating
turns, the submersible is accelerated from rest by a constant
vehicle axial thrust. In the decelerating turns, the submersible
is decelerated from a near maximum cruise velocity of 6 feet/second
by adjusting propeller speed to maintain a near zero axial thrust
on the submersible. The simulation was halted in both cases after
the submersible had achieved a 90° change in yaw angle. The results
for the accelerating and decelerating turns are shown in Figures
37 and 38 respectively. The numbers in brackets represent the
position of the vessel in the axis system at the completion of
the 90° turns. The time to complete each maneuver is also given
in the figures.

In the case of the standard turning circle maneuver,
the performance of the two steering devices is about the same.
The accelerating and decelerating turns, however, reveal notice-
able differences,with the WSN out performing the tiltable shroud
in the accelerating turn but performing less effectively in the
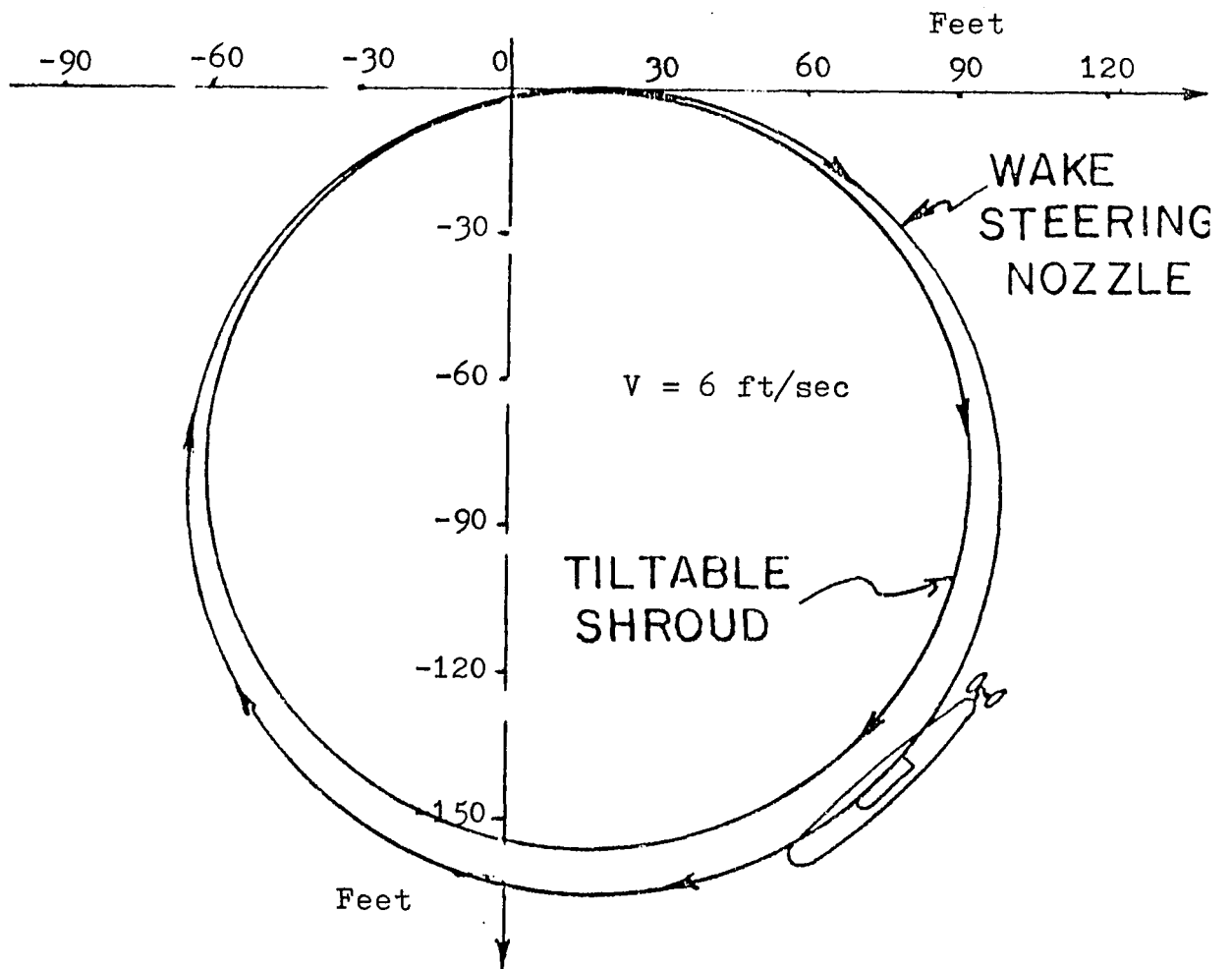
Figure 36   Turning Circle Simulation of DSRV Comparing
WSN and Tiltable Shroud
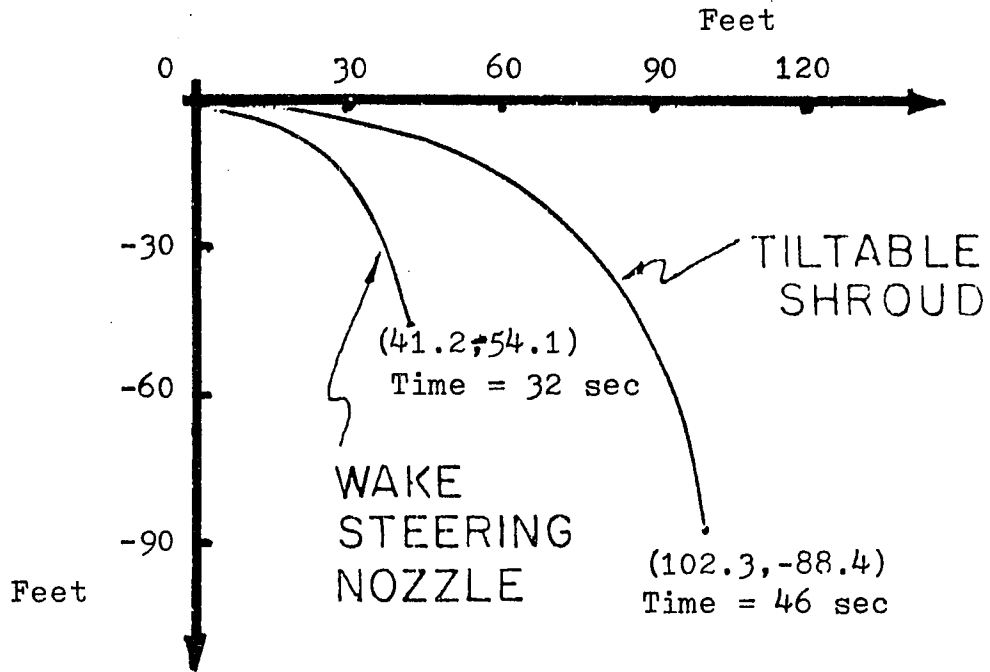
Figure 37 Simulated 90^{0} Accelerated Turn Comparing
Wake Steering Nozzle and Tiltable Shroud
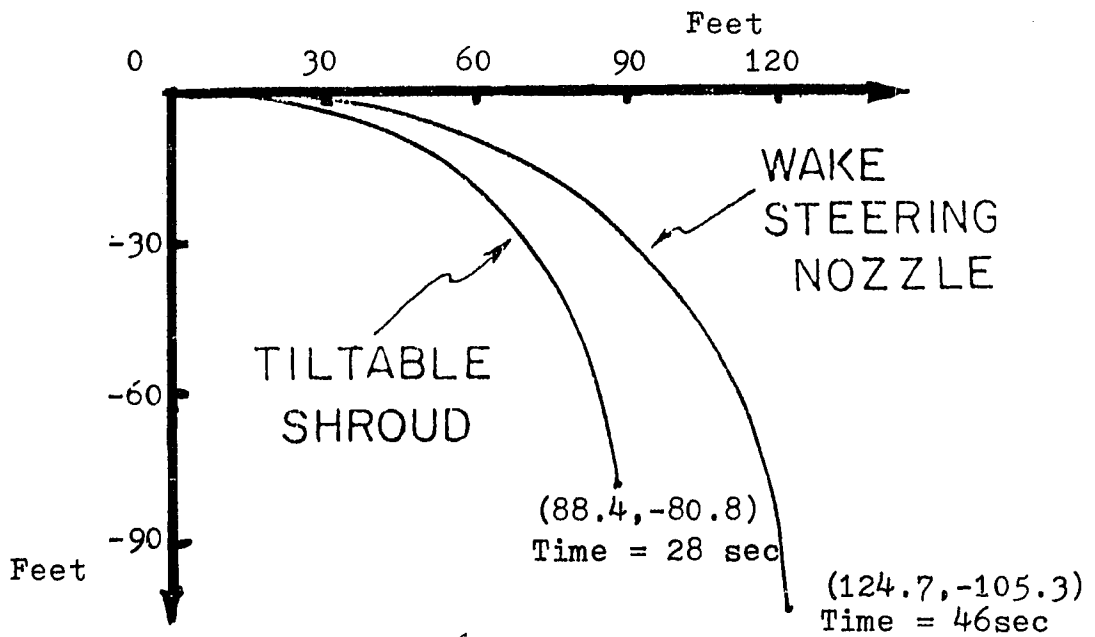
Figure 38 Simulated 90^{0} Deccelerated Turn Comparing
Wake Steering Nozzle and Tiltable Shroud

decelerating turn. This is to be expected since the high propeller-nozzle thrust of the accelerating turn creates a comparatively high WSN radial or steering thrust while the high forward velocity and low propeller-nozzle thrust of the decelerating turn favor the tiltable shroud.

It should be pointed out that the steering effectiveness of the WSN could be improved by choosing a larger diameter WSN. For example, using a 3.4 foot diameter nozzle as opposed to the 2.7 foot diameter nozzle used, increases steering effectiveness K_{TR-A} by about 15% according to the analysis of Appendix D. However, this is done at a sacrifice of a larger shroud size and a lower axial thrusting efficiency.

6-D   A Proposed System for Hovering Control

The proposed use of two WSN, one mounted fore and the other aft, was introduced in Chapter I and is illustrated in Figure 4. This system has the potential capability of replacing the existing thruster-steering system for a submersible such as the DSRV, which has a main propeller, tiltable shroud and four ducted thrusters.

The arrangement is capable of generating independent forces and moments through cancellation of the axial thrust generated by the two opposing WSN. The resulting thrust cones

generated by operating in this configuration are shown in Figure 39. By reversing the propeller on the front WSN during cruising, a push-pull type of thrusting is possible.
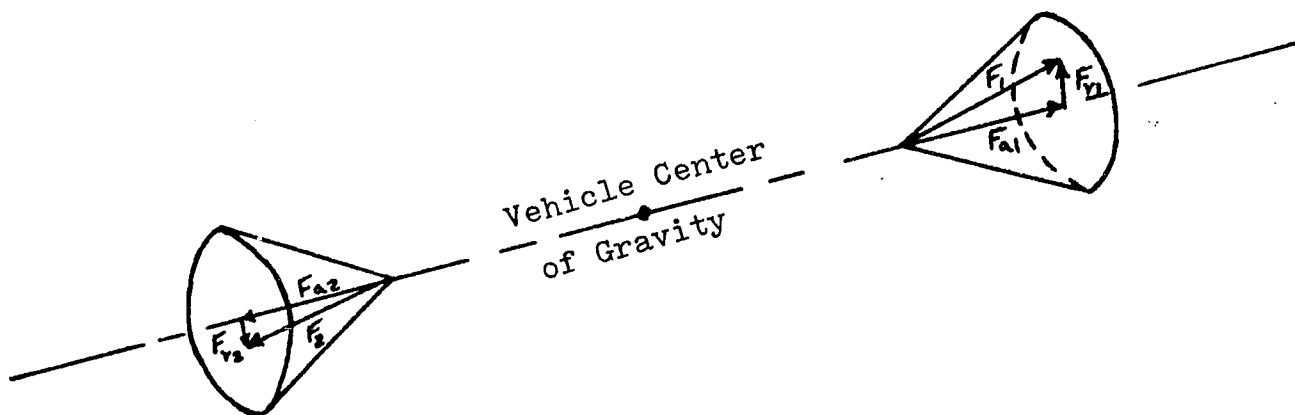
Figure 39   Thrust Vectors Obtained by Mounting WSN on the
Tail and Bow of a Submersible

An additional advantage of this system is the potential ability of the WSN mounted on the front of the submersible to produce a radial thrust for both forward and reverse propeller operation. This would improve the submersible steering effectiveness for cruising and for hovering in a current. This would require additional ports on the nozzle fore section. Future testwork must be conducted on both the forward and reverse operation of the WSN.

The magnitude of the radial thrusts and thus the control forces and moments generated are a function of the WSN size, propeller speed and the characteristic thrust coefficients. Considering

a WSN having the same dimensions as the nozzle used in the simu-
lation and using a maximum propeller speed of 5 rev/sec, the
maximum radial thrust of this WSN at low advance ratios is about
2,750 pounds. This is the same order of magnitude as the maximum
thrust of the ducted thrusters on the DSRV.[20] Thus two WSN could
produce the same yaw and heave forces as the four ducted thrusters.
Because the WSN would be located further from the vehicle center
of gravity than the ducted thruster, the pitch and yaw moments
generated would be increased an average of about 40%, based on the
dimensions of the WSN and DSRV.

6-E   Summary

A comparison of the WSN with some conventional propulsion-
steering systems has been conducted. The results reveal that one
tail mounted WSN is capable of providing submersible steering forces
comparable to a tiltable shroud and that mounting another WSN on
the front can provide the same forces and moments as the four ducted
thrusters, main propeller and tiltable shroud of the DSRV. Although
the axial thrusting efficiency of the WSN is lower than some of the
conventional ducted thrusters, it can no doubt be increased, as can
the range of forward velocity operation of the device, through opti-
mization of the propeller and nozzle design. Shapes other than the
arc of a circle need to be investigated. Additional testwork is
required to investigate methods of controlling radial force direc-
tion and the effect on WSN performance of flows around the nozzle
which are not symmetric to the propeller axis.

CHAPTER VII

ORGANIZATIONAL ASPECTS OF THE WAKE STEERING PROJECT

7-A General

The research of the wake steering project involved the coordinated efforts of a number of people. This approach typifies the current trend towards the use of project groups, as an alternative to the lone investigator, as a means of solving today's more complex research problems. The success of the project group approach depends to a great extent on the ability of the group to work together effectively. This is often hampered by nontechnical issues which require considerable managerial skill and understanding in order to be resolved. Thus, those concerned with the management of the project, who are traditionally scientists and engineers, must acquire and develop new skills to manage these situations.

The purpose of this chapter is to examine some of the organizational aspects of research projects which the author has found particularly relevant in the management of groups as a consequence of his role in the management of the wake steering project. The main focus of this chapter is on the project's intergroup and interpersonal dynamics. However, as a prelude, there is a brief discussion of project organized research and in particular the various phases in the life cycle of a project. This serves to define an overall framework or continuum into which any project, but more specifically the wake steering project, can be placed.

7-B   Project Organized Research

Projects, as defined by Archibald and Flaks[58] are "unique well-defined efforts to produce certain specified results at a particular point in time". A project is characterized by a carefully bounded limit. There is a beginning, intermediate stage and an end, therefore it has a life cycle. This life cycle can be separated into at least four distinct phases:

Phase 1 - Conceptualization

The conceptualization stage is the generation of concepts or "paper ideas" to fulfill needs; existing or anticipated. The recognition and definition of these needs can come from several sources; those directly involved with the research, those in the management of the organization or from someone outside the organization. Very few people are involved at this stage and the project exists primarily on paper. A cursory evaluation or screening of ideas is also part of this phase which can be viewed as the initial "brainstorming". In the university environment, this phase is often conducted without funding or is funded under an open-ended type of grant with broadly defined objectives.

Phase 2 - Preliminary Evaluation

A funded program is planned and executed around the most promising idea or concept to emerge from Phase 1. The purpose of the program is to conduct a preliminary evaluation of the concept. More people are involved and organization and management

problems therefore increase. The project objectives are more
clearly and precisely defined. The time and resource require-
ments are estimated. Specifications, such as physical charac-
teristics, performance criteria and cost limits are established
for the end product. A model of the basic concept is constructed
for experimental evaluation. The model is modified to meet initial
performance criteria.

Phase 3 - Prototype Evaluation

Using design information obtained from the results of
the preliminary evaluation, a prototype is built and tested. This
phase is for working any bugs out of the new system or pro-
duct. If any flaws are discovered, the design may have to be
further modified and evaluated by revising and retesting the
model. The prototype design is studied for production operations
and testing may be conducted in its ultimate working environment.
The whole project is given a final and thorough evaluation at
this point. Does the end product meet the standards of perfor-
mance identified at the outset? Can it be produced within a
specified budget and time period? If the results of this evaluation
are positive, the project enters its final phase.

Phase 4 - Utilization

This phase represents commercial production of the
concept and close-out of the project. The product can now be put
to its intended use. The transition from Phase 3 to this phase
often gives the most serious management problems because of the

magnitude of the organizational changes involved. The manu-
facture of the product must be integrated into the company,
often carrying with it portions of the project organization.

A flow chart of this whole process is diagrammed in
Figure 40. Each of the circular nodes represents an evaluation
point in the project where a decision must be made. The project
may proceed to the next phase, continue with the phase it is
already in, stop altogether or return to one of the preceeding
phases. This decision is obviously influenced by many factors
such as a change in the project's goals, the technical success
or failure of the project or a change in the available resources.
Consideration should be given to predicted future values of
these factors as well as the current values.
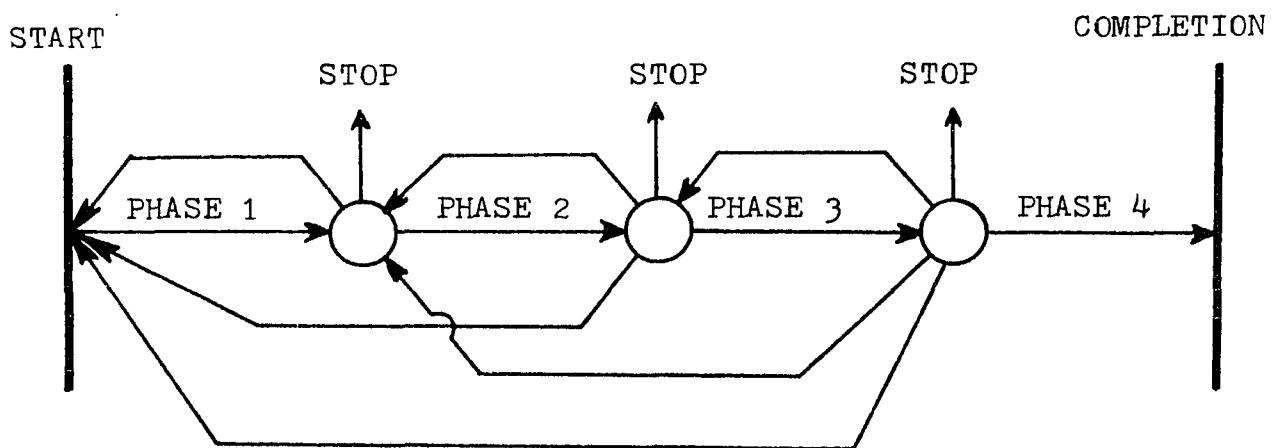
Fig. 40   A Project Flow Diagram

Research on the subject of creativity has shown that
a loosely structered and informal type of atmosphere is the most
fertile source of ideas.[59,60] Gordon[59] emphasizes the im-
portance of removing people from the day to day tasks of their
immediate work environment and creating a shirt sleeve type of
setting. The contention being that this type of atmosphere is
more conducive to idea formulation rather than a purely production
oriented atmosphere. He also feels the group should have an inter-
disciplinary flavor to provide the fresh approach to problems
so often needed. In the conceptualization phase where the creation
of a good core idea to form the basis of a project is the primary
concern, the project manager might conciously try to adopt some
of these techniques. On the other hand in Phase 3, which is
concerned with prototype evaluation, more effort directed to-
wards the detailed planning and scheduling of activities with an
increased awareness of deadlines and costs would likely be more
effective. This is not meant to imply that creativity is any
less important in Phase 3, only that it is directed more towards
the problems at hand. Phase 2 would lie somewhere in between
these two phases, but probably closer to Phase 3 than Phase 1.

It is also important to those concerned with the final
outcome of the project to realize which phase a project is in.
This recognition is an aid in leading to a common agreed to set
of goals and expectations on the part of all concerned. In the
wake steering project it was generally agreed that Phase 1 had

previously been completed by Wozniak, Taft and Alperi [30] who had originated the basic concept after examining a number of possibilities. Consequently, it was apparent to our group that it would be unwise to discard their original concept and begin reconceptualizing before completing a thorough investigation of their concept. This consensus did not always hold as there was a tendancy for the group to reconceptualize, particularly when faced with discouraging results such as the failure of the aluminum shrouds to operate reliably.

It was also apparent to our group that Phase 2 of this project had not yet been completed. Therefore, the investigation of the wake steering nozzle reported in chapters 4 to 6 constitutes, for the most part, our development of Phase 2

Phase 3 was examined and it was felt that it would be unrealistic for us to devote time and resources to the design and construction of a full scale prototype of the nozzle.

The main goal in any phase of a project is usually to achieve a technical success. The contribution of management towards this objective is through the best utilization of the project's resources, the most important of these being its personnel. The next two sections are devoted to relating certain concepts of management which, based on the writer's experience, are considered important in ensuring the success of a project.

7-C   Planning for Research

7-C.1   Establishing Objectives

The planning and successful completion of a project requires a base or a set of congruent objectives and goals. The term congruent does not imply that all the goals are basically the same but rather that they act in a complementary fashion thus minimizing any conflict. The first step in achieving this degree of congruency is a common awareness of just what the goals of the organization or group are.

Groups typically have multiple goals and some of these are not very obvious. Litterer makes a distinction between official and operative goals[61]. Official goals are for the public consumption and are openly stated. Operative goals are those actually pursued and determine the operation of the organization. Operative goals are not neccessarily different from the official ones but often are much less specific. It is a matter of distinguishing between a group's stated goals and its real goals.

In the wake steering project the official goals were established by the Advanced Research Projects Agency who funded the project*, and were based on a proposal by Dr. Charles K. Taft, the principle investigator and project director. The basic objective was to conduct an experimental and analytical investigation of the potential of the wake steering concept. This objective was communicated to the group members by Dr. Taft

* The contract was administered by the Office of Naval Research under contract number N00014-67-A-0158-006.

during the recruiting phase of the project and in the initial
group meetings.

These official goals were also part of the operative
goals of our project. That is, they were very real goals to
which the members of the group were directing their efforts.
Other operative goals were the provision of thesis topics for
graduate students, publications for students and faculty and
continued project funding. These goals were eventually discussed
by our group with a view to establishing as high a degree of
congruency as possible in the efforts directed towards these
goals. Consequently, most of the project related work of the
graduate students also provided thesis or M.Sc. project topics.
In addition, one paper has been written with more likely to fol-
low.

It is the writer's conviction that the recognition
and open discussion of all the operative even though unstated
goals of the project increased our group's productivity by
minimizing goal conflict. A particular example was the initial
frustration of some of the students as to how to direct their
research efforts in a way which was in the best interests of
the project but which would also lead to a thesis topic. In
one instance this was resulting in a student spending time
researching in a completely different area. Since most of the
faculty on our project were also advisors to the students,
a discussion of this difficulty led to a definition of work that

would simultaneously achieve both goals.

7-C.2 The Planning Function

Achieving the goals of an organization involves a certain amount of planning at some stage. This plan may only exist in an abstract sense in the minds of management. Planning for research may be objected to by the people involved in research because it is viewed as setting boundaries or guidelines on creativity. It seems somehow to run counter to imagination, genius and insight. Planning is also objectionable perhaps because trying to translate possible eventualities into concrete actions is such a difficult mental process, particularly when the need for such actions may never arise. Yet, planning is important to achieving one's goals and in deciding among the various alternatives. [62,63]

Acting as project coordinator for the wake steering project, the planning function was one of the prime concerns of the writer of this dissertation. Several plans were developed around project networks similar to PERT. The first schedules developed were not very successful. That is to say that little attention was given to doing the tasks as outlined and often with total disregard to completion times. Consequently, the wake steering project fell far behind on most of its early commitments. Later schedules were much more successful. The construction of these later schedules differed from the earlier ones in a number of important aspects:

1) There was an increased awareness by our group that such schedules could serve a useful purpose. Initially, many of the members of the project were apathetic to any sort of detailed planning and general scheduling of activities. After the project had been underway for a few months, the group became increasingly frustrated with our relatively slow rate of progress. As a result people were more receptive to their use.

2) There was also an increased input to the planning by the people who were conducting the work. One contributing factor to this change was that the project coordinator was planning with the people involved rather than for them as was the case in the earlier schedules. Churchman(64)points out that one of the most critical problems in organizing for planning is the potential alienation of the planning function. He and others(65,66)emphasize the importance of active involvement of the people who will be doing the work.

3) The task time estimates associated with each activity were more realistic. This was achieved thanks to Mr. Fellows, an M.Sc. student on the project, who helped ensure that a careful examination of the various interactions was conducted and sufficient detail describing the various tasks included. Assistance was also provided by Mr. O'Connel an MBA student participating in the project.*

An example of the success of one of the later schedules is that it assisted Mr. Hudson, an M.Sc. student, in completing a substantial set of the forward velocity tests on time. The

*Mr. O'Connel acted as an observer and management consultant to the author during the later part of the project.

project schedule enabled the project coordinator to assist
Mr. Hudson in completing this work because the areas or tasks
where assistance was required were evident and provisions could
be made ahead of time.

An additional benefit of planning is that by necessity
it leads to clarification of the goals of the project since in
planning out <u>what</u> is to be done consideration must be given to
<u>where</u> one is going. This aspect of planning helped identify
and clarify the subgoals of the wake steering project.

7-D   The Leadership Role

7-D.1   Responding to Individual Needs

Classical management theories tended to stress the im-
portance of control of subordinates by authoritative means.
It was assumed that the average human being had no interest
in the organization's goals, an inherent dislike for work
and a need to be continually directed.

Recent management theory is directed more towards
providing an atmosphere which makes possible the satisfaction
of individual goals and needs through achievement of the or-
ganization's goals. Typical examples are McGregor's [67]
Theory y type of manager and the "9.9" manager described by
Blake and Mouton.[68]   These authors stress the importance of
recognizing that the individual has a set of needs, many of
which are continually changing. It has been demonstrated
that sensitive and supportive attitudes by management towards
employee needs is a contributing factor in achieving high per-
formance.[69]

One framework suitable for examining individual needs in work groups is that proposed by Herzberg.[70] He has divided individual needs into two categories; satisfiers and dissatisfiers. The _satisfiers_ are _motivators_ in that they motivate the individual to superior performance and effort. They are all _task_ oriented and consist of achievement, recognition, work itself, responsibility and advancement. The _dissatisfiers_ are in the _environment_. They include such things as company policies, salary and the type of supervision received. The dissatisfiers serve primarily to prevent satisfaction while having little effect on positive job attitudes. They are of relatively _short_ duration in contrast with the motivators which were found to have a _long_ lasting effect in motivating employees to superior job performance. Thus one of the primary functions of management should be to create or enhance the potential job satisfiers. Too often this is not the case and it is the dissatisfiers that get most of the attention.

The primary reason for this is the dissatisfiers constitute a more tangible and often less personal category of needs and therefore tend to be the focal point of both management and workers. How often have you heard employees complaining about company "red tape", their salary or their supervisor when really they were asking for a more fulfilling job through increased responsibility and recognition? The effective project manager will be aware that much more significant factors underly what often may appear on the surface as petty and

easily resolved employee complaints.

The atmosphere created in the wake steering project
was one which was generally responsive and supportive to in-
dividual needs, particularly the more task oriented motiva-
tors. An example of this was the case of Mr. Clark, an M.Sc.
student on our project, who had a number of ideas relating
to the experimental testing of the nozzles. These ideas re-
flected Mr. Clark's background as a machinist and his current
interests in mechanical instrumentation design. Mr. Clark
was encouraged by the leadership of the project to present his
ideas to the group. One of the proposed ideas, the variable
nozzle holder, was enthusiastically received by the group.
Mr. Clark was encouraged to pursue the idea and given responsi-
bility for its development. Out of this evolved the nozzle
variation system illustrated in Figure 17, Chapter 4. This
system enabled the nozzle inside shape to be rapidly varied at
a much lower cost compared to some of the other methods con-
sidered. It is fair to say that Mr. Clark received a good
deal of satisfaction from this accomplishment and the project
an excellent piece of equipment. This may not have been pos-
sible under a leadership style which was unresponsive to in-
dividual needs.

This does not mean to imply that every individual on
our project obtained a high degree of satisfaction. In the case
of one individual there was extreme discouragement and frustra-
tion. The main reason for this, which finally became apparent
to the author, was that this person felt he was not getting

adequate recognition for the results he had achieved, particularly from the project director. This was resulting in a complete breakdown in communications and an increasing amount of tension between this individual and the project director. Some discussions were held with these individuals during which this issue was raised. These discussions helped to correct the situation somewhat but it still remained un-satisfactory. An earlier realization by the author as to the reason for the high level of dissatisfaction of this individual perhaps could have avoided this situation.

7-D.2 The Functional Aspects of Leadership

People are in leadership positions because they were appointed to that position (formal) or because they emerged (informal). At any rate they have the ability to influence the group and they exercise it. This power to influence others can be viewed as stemming from five bases:[71] legitimate, expert, referent, reward and penalty. Leadership can be based on one or all of the preceeding sources of influence. For example, a formal leader would have legitimate power because of his officially designated position. Along with this he would likely have the ability to dispense organizational rewards or penalties. The emergent leader, on the other hand, derives his support from his special knowledge or expertise and/or because project personnel feel personally attracted to him.

The leadership positions of the group, both formal and informal can be held by one or several persons in the group.

In an __authoritative__ setting the designated leader is usually
the only leader. All leadership functions are performed by
him. The expertise of others in the group is not utilized.
This is contrasted with the __functional__ concept of shared
leadership which recognizes and utilizes the special abili-
ties of others in the group. It focuses attention on __what__
must be done to move the group towards its goals rather than
__who__ must do it.[72] Studies conducted by Gemmill and Thamain
[73,74] have demonstrated that a functional approach to
project management based on expert power is the most effective
in gaining the support of project personnel.

This functional concept of group leadership was recog-
nized by Professor Taft. In his role as the official leader
of our project, he was influential in creating an environment
where the leadership was shared. This enabled our group to
utilize the talents and expertise in fluid mechanics of Pro-
fessors Wilson and Alperi and the machine design capabilities
of Mr. Clark to mention a few. As an example, at the instigation
and under the direction of Professor Wilson, a water tunnel was
rapidly constructed to provide a facility for the forward vel-
ocity testing.

7-D.3 The Role of the Project Coordinator

The role of project coordinator is vital to the
leadership and management of a project. A description of
the type of project coordinator role that the writer assumed
in the management of the wake steering project is a combination

of what Archibald and Flaks[58] describe as a project ex-
pediter and a project coordinator.

As project _expediter_:

 .1) He deals with all persons involved with the work to
    expedite and ensure that schedules are kept.

 2) He is a center of communication and is able to supply
    information to higher management on request.

As project _coordinator_

 1) He has independent authority to act and is therefore
    responsible for results.

 2) He exercises leadership of the project through personal
    interaction rather than through actual authority.

 3) He controls disbursement of funds but does not estab-
    lish the budget.

An additional dimension to the writer's role of
project coordinator was that of "team member". In the early
stages of our project, the activities of the writer were confined
almost exclusively to this role. This soon proved ineffective
in terms of the overall project as Professor Taft was becoming
overburdened with the leadership duties of the project. Al-
though this was apparent to the project coordinator, some time
elapsed before the assumption of a very active role in the
leadership of the project. A contributing factor to this delay
was the tendency to avoid the difficulty and risks involved in
such a change in the established role. As Zaleznik[75] points
out, this changes many of the basic interpersonal relationships.
This situation was leading to increased levels of frustration.

Professor Taft was becoming frustrated with the project coordinator because he felt that the project coordinator should be assuming a more active role in the leadership of the project. The project coordinator now felt that he could do more to assist the group in achieving its goals in a management role than as a team member. These feelings were heightened by a lack of communication and had the situation continued it could have become a real problem. Fortunately, this misinterpretation of roles was discussed. The role of the project coordinator was more clearly defined. Some common expectations were established leading to a more active management role for the project coordinator.

It is recommended in the future that the role of the student manager is discussed with both the key project personnel and the student's Ph.D. committee prior to commencement of the student's managerial role. This provides at least an initial clear cut starting point. What happens to this "official" role during the remainder of the project is then part of the learning experience.

The author also found that to continue his individual research while simultaneously coordinating the activities of the project was generally not in the best interests of both. Too often matters were let slide in the project with the hope that they would work themselves out which they rarely did. Not enough time was spent on "housekeeping" chores, such as the development of good bookkeeping, filing and accounting systems, essential to well organized management. In short, project management is a full time job and this should be taken into

consideration in designing a Ph.D. program.

7-E

Certain organizational aspects of project or group oriented research were examined in this chapter. These are based on the writer's experience as project coordinator for the wake steering project. This experience has provided a set of key concepts considered by the writer to be important in managing projects of this type. These concepts range from topics at the larger organizational level, such as goals and objectives, to a consideration of interpersonal factors, such as leadership roles.

At the larger or macro-level, projects can be viewed as having a life cycle, which can be divided into various phases. Each phase has distinguishing characteristics which influence such managerial considerations as the planning and scheduling of work and setting the project's goals. Recognition of which phase a project is in should lead to a common set of goals and expectations for the group, thus improving their effectiveness.

It must be recognized that project groups have goals other than their official goals. Recognition and open discussion of these operative goals increases the productivity of the group by minimizing goal conflict and establishing a high degree of congruency between the goals.

Planning is required at all phases of a project but becomes more extensive in the later phases. To be most

effective, this planning is best carried out by <u>those</u> who will be <u>doing</u> the work. Care must be taken to ensure enough detail is included to provide an adequate description of the various tasks.

The successful outcome of a project depends on the ability of the group to work together effectively. A climate of <u>responsible</u> <u>freedom</u> must be created where the individual is encouraged to extend himself. Probably the single most important factor influencing the creation of this environment is the leadership of the group. The truly effective project manager must be able to recognize the individual need <u>satisfiers</u> and work to create the opportunity for the individual to realize these <u>task</u> <u>oriented</u> <u>needs</u>. Leadership must also be responsive to the overall needs of the project as well as in- dividual needs. It must recognize where the pressure points are and know how to relieve them. Operating out of a <u>functional</u> concept and <u>democratic</u> style, the leadership role can be shared by the whole group thereby making maximum utilization out of the pooled leadership abilities of the group.

CONCLUSIONS AND RECOMMENDATIONS

Some methods of improving the maneuverability of
a submersible have been examined. The main thrust of this
investigation was the development of techniques for generating
independent control forces and moments in the various degrees
of freedom. As part of the effort to achieve this goal, de-
coupling feedback control laws were derived and applied to
decouple some of the motions of the DSRV.

The equations of motion of the DSRV are a complex
coupled nonlinear set of differential equations. Existing
linear decoupling theory was shown to be unsatisfactory as
a means of developing control laws which would enable single
input-output control.[21] These results motivated the devel-
opment of a nonlinear theory for the direct decoupling of
nonlinear systems. Conditions for decoupling two classes of
systems were developed; Class 1 systems in which the inputs
appear linearly in the describing equations and Class 2 systems
in which the inputs are nonlinear. The Class 1 systems have
recently been treated by other authors using different approaches.
The end results are basically the same and the choice is largely
one of individual preference. Readers familiar with the linear
theory of Wolovich and Falb [9] for linear systems are likely
to prefer the approach used in this thesis.

As far as decoupling the motions of the submersible
are concerned, the Class 2 systems are really of more interest
since the submersible is of this class. Except for the work of
Tubalkain and Limbert [39], this area of systems has not been

considered in any detail by other authors. By expressing the
equations in vector form, conditions were developed in a more
direct manner to include systems which could not be decoupled
using their method. However, the principle advantage is that
decoupling is achieved using only state feedback rather than
state plus input feedback. Feeding back the inputs $\bar{u}$ intro-
duces a set of hidden variables into the closed loop system
which further complicates an evaluation of the closed loop
stability of the system.

The ability to decouple Class 1 systems was shown to
depend on the invertibility of a matrix $D^*(\bar{x},t)$. Values of
the system states where this condition is not met serve to
define regions where the system cannot be decoupled. The
decoupling of Class 2 systems was shown to depend on the
ability to solve a set of nonlinear algebraic equations for
all the components of the input vector $\bar{u}$. Decoupling is pos-
sible where these solutions are real and finite. The results
for Class 1 and Class 2 systems were extended to develop
feedback control laws for the on-line regulation of these
systems.

The main difficulty complicating the practical appli-
cation of the decoupling theory in general, both linear and
nonlinear, is that it is ineffective if saturation of any of
the inputs $\bar{u}$ occurs. The theory delineates those regions where
the inputs become infinite. In practice saturation will occur
at finite values. This can act to greatly reduce the region
in state space over which the decoupling control laws are
applicable. Redefining the region over which the control laws

are effective could require an extensive search procedure
since the inputs are functions of several variables; the new
system inputs, system states and the specified closed loop
dynamics. The development of numerical search routines in-
corporating the decoupling theory would advance the state of
the art considerably.

The nonlinear decoupling theory developed in Chapter
II was successfully applied to exactly decouple the roll-surge
equations which the linear theory had previously failed to
satisfactorily decouple. The nonlinear theory was then applied
to a more exact set of roll-surge equations which included the
input dynamics and constraints on the input magnitudes. By
introducing rate limiting filters on the new system inputs,
the amount of roll-surge cross-coupling was reduced almost
to zero without appreciably slowing the dynamic response of
the submersible.

The method of solving the problem of completely de-
coupling the six degrees of freedom of the DSRV during hovering
nameuvers was also established. The explicit solutions to
this problem were not obtained by the procedure one would
follow is basically the same as was done for the roll-surge
motions. The main difference and difficulty is that a more
extensive search routine would have to be employed since the
inputs are functions of more variables. Additional research
in this area is required if the full benefits of the decoupling
theory are to be realized.

Although the control laws have been developed for a

specific submersible; the DSRV, they are quite readily extendable to other submersibles. The potential application of the control laws develped in this thesis is promising. The extremely rapid developments in recent years in the areas of signal processing and digital computers are greatly reducing the time and cost of employing some of these more elaborate control techniques.

The thrusting and steering characteristics of the wake steering nozzle were also investigated. This device has the potential of reducing the amount of submersible hydrodynamic cross-coupling between the motions by increasing vessel geometric symmetry. This may be done using fewer thrusters but still maintaining comparable levels of maneuverability overall.

The performance of the wake steering nozzle was first investigated at zero forward velocity. Preliminary tests revealed that the radial steering thrust of the nozzles increases as the nozzle divergence increases. However, higher nozzle divergence resulted in an unreliable mode of operation where the wake remains deflected after closing the control port producing an unwanted component of radial thrust.

A further set of tests of several propeller and nozzle combinations served to define a set of shrouds which operated reliably while producing reasonably large radial thrusts. These combinations tended to be the longer nozzles and were about midrange in terms of divergence and propeller pitch of those tested.

Two nozzles from the static tests which were midrange in terms of divergence were chosen for forward velocity testing. The reliability of these nozzles showed an improvement over the static tests. Also, the radial thrust coefficient was found to increase with forward velocity. Locating a series of slots at different axial locations along the aft section of the shroud was demonstrated to be a realistic means of controlling the magnitude of the radial force.

Based on the static and forward velocity test results, a preliminary comparison of the WSN with some conventional submersible propulsion and steering systems was conducted. The WSN was found to be somewhat less efficient as a forward thruster than a conventional nozzled propeller, Nozzle 19a. However this is to be expected since nozzle 19a is a highly developed nozzle design representing the state of the art in conventional non-steering nozzles, whereas the WSN design has not yet been optimized. The real significance of the comparison is that it provides the impetus and direction for future work on the WSN indicating that parameters such as nozzle length and propeller type must be optimized from the point of view of efficiency as well as radial thrust. In terms of steering effectiveness, the WSN was shown to be as effective as a conventional tail mounted steering device, a tiltable shroud. By mounting a WSN on the bow of a submersible, in addition to one on the tail, the WSN can be considered a potential candidate for replacing the propulsion and steering system of a conventional submersible such as

the DSRV which has a main propeller, tiltable shroud and four ducted thrusters.

Future work on the WSN should be directed towards maximizing the radial thrust of the WSN subject to the constraints of reliable operation and acceptable thrusting efficiency. Other factors must also be taken into consideration. The following is a list of recommendations concerning future investigations of the wake steering nozzle:

1) The test work should be conducted on model sizes larger than those used in our test program. This would enable the investi₍ tion of a much wider range of commercially available propeller types.

2) Propellers having more than two blades should be tested and the effect on performance of propeller hubs be studied more closely.

3) Inside shapes other than the arc of a circle must be investigated. The effect of the outside shape of the nozzle also needs to be considered.

4) Additional test work on the effect of control port location is required.

5) The effect of control port configuration should also be investigated. By proper port sizing and the use of retractable inlet scoops, an increase in both the radial thrust and nozzle reliability could possibly be achieved.

6) The effect on WSN performance characteristics of fluid flow at nonzero angles of attack should also be part of any future test program. The reliability of the

device could be greatly affected by flow at right angles to the nozzle.

The research on the wake steering nozzle reported in this thesis represents the organized efforts of a number of people. As such the results are significantly more than could be accomplished by the author working alone. This group approach to research is fast becoming the accepted method of tackling today's more complex problems. Group research introduces another dimension to the problem; the effective management of the activities of the group.

To the uninitiated researcher with a very limited experience in administration, such as the case of the writer of this dissertation, involvement in the administration of the wake steering project as part of an academic program was an ideal opportunity. Combining course work in organizational behavior and consultation with experts in this field with ongoing project management experience provided an accelerated type of learning. This program has provided the author with a set of key concepts considered important in project management. Briefly, these are:

1) Projects are viewed as having a _life cycle_ which can be divided into various _phases_. These act to influence the project's goals and the planning and scheduling of activities.

2) Goals must be established early in a project. Recognition and discussion of _all_ these goals can increase the productivity of the group by establishing a high degree of _congruency_ between these goals.

3) To achieve the goals of a project requires careful
planning. This planning is best conducted by <u>those</u>
who will be <u>doing</u> the work.

4) The key factor in the success of a research group
is the type and style of leadership provided. Leader-
ship must be <u>sensitive</u> to <u>individual</u> needs and maximize
the opportunity for satisfaction of those needs within
the project framework while meeting the objectives of
the project. Leadership which recognizes the special
abilities of individuals in the group and which actually
utilizes these abilities should have the greatest like-
lihood of accomplishing this seemingly impossible task.

To further improve and accelerate the management
learning experience, some recommendations are offered for de-
signing programs of this type:

1) At least some of the formal course work in organiza-
tional behavior theory should preceed the actual project
management experience. Otherwise too much of the use-
ful knowledge is gained too late to be applied. Prefer-
ably these initial courses would be a condensed overview
type of course geared specifically to this type of
program.

2) The specific role that the student manager will assume
in the project should be discussed in depth by those in-
volved prior to commencement of the project. This pro-
vides an initial and immediate starting point.

3) A person outside of the project with some expertise in

organizational behavior should participate in the project
as a managerial consultant and source of feedback to the
student manager.

4) The student manager should keep a complete diary for
the project to provide the data later required for an
objective overview.

5) Recognition must be given to the fact that the manage-
ment of a project is a full time job. Engineers, es-
pecially those with limited management experience such
as the author, tend to underestimate the amount of time
required to manage a project. This factor must be taken
into account in determining the length of the program
and the individual research expectations of the student
manager. The project management part of the program might
best be conducted completely separate from the student's
individual research effort. That is, the student would
act as a _full time_ project manager for a specific time
during his Ph.D. program while the remaining time would
be devoted to course work and individual research.

LIST OF REFERENCES

1. Taggert,R., "Dynamic Positioning for Small Submersibles",
   Ocean Industry, August, 1968, pp.44-49.

2. Meiry,J.L., "Space and Deep Submergence Vehicles: Integrated
   System Synthesis", Journal of Hydronautics, Vol. 3,
   No.2, April, 1969, pp.88-94.

3. Meiry,J.L., "The Control System of the Deep Submergence
   Rescue Vehicle", Fourth National ISA Marine
   Instrumentation Symposium, Crown Beach, Florida,
   January, 1968.

4. Broxmeyer et al, "Deep Submergence Rescue Vehicle Simulation
   and Ship Control Analysis", MIT Report R-570-A,
   February, 1967.

5. Boksenbom,A.S. and Hood,R., "General Algebraic Method Applied
   to Control Analysis of Complex Engine Types",
   NACA Report 980, 1950.

6. Chein,K.L., Ergin,E.I. and Ling,C., "The Noninteracting
   Controller for a Steam Generating System ", Control
   Engineering, Vol.5, October, 1958, pp.95-101.

7. Chatterjee,H.K., "Multivariable Process Control", Proc. of
   Int. Fed. of Automatic Control, 1960, pp.132-141.

8. Morgan, B.S., "The Synthesis of Linear Multivariable Systems
   by State Feedback", Transactions of the Joint
   Automatic Control Conference, 1964, pp.468-472.

9. Falb,P.L. and Wolovich,W.A., "Decoupling in the Design and Synthesis of Multivariable Control Systems", IEEE Transactions on Automatic Control, Vol. AC-12, December, 1967, pp.651-659.

10. Gilbert, E.G., "The Decoupling of Multivariable Systems by State Feedback", Society of Industrial and Applied Mathematics Journal of Control, Vol.7, February, 1969, pp.50-63.

11. Morse,A.S. and Wonham,W.A., "Decoupling by Pole Assignment by Dynamic Compensation", Society of Industrial and Applied Mathematics Journal of Control, Vol.8, August, 1970, pp.317-337.

12. Morse,A.S. and Wonham,W.A., "Decoupling and Pole Assignment in Linear Multivariable Systems: A Geometric Approach", Society of Industrial and Applied Mathematics Journal of Control, Vol.8, February, 1970, pp.1-18.

13. Freund,E., "Design of Time-Variable Systems by Decoupling and the Inverse", IEEE Transactions on Automatic Control, Vol. AC-16, April, 1971, pp.183-185.

14. Sato,S.M. and Lopresti,P.V., "On the Generalization of State Feedback Decoupling Theory", IEEE Transactions on Automatic Control, Vol. AC-16, April, 1971, pp.133-139.

15. Slivinsky,C.R., Schultz,D.G. and Weaver,L.E., "The Design
    of Linear Multivariable Control Systems Using
    Modern Control Theory, (With Applications to
    Coupled Core Reaction Control)", University of
    Arizona, Tucson, NASA CR 1345, 1968.

16. Cliff,E.M. and Lutze,F.H., "Application of Geometric De-
    -coupling Theory to the Synthesis of Aircraft
    Lateral Control Systems", Journal of Aircraft,
    Vol.9, No.11, November,1972, pp.770-776.

17. Cliff,E.M. and Lutze,F.H., "Decoupling Longitudinal Motions
    of an Aircraft", Transactions of the Joint Auto-
    -matic Control Conference, June, 1973, pp.86-91.

18. Rajagopalan,T. and Seshadri,V.,"Noninteracting Control of
    a Continuous Stirred Tank Reactor", Int, Journal
    of Control, Vol.16, August, 1972, pp.129-144.

19. Bryant,G.F. and Higham,J.D., "A Method for Realizable Non-
    -interactive Control Design for a Five Stand Cold
    Rolling Mill", Automatica, Vol.9, 1973, pp.453-
    -466.

20. Lockheed Missiles and Space Company, "DSRV Model for Analysis",
    Report No. RV-R-0037A, May, 1968.

21. Schoenau,C.J., NASA Grant NGR 30-002-056, Final Report,
    Appendix V, December, 1971.

22. Strumpf,A., "Cruising and Hovering Response of a Tail-Stab-
    -ilized Submersible", Journal of Hydronautics,
    Vol. 1, October, 1967.
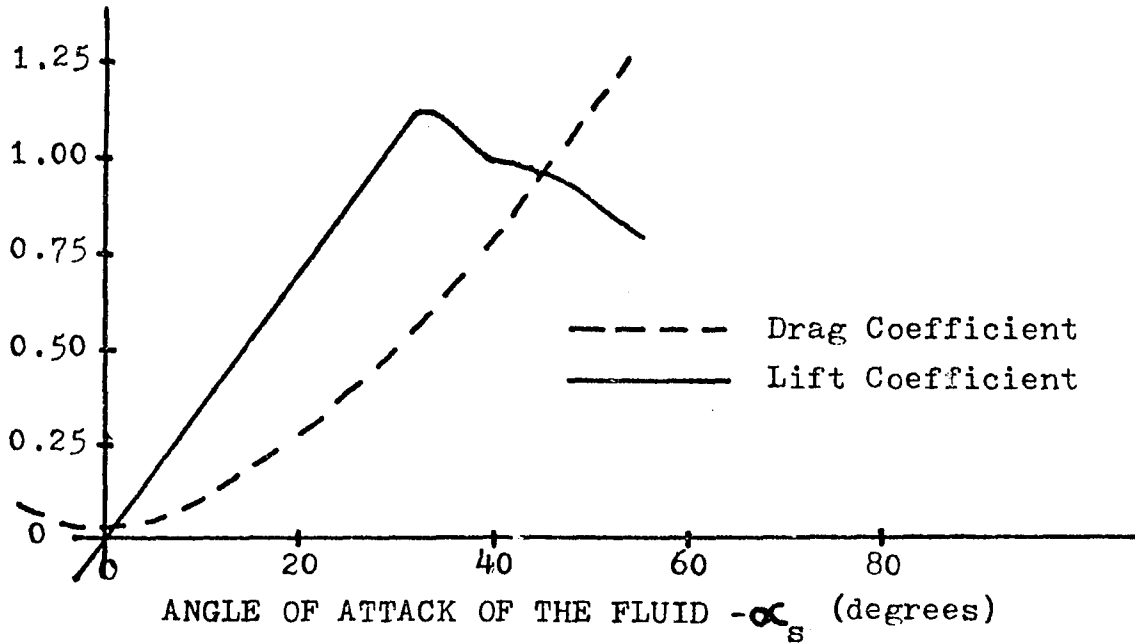
Figure 41   Lift and Drag Coefficients for the Tiltable
Shroud
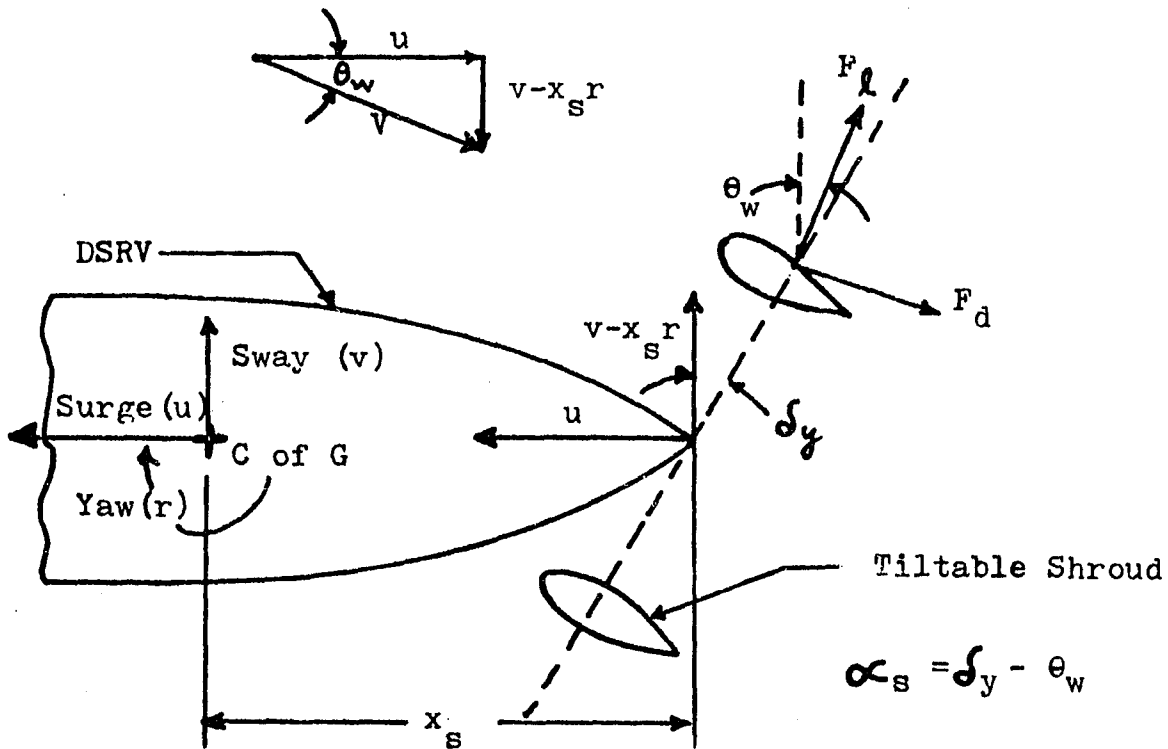
Figure 42   Tiltable Shroud Lift and Drag Forces Relative
to the Motions of the DSRV

23. Oosterveld, M.W.C., "Wake Adopted Ducted Propellers", Netherlands Ship Model Basin Publication No. 345, 1965.

24. Van Manen,J.D., Oosterveld,M.W.C., "Analysis of Ducted--Propeller Design", Society of Naval Architects and Marine Engineers Annual Meeting, Paper No.13, November, 1966.

25. Van Manen,J.D., "Recent Research on Propellers and Nozzles", Journal of Ship Research, Vol.1, July, 1957, pp.13-46.

26. Morgan,W.B., "Some Results from the Inverse Problem of the Annular Airfoil and Ducted Propeller, Journal of Ship Research, Vol.13, 1969, pp.40-52.

27. Morgan,W.B. and Caster,E.B., "Comparison of Theory and Experiment on Ducted Propellers", Seventh Symposium on Naval Hydrodynamics, August, 1968.

28. Chaplin,H.R., "A Method for Numerical Calculation of Slip--stream Contraction of a Shrouded Impulse Disc in the Static Case with Application to Other Axisym--metric Potential Flow Problems", David Taylor Model Basin Report No.1857, June, 1964.

29. Wozniak,J.J., "A Novel Approach to Submersible Vehicle Pro--pulsion, Steering and Control", M.S. Thesis, University of New Hampshire, Durham, N.H., June, 1971.

30. Wozniak,J.J., Taft,C.K. and Alperi,R.W., "Wake Steering: A New Approach to Propulsion and Control", <u>Proceed-</u> <u>-ings of the Marine Technology Society</u>, September, 1972, pp.681-698.

31. Clark,J.A., "Design of a Five-Component Water Tunnel Dynamic Balance", <u>M.S. Project</u>, University of New Hampshire, Durham, N.H. January, 1973.

32. Fellows,B.W., "Experimental Investigation of the Static Performance of Propellered Fluidic Nozzles for Thrust Vector Propulsion of Submersible Vehicles", <u>M.S. Project</u>, University of New Hampshire, February, 1974.

33. Fellows,B.W., Schoenau,G.J. and Taft,C.K., "Propellered Fluidic Nozzles for Thrust Vector Propulsion of Submersible Vehicles",To be presented at the Seventh Cranfield Fluidics Conference, March, 1974

34. Hudson,R., "Forward Velocity Tests on Wake Steering Nozzles", <u>M.S. Project</u>, University of New Hampshire, Durham, New Hampshire, January, 1974.

35. Abkowitz,M.A., <u>Stability and Motion Control of Ocean Vehicles</u>, MIT Press, Cambridge, Mass., 1969.

36. Schoenau,G.J. and Limbert,D.E., "Decoupling Certain Classes of Nonlinear Systems by Nonlinear State Feedback", <u>Transactions of the Joint Control Conference</u>, June, 1973, pp.65-71.

37. Singh,S.N. and Rugh,W.J., "Decoupling in a Class of Nonlinear Systems by State Variable Feedback", *Journal of Dynamic Systems Measurement and Control*, Vol. 94, December, 1972, pp.323-329.

38. Tokumaru,H. and Iwai,Z., "Noninteracting Control of Nonlinear Multivariable Systems", *International Journal of Control*, Vol.16, December, 1972, pp.945-958.

39. Tulbakain,K. and Limbert,D.E., "Decoupling and Synthesis of Certain Nonlinear Systems", *Transactions of the Joint Automatic Control Conference*, August, 1972, pp.893--898.

40. Rudin,W., *Principles of Mathematical Analysis*, McGraw-Hill, New York, N.Y., 1964.

41. Schoenau,G.J., "Regulatory Feedback Control of Nonlinear Population Dynamics", *IEEE International Conference on Cybernetics and Society*, November, 1973, pp.280--281.

42. Wonham,W.M., "On Pole Assignment in Multi-Input Controllable Linear Systems", *IEEE Transactions on Automatic Control*, Vol. AC-12, December, 1967, pp.660-665.

43. Willems,J.C. and Mitter,S.J., "Controllability, Observability, Pole Allocation and State Reconstruction", *IEEE Transactions on Automatic Control*, Vol. AC-16, December, 1967.

44. Silverman,L.M., "Realization of Linear Dynamical Systems",
    IEEE Transactions on Automatic Control, Vol. AC-16,
    December, 1971, pp.554-567.

45. Schultz,D.G. and Melsa,J.L. State Functions and Linear Control
    Systems, McGraw-Hill, New York, N.Y., 1967.

46, Kostyukovskii,Yu.M., "Observability of Nonlinear Controlled
    Systems", Avtomatica i Telemakhanika, No.9, 1968,
    pp.1384-1396.

47. Kostyukovskii,Yu.M., "Simple Conditions of Observability of
    Nonlinear Controlled Systems", Avtomatica i Telemek-
    -hanika, No.10, 1968, pp.1575-1584.

48. Tokumaru,H. and Adachi,N., "On the Controllability of
    Nonlinear Systems", Automatica, Vol.6, 1970, pp.715-
    -720.

49. Gershwin,S.B. and Jacobsen,D.H., "A Controllability Theory
    for Nonlinear Systems", IEEE Transactions on Automatic
    Control, Vol. AC-16, February, 1971, pp.37-46.

50. Davison,E.J., Silverman,L.M. and Varaya,P.P.,"Controllability
    of a Class of Nonlinear Time Variable Systems", IEEE
    Transactions on Automatic Control, Vol. AC-12,
    December, 1967, pp.791-792.

51. Ogata,K., State Space Analysis of Control Systems, Prentice
    Hall, Englewood Cliffs, New Jersey, 1967.

52. IBM, System/360 Continuous System Modelling Program User's
    Manual, No. GH20-0367-3, October, 1969.

53. Abbott,I.H. and Von Doenhoff, <u>Theory of Wing Sections</u>, Dover
    Publications, New York, N.Y., 1958.

54. U.N.H. Technical Report No.1, "Submersible Maneuvering", ONR
    Contract No. N00014-67-A-0158-0006, September 1,
    1972.

55. U.N.H. Technical Report No.2, "Submersible Maneuvering", ONR
    Contract No. N00014-67-A-0158-006, February, 1973.

56. Cunningham,W.J., <u>Introduction to Nonlinear Analysis</u>, McGraw-
    -Hill, New York, N.Y., 1958.

57. Comstock,J.P. (Editor), <u>Principles of Naval Architecture</u>,
    The Society of Naval Architects and Marine Engineers,
    New York, N.Y., 1967.

58. Archibald, R.D. and Flaks, M., "An EE's Guide to Project
    Management", <u>The Electronic Engineer</u>, April, 1968,
    pp. 29-34.

59. Gorden,W.J.J., <u>Synectics</u>, Harper and Row, New York, New York,
    1967.

60. Taylor,F. and Barron,R., <u>Scientific Creativity: Its Recognition
    and Development</u>, J.Wiley and Sons, New York, New
    York, 1963.

61. Litterer,J.A., <u>The Analysis of Organizations</u>, J. Wiley and
    Sons, New York, New York, 1965.

62. Moder,J.J. and Phillips,C.R., <u>Project Management with CPM and
    PERT</u>, Van Nostrand Reinhold Company, New York, New
    York, 1970.

63. Baumgartner,J.S., _Project Management_, Richard D. Irwin,
    Homewood, Illinois, 1963.

64. Churchman,C.W., _The Systems Approach_, Dell Publishing Company,
    New York, New York, 1968.

65. Corell,R.W., " Design Studies of the Development of the Case Re-
    search Arm-Aid", Ph.D. Thesis, Case Western Reserve, 1964.

66. Bennis,W.G., _Changing Organizations_, McGraw-Hill, New York,
    New York,1966.

67. McGregor,D., _Leadership and Motivation_, The MIT Press, Cam-
    bridge, Mass., 1966.

68. Blake,R.R. and Mouton,J.S., _Building a Dynamic Corporation_
    through Grid Organization Development, Addison-
    Wesley Publishing Company, Reading, Mass., 1969.

69. Likert,R., _The Human Organization_, McGraw-Hill Book Company,
    New York, New York, 1967.

70. Herzberg,F., "New Approaches in Management Organization and
    Job Design", _Industrial Medicine and Surgery_,
    November, 1962, pp. 477 - 481.

71. French,J. and Raven,B., "The Bases of Social Power", _Studies_
    in Social Power, D. Cartwright-Editor, Ann Arbor,
    Michigan Research Center for Group Dynamics, 1959,
    pp. 150-165.

72. Willits,R.D., Unpublished Notes, University of New Hampshire,
    Durham, New Hampshire.

73. Gemmill,G. and Thamain,H., "The Power Styles of Project
      Managers: Some Efficiency Correlates", 20th Annual
      JEMC, Managing for Improved Engineering Effective-
      ness, 1972, pp. 89-96.

74. Gemmill,G. and Thamain,H., "The Effectiveness of Different
      Power Styles of Project Managers in Gaining Project
      Support", IEEE Transactions on Engineering Management,
      Vol EM-20, May, 1973, pp. 38-44.

75. Zaleznik,A., "The Human Dilemmas of Leadership", The Harvard
      Business Review, Vol 41, July/August, 1963, pp. 49-55.

APPENDIX A

DSRV EQUATIONS OF MOTION

The dynamic equations considered necessary for adequately describing the motion of a submersible such as the DSRV are a complex coupled set of nonlinear differential equations.[35] The equations of motion for the DSRV in all six degrees of freedom, relative to an axis system located at the vehicle center of gravity, are given in this appendix. These equations are taken from Reference 20. A detailed derivation of the terms in these equations is contained in References 4 and 20. General information on the standard naval architecture approaches to modelling submersibles is given in Reference 35. To keep track of the large number of terms, the nomenclature for the equations is provided in this appendix.

Definitions and Nomenclature

The DSRV's axis coordinate system is located at the vehicle center of gravity as shown in Figure 1, Chapter 1.

The x-axis is defined to be on the longitudinal centerline, the positive direction being forward, toward the bow.

The y-axis is defined to be perpendicular to the x-axis, the positive direction being to starboard.

The z-axis is defined to be perpendicular to both the x-axis and the y-axis with positive direction being down, toward the transfer skirt.

X, Y and Z are used to describe forces in the direction
of the x, y and z axes respectively. K, M and N are used to describe
moments about the x, y and z axes. Angular displacements are taken
as positive in accordance with the "right hand rule".

Symbol	Definition
b_s	Shroud span (ft.)
C_s	Shroud chord (ft.)
I_x, I_y, I_z	Vehicle roll, pitch and yaw moments of inertia, respectively (slug-ft^2)
K_p, M_p, N_p	Moments due to main propeller (ft. - lbs.)
K_t, M_t, N_t	Moments due to ducted thrusters (ft. - lbs.)
L_v	Vehicle overall length (ft.)
L_b	Distance from the origin of the axis system to the tip of the bow of the vessel (ft.)
L_s	Distance from the tip of the bow of the vessel to the leading edge of the shroud (ft.)

k_s	L_b/L_s
m	Vehicle mass in the submerged state including entrained water (slugs)
n	Main propeller speed (rev/sec)
ϕ, θ, ψ	Angular displacement components relative to the body axes roll, pitch and yaw, respectively (radians)
p, q, r	Angular velocity components relative to the body axes roll, pitch and yaw, respectively (rad/sec)
$\dot{p}, \dot{q}, \dot{r}$	Angular acceleration components relative to the body axes roll, pitch and yaw, respectively (rad/sec^2)
u, v, w	Velocity components of the origin of the body axes; x, y and z, relative to the fluid (ft/sec)
$\dot{u}, \dot{v}, \dot{w}$	Acceleration components of the origin of the body axes; x, y and z, relative to the fluid (ft/sec^2)
V	Velocity of the origin of the body axes relative to the fluid
x_G, y_G, z_G	Coordinates of the center of mass relative to the body axes (ft)

X_{oi}, Y_{oi}, Z_{oi} Initial values of the vehicle position in the _fixed_ coordinate frame (ft)

X_p, Y_p, Z_p Forces due to the main propeller (lbs)

X_s, Y_s, Z_s Forces produced by the shroud (lbs)

X_t, Y_t, Z_t Forces due to the ducted thrusters (lbs)

x_{ti}, y_{ti}, z_{ti} Coordinates of the ballast tanks relative to the vehicle axes (ft)

α_s Shroud effective angle of attack (Degrees)

W_{ti} Change in variable ballast from initial conditions[*] (lbs)

Vehicle Equations of Motion

Note that in the following equations all _single subscripted capital letters preceding_ the _acceleration_ terms in the equations are constants and subscripted according to the terms they precede. For example, the constant $X_{\dot{u}}$ in the term $X_{\dot{u}}\dot{u}$. Note also that all _double subscripted capital_ letters _preceding_ the velocity terms in the equations are constants and are subscripted according to the terms they precede. For example, the constant X_{rv} in the term $X_{rv}rv$. The values for all these constants are contained in Table 9 in this appendix.

_____

[*] For additional information refer to Reference 20.

Vehicle Equations of Motion

Surge:

$$m \left(\dot{u} + qw - rv - x_G(q^2 + r^2) + y_G(pq - \dot{r}) + z_G(pr + \dot{q}) \right) =$$

$$X_{\dot{u}}\dot{u} + X_{qw}qw + X_{rv}rv + X_{u|u|}u|u| + X_{rr}r^2 + X_{qq}q^2 +$$

$$X_{rp}rp - W_{ti}\sin\theta + X_s + X_p + X_t \tag{A.1}$$

Roll:

$$I_x\dot{p} + (I_z - I_y)qr + m\left(y_G(\dot{w} + pv - qu) - z_G(\dot{v} + ru - pw) \right) =$$

$$K_{\dot{p}}\dot{p} + K_{\dot{v}}\dot{v} + K_{qr}qr + K_{v|w|}v|w| + K_{rw}rw + K_{vq}vq +$$

$$K_{pw}pw + K_{v|u|}v|u| + K_{v|v|}v|v| + K_{p|u|}p|u| + K_{r|u|}r|u| +$$

$$K_{p|p|}p|p| + W_o y_G \cos\theta\cos\phi - z_{ti}W_{ti}\cos\theta\sin\phi + K_p$$

$$\tag{A.2}$$

Sway:

$$m\left(\dot{v} + ru - pw - y_G(r^2 + p^2) + z_G(qr - \dot{p}) + x_G(qp + \dot{r}) \right) =$$

$$Y_{\dot{v}}\dot{v} + Y_{\dot{r}}\dot{r} + Y_{\dot{p}}\dot{p} + Y_{r|u|}r|u| + Y_{pw}pw + Y_{qp}qp +$$

$$Y_{v|w|}v|w| + Y_{p|u|}p|u| + Y_{v|u|}v|u| +$$

$$\left(C_{1v}v|v| + C_{2v}r|v| + C_{3v}\frac{v}{|v|}r^2 \right)^{**} +$$

$$\left(C_{4v}\frac{r}{|r|}\frac{v^3}{r} + C_{5v}\frac{r}{|r|}v^2 + C_{6v}v|r| + C_{7v}r|r| \right)^{*}$$

$$+ W_{ti}\cos\theta\sin\phi + Y_s + Y_p + Y_t \tag{A.3}$$

* Terms are cancelled when $\frac{v}{-rL_s} > k_s$ or $\frac{v}{-rL_s} < k_s - 1$

** Terms are cancelled when $k_s \gtrless \frac{v}{-rL_s} \gtrless k_s - 1$

where

$$C_{1v} = \tfrac{1}{2}\rho L_s^2 Y_{v|v|}^{\cdot} \qquad\qquad C_{5v} = \tfrac{1}{2}\rho L_s^2 (2k_s - 1) Y_{v|v|}^{\cdot}$$

$$C_{2v} = \tfrac{1}{2}\rho L_s^3 (2k_s - 1) Y_{v|v|}^{\cdot} \qquad C_{6v} = \tfrac{1}{2}\rho L_s^3 \left((1-k_s)^2 + k_s^2 \right) Y_{v|v|}^{\cdot}$$

$$C_{3v} = \tfrac{1}{2}\rho L_s^4/3 (1-3k_s + 3k_s^2) Y_{v|v|}^{\cdot} \quad C_{7v} = \tfrac{1}{2}\rho L_s^4/3 (1-k_s + k_s^2)(2k_s-1) Y_{v|}^{\cdot}$$

$$C_{4v} = \tfrac{1}{2}\rho \frac{2L_s}{3} Y_{v|v|}^{\cdot}$$

Heave:

$$m\left(\dot{w} + pv - qu - z_G(p^2 + q^2) + x_G(rp - \dot{q}) + y_G(rq + \dot{p}) \right) =$$

$$Z_{\dot{w}}\dot{w} + Z_{\dot{q}}\dot{q} + Z_{pp}p^2 + Z_{pv}pv + Z_{pr}pr +$$

$$Z_{vv}v^2 + Z_{rv}rv + Z_{rr}r^2 + Z_{u|u|}u|u| + Z_{w|u|}w|u| +$$

$$Z_{q|u|}q|u| + W_{ti} \cos \theta \cos \phi$$

$$+ \left(C_{1w}w|w| + C_{2w}q|w| + C_{3w}\frac{w}{|w|}q^2 \right)^{**}$$

$$+ \left(C_{4w}\frac{q}{|q|}\frac{w^3}{q} + C_{5w}\frac{q}{|q|}w^2 + C_{6w}w|q| + C_{7w}q|q| \right)^{*}$$

$$+ Z_s + Z_p + Z_t \qquad\qquad\qquad\qquad (A.4)$$

where

$$C_{1w} = \tfrac{1}{2}\rho L_s^2 Z_{w|w|}^{\cdot}$$

$$C_{2w} = \tfrac{1}{2}\rho L_s^3 (1-2k_s) Z_{w|w|}^{\cdot}$$

* Terms are cancelled when $w/qL_s > k_s$ or $w/qL_s < k_s - 1$

** Terms are cancelled when $k_s \geqq w/qL_s \geqq k_s - 1$

$$C_{3w} = \tfrac{1}{2}\rho L_s^4/3\,(1-3k_s + 3k_s^2)Z_w^{\cdot}\,|w|$$

$$C_{4w} = \tfrac{1}{2}\rho\, 2L_s/3 Z_w^{\cdot}\,|w|$$

$$C_{5w} = \tfrac{1}{2}\rho L_s^2\,(1-2k_s)Z_w^{\cdot}\,|w|$$

$$C_{6w} = \tfrac{1}{2}\rho L_s^3\left((1-k_s)^2 + k_s^2\right)Z_w^{\cdot}\,|w|$$

$$C_{7w} = \tfrac{1}{2}\rho L_s^4/3\,(1-k_s + k_s^2)\,(1-2k_s)Z_w^{\cdot}\,|w|$$

Yaw:

$$I_z\dot{r} + (I_y - I_x)pq + m\left(x_G(\dot{v} + ru - pw) - y_G(\dot{u} + qw - rv)\right) =$$

$$N_{\dot{r}}\dot{r} + N_{\dot{v}}\dot{v} + N_{pq}pq + N_{|u|v}|u|v + N_{r|u|}r|u| + N_{wp}wp +$$

$$N_{vq}vq + N_{p|u|}p|u| + N_{w|v|}w|v| +$$

$$W_{ti}\cos\theta\sin\phi + Woy_G\sin\theta + x_s y_s +$$

$$N_t + N_p +$$

$$\left(C_{1r}r|r| + C_{2r}\frac{r}{|r|}v^2 + C_{3r}\frac{r}{|r|}\frac{v^4}{r^2} + C_{4r}r|v|\right)^*$$

$$+\left(C_{5r}v|r| + C_{6r}v|v| + C_{7r}\frac{v}{|v|}r^2\right)^{**}$$

(A.5)

* Terms are cancelled when $-\dfrac{v}{rL_s} > k_s$ or $-\dfrac{v}{rL_s} < k_s - 1$

** Terms are cancelled when $k_s \geqq -\dfrac{v}{rL_s} \geqq k_s - 1$

where

$$C_{1r} = \tfrac{1}{2}\rho \, L_s^5/4 \left(k_s^4 + (1-k_s)^4 \right) Y_{v|v|}^{\cdot}$$

$$C_{2r} = \tfrac{1}{2}\rho L_s^3/2 \left(k_s^2 + (1-k_s)^2 \right) Y_{v|v|}^{\cdot}$$

$$C_{3r} = \tfrac{1}{2}\rho \, L_s/6 \, Y_{v|v|}^{\cdot}$$

$$C_{4r} = \tfrac{1}{2}\rho \frac{2L_s}{3} \left(k_s^3 - (1-k_s)^3 \right) Y_{v|v|}^{\cdot}$$

$$C_{5r} = \tfrac{1}{2}\rho \frac{2L_s}{3} \left(k_s^3 - (1-k_s)^3 \right) Y_{v|v|}^{\cdot}$$

$$C_{6r} = \tfrac{1}{2}\rho L_s^3/2 \left(k_s^2 - (1-k_s)^2 \right) Y_{v|v|}^{\cdot}$$

$$C_{7r} = \tfrac{1}{2}\rho \, L_s^5/4 \left(k_s^4 - (1-k_s)^4 \right) Y_{v|v|}^{\cdot}$$

Pitch:

$$I_y \dot{q} + (I_x - I_z)pr + m \left(z_G(\dot{u} + qw - rv) - x_G(\dot{w} + pv - qu) \right) =$$

$$M_{\dot{q}}\dot{q} + M_{\dot{w}}\dot{w} + M_{pr}pr + M_{u|w|}u|w| + M_{q|u|}q|u| + M_{vp}vp +$$

$$M_{u|u|}u|u| + M_{vv}v^2 + M_{rv}rv + M_{rr}r^2 - (W_o z_G + W_{ti}z_{ti})\sin\theta$$

$$-x_{ti}W_{ti}\cos\theta\cos\phi - x_s Z_s + M_p + M_t$$

$$+ \left(C_{1q}q|q| + C_{2q}\frac{q}{|q|}w^2 + C_{3q}\frac{q}{|q|}\frac{w^4}{q^2} + C_{4q}q|w| \right)^*$$

$$+ \left(C_{5q}w|q| + C_{6q}w|w| + C_{7q}\frac{w}{|w|}q^2 \right)^{**} \qquad (A.6)$$

* Terms are cancelled when $w/qL_s > k_s$ or $w/qL_s < k_s - 1$

** Terms are cancelled when $k_s \gtrless w/qL_s \gtrless k_s - 1$

where

$$C_{1q} = \tfrac{1}{2}\rho L_s^5/4 \left(k_s^4 + (1-k_s)^4 \right) Z'_{w|w|}$$

$$C_{2q} = \tfrac{1}{2}\rho L_s^3/2 \left(k_s^2 + (1-k_s)^2 \right) Z'_{w|w|}$$

$$C_{3q} = \tfrac{1}{2}\rho L_s/6 \; Z'_{w|w|}$$

$$C_{4q} = \tfrac{1}{2}\rho \, 2/3 L_s^4 \left(-k_s^3 + (1-k_s)^3 \right) Z'_{w|w|}$$

$$C_{5q} = \tfrac{1}{2}\rho \, 2/3 L_s^4 \left(k_s^3 + (1-k_s)^3 \right) Z'_{w|w|}$$

$$C_{6q} = \tfrac{1}{2}\rho L_s^3/2 \left(-k_s^2 + (1-k_s)^2 \right) Z'_{w|w|}$$

$$C_{7q} = \tfrac{1}{2}\rho L_s^5/4 \left(-k_s^4 + (1-k_s)^4 \right) Z'_{w|w|}$$

Euler Angle Rates

$$\dot{\psi} = \frac{r \cos\phi + q \sin\phi}{\cos\theta} \tag{A.7}$$

$$\dot{\theta} = q \cos\phi - r \sin\phi \tag{A.8}$$

$$\dot{\phi} = p + \dot{\psi} \sin\theta \tag{A.9}$$

Trajectory Rates in the Fixed Axes

$$\dot{X}_o = u \cos\psi \cos\theta + v(\cos\psi \sin\theta \sin\phi - \sin\psi \cos\phi)$$
$$+ w(\sin\psi \sin\phi + \cos\psi \sin\theta \sin\phi) \tag{A.10}$$

$$\dot{Y}_o = u \sin \quad \cos\theta + v(\cos\psi \cos\phi + \sin\psi \sin\theta \sin\phi)$$
$$+ w(\sin\psi \sin\theta \cos\phi - \cos\psi \sin\phi) \tag{A.11}$$

$$\dot{Z}_o = u \sin\theta + v \cos\theta \sin\phi + w \cos\theta \cos\phi \tag{A.12}$$

Displacements in the Fixed Axes

$$X_o = \int \dot{X}_o \, dt + X_{oi} \qquad (A.13)$$

$$Y_o = \int \dot{Y}_o \, dt + Y_{oi} \qquad (A.14)$$

$$Z_o = \int \dot{z}_o \, dt + Z_{oi} \qquad (A.15)$$

Main Propeller Forces

$$X_p = 755 \, n \, n - 58 \, un - 3.8u^2 + 26n \left(v_p^2 + w_p^2 \right)^{\frac{1}{2}}$$

$$\text{for } u \geq 0, \frac{n}{n} \geq -0.21 \qquad (A.16)$$

$$= -365n^2 - 172un - 45u^2 + 26n \left(v_p^2 + w_p^2 \right)^{\frac{1}{2}}$$

$$\text{for } u \geq 0, \frac{n}{n} \leq -0.21 \qquad (A.17)$$

$$= 755n^2 + 60un + 22u^2 + 26n \left(v_p^2 + w_p^2 \right)^{\frac{1}{2}}$$

$$\text{for } u < 0, n \geq 0 \qquad (A.18)$$

$$= -365n^2 - 13un + 22u^2 + 26n \left(v_p^2 + w_p^2 \right)^{\frac{1}{2}}$$

$$\text{for } u < 0, n < 0 \qquad (A.19)$$

$$Y_p = -30nv_p$$

$$\text{for } n \geq 0 \qquad (A.20)$$

$$= -12nv_p$$

$$\text{for } n < 0 \qquad (A.21)$$

$$Z_p = -30nw_p$$

$$\text{for } n \geq 0 \qquad (A.22)$$

$$= -12nw_p$$

$$\text{for } n < 0 \qquad (A.23)$$

$$K_p = 530n|n| - 6.5un - 4.05u^2 + 22n\left(v_p{}^2 + w_p{}^2 \right)^{\frac{1}{2}} + 131\dot{n}$$

$$\text{for } u \geq 0, \frac{n}{n} \geq - 0.21 \tag{A.24}$$

$$= -468n^2 - 155un - 38u^2 + 22n\left(v_p{}^2 + w_p{}^2 \right)^{\frac{1}{2}} + 131\dot{n}$$

$$\text{for } u \geq 0, \frac{n}{n} \leq - 0.21 \tag{A.25}$$

$$= 530n^2 + 80un + 15.2u^2 + 22n\left(v_p + w_p{}^2 \right)^{\frac{1}{2}} + 131\dot{n}$$

$$\text{for } u < 0, n \geq 0 \tag{A.26}$$

$$= -468n^2 - 8un + 15.2u^2 + 22n\left(v_p{}^2 + w_p{}^2 \right)^{\frac{1}{2}} + 131\dot{n}$$

$$\text{for } u \leq 0, n < 0 \tag{A.27}$$

$$M_p = -765nw_p$$

$$\text{for } n \geq 0 \tag{A.28}$$

$$= -306nw_p$$

$$\text{for } n < 0 \tag{A.29}$$

$$N_p = 765nv_p$$

$$\text{for } n \geq 0 \tag{A.30}$$

$$= 306nv_p$$

$$\text{for } n < 0 \tag{A.31}$$

$$\text{where} \quad v_p = v - 25.5r$$

$$w_p = w + 25.5q$$

TABLE 8
VEHICLE CONSTANTS

m = 4,363 slugs		z_{Go} = .1335 ft	
I_{xx} = 38,224 slug-ft²		L_v = 49.33 ft	
I_{yy} = 477,270 slug-ft²		L_s = 48.89 ft	
I_{zz} = 475,868 slug-ft²		L_l = 23.4 ft	

TABLE 9
HYDRODYNAMIC DERIVATIVES

COEFF.	NON DIM.	FACTOR	DIMENSIONAL
X_u	-1.583 10^{-3}	$\frac{\rho}{2}L_v^3$	-1.9 10^2
X_{rv}	3.358 10^{-2}	"	4.03 10^3
X_{qw}	-3.200 10^{-2}	"	-3.84 10^3
X_{rr}	-1.81 10^{-4}	$\frac{\rho}{2}L_v^4$	-1.071 10^3
X_{qq}	-7.0 10^{-5}	"	-4.14 10^2
X_{pr}	-1.8 10^{-4}	"	-9.47 10^2
$X_{u|u|}$	(F) -5.07 10^{-3}	$\frac{\rho}{2}L_v^2$	-1.234 10^1
	(B) -1.1 10^{-2}	"	-2/676 10^1
Y_v	-3.358 10^{-2}	$\frac{\rho}{2}L_v$	-4.03 10^3
Y_r	1.81 10^{-4}	$\frac{\rho}{2}L_v^4$	1.071 10^3
$Y_{\dot{p}}$	1.60 10^{-4}	"	9.47 10^2
Y_{pq}	7.0 10^{-5}	"	4.14 10^2
Y_{pw}	3.2 10^{-2}	$\frac{\rho}{2}L_v^3$	3.84 10^3
*$Y_{v|w|}$	-5.0 10^{-2}	$\frac{\rho}{2}L_v^2$	-1.22 10^2
$Y_{v|v|}$	-1.082 10^{-1}	$\frac{\rho}{2}L_v^2$	-2.38 10^2
$Y_{v|u|}$	(F) -5.6 10^{-2}	$\frac{\rho}{2}L_v^2$	-1.362 10^2
	(B) -9.4 10^{-2}	"	-2.29 10^2

COEFF.	NON DIM.	FACTOR	DIMENSIONAL
$Y_{r|u|}$	(F) 6.6 10^{-3}	$\frac{\rho}{2}L_v^3$	7.92 10^2
	(B) -1.9 10^{-3}	"	-2.3 10^2
$Y_{p|u|}$	(F) 3.0 10^{-3}	"	3.6 10^2
	(B) 5.75 10^{-3}	"	6. 10^2
Z_w	-3.2 10^{-2}		-3.84 10^3
$Z_{\dot{r}}$	-7. 10^{-5}	$\frac{\rho}{2}L_v^4$	-4.14 10^2
Z_{pr}	1.81 10^{-4}	"	1.071 10^3
Z_{pp}	1.60 10^{-4}	"	9.47 10^2
Z_{pv}	-3.358 10^{-2}	$\frac{\rho}{2}L_v^3$	-4.03 10^3
$Z_{w|w|}$	-9.408 10^{-2}	$\frac{\rho}{2}L_v^2$	-2.088 10^2
$Z_{n|u|}$	(F) 2.34 10^{-3}	$\frac{\rho}{2}L_v^2$	5.693
	(B) -2.34 10^{-3}	"	-5.693
$Z_{w|u|}$	(F) -3.12 10^{-2}	"	-7.59 10^1
	(B) -4.4 10^{-2}	"	-1.07 10^2
$Z_{q|u|}$	F -3.4 10^{-3}	$\frac{\rho}{2}L_v^3$	-4.10 10^2
	B 7.42 10^{-3}		8.9 10^2

(F) Forward Motion, u > 0

(B) Backward motion, u < 0

* (Splitter-board is in DSRV null wake, when w < 0 no lift occurs; this coefficient value is then zero)

TABLE 9
HYDRODYNAMIC DERIVATIVES, Continued

COEFF.	NON DIM.	FACTOR	DIMENSIONAL	COEFF.	NON DIM.	FACTOR	DIMENSIONAL
$M_{\dot{w}}$	-7.0×10^{-5}	$\frac{\rho}{2}L^4 v$	-4.14×10^2	$K_{v|u|}$	(F) 3.0×10^{-3}	$\frac{\rho}{2}L^3 v$	3.6×10^2
$M_{\dot{q}}$	-1.174×10^{-3}	$\frac{\rho}{2}L^5 v$	-3.43×10^5		(B) 5.75×10^{-3}	"	6.9×10^2
M_{pv}	-1.81×10^{-4}	$\frac{\rho}{2}L^4 v$	-1.071×10^3	$K_{p|u|}$	(F)-3.42×10^{-4}	$\frac{\rho}{2}L^4 v$	-2.02×10^3
M_{pr}	1.185×10^{-3}	$\frac{\rho}{2}L^5 v$	3.46×10^5		(B)-6.55×10^{-4}	"	-3.88×10^3
M_{rv}	1.6×10^{-4}	$\frac{\rho}{2}L^4 v$	9.47×10^2	$K_{r|u|}$	(F)-2.06×10^{-4}	"	-1.219×10^3
$M_{u|u|}$	(F)-2.7×10^{-4}	$\frac{\rho}{2}L^3 v$	-3.24×10^1		(B)-8.0×10^{-4}	"	-4.75×10^3
	(B)-5.23×10^{-4}	"	-6.28×10^1	*$K_{v|w|}$	5.73×10^{-3}	$\frac{\rho}{2}L^3 v$	6.87×10^2
$M_{w|u|}$	(F) 2.71×10^{-2}	"	3.252×10^2	$N_{\dot{r}}$	-1.202×10^{-3}	$\frac{\rho}{2}L^5 v$	-3.51×10^5
	(B)-2.3×10^{-2}	"	-2.76×10^3	$N_{\dot{v}}$	1.81×10^{-4}	$\frac{\rho}{2}L^4 v$	1.071×10^3
$M_{q|u|}$	(F)-8.3×10^{-3}	$\frac{\rho}{2}L^4 v$	-4.915×10^4	N_{pq}	-1.157×10^{-3}	$\frac{\rho}{2}L^5 v$	-3.38×10^5
	(B)-1.19×10^{-2}	"	-7.06×10^4	N_{pw}	-7.0×10^{-5}	$\frac{\rho}{2}L^4 v$	-4.14×10^2
$K_{\dot{p}}$	-1.815×10^{-5}	$\frac{\rho}{2}L^5 v$	-5.3×10^3	N_{vq}	-1.6×10^{-4}	"	-9.47×10^2
$K_{\dot{v}}$	1.6×10^{-4}	$\frac{\rho}{2}L^4 v$	9.47×10^2	*$N_{v|w|}$	8.4×10^{-3}	$\frac{\rho}{2}L^3 v$	7.7×10^2
K_{rw}	-1.11×10^{-4}	"	-6.57×10^2	$N_{v|u|}$	(F)-2.54×10^{-2}	"	-3.05×10^3
K_{vq}	1.11×10^{-4}	"	6.57×10^2		(B) 3.01×10^{-2}	"	3.60×10^3
K_{pw}	-1.6×10^{-4}	"	-9.47×10^2	$N_{p|u|}$	(F)-1.1×10^{-4}	$\frac{\rho}{2}L^4 v$	-6.5×10^2
K_{qr}	-2.74×10^{-5}	$\frac{\rho}{2}L^5 v$	-8.0×10^3		(B)-1.31×10^{-3}	"	-7.1×10^3
$K_{p|p|}$	-1.42×10^{-4}	"	-4.146×10^4	$N_{r|u|}$	(F)-8.29×10^{-3}	"	-4.92×10^4
$K_{v|v|}$	1.42×10^{-3}	$\frac{\rho}{2}L^3 v$	1.704×10^2		(B)-1.32×10^{-2}	"	-7.8×10^4

(F) Forward Motion, u > 0
(B) Backward motion, u < 0
* (Splitter-board is in DSRV hull wake, when w < 0 no lift occurs; this coefficient value is then zero)

APPENDIX B

NUMERICAL EXAMPLES OF DECOUPLING

In this appendix representative examples of the decoupling procedure applied to Class 1 and Class 2 systems are given.

Class 1 System Example

The Class 1 system of Chapter 2 is written in state vector form as

$$\dot{\bar{x}} = a(\bar{x},t) + B(\bar{x},t)\bar{u}$$
$$\bar{y} = c(\bar{x},t)$$

(B.1)

which is decoupled using feedback of the form

$$\bar{u} = f(\bar{x},t) + G(\bar{x},t)\bar{w}$$

(B.2)

giving the general closed loop system equation

$$\dot{\bar{x}} = a(\bar{x},t) + B(\bar{x},t)(f(\bar{x},t) + G(\bar{x},t)\bar{w})$$
$$\bar{y} = c(\bar{x},t)$$

(B.3)

The entries for the vector and matrix functions used in this example are

$$a(\bar{x},t) = \begin{bmatrix} x_1 + e^{-2t}e^{x_2} \\ \tan x_2 \\ x_2 \end{bmatrix}, \quad B(\bar{x},t) = \begin{bmatrix} x_1 - 1 & 0 \\ x_2 e^{x_1} & 1 \\ 0 & 0 \end{bmatrix}, \quad c(\bar{x},t) = \begin{bmatrix} x_1 \\ x_3 \end{bmatrix}$$

The terms in the vector feedback equation (B.2) to decouple the system, as given in Theorem 1 and the synthesis procedure in Chapter 2, are

$$G(\bar{x},t) = \Lambda\, D^{*^{-1}}(\bar{x},t)\,(r(\bar{x},t) - a^*(\bar{x},t)) \qquad (B.4)$$

The entries of Λ and $r(\bar{x},t)$ are chosen by the designer in the synthesis procedure. $D^*(\bar{x},t)$ and $a^*(\bar{x},t)$ are given in the de--coupling theorem generated by differentiating the outputs.

Differentiating the first output:

$$y_1 = x_1$$

$$y_1^{(1)} = \nabla y_1 \dot{\bar{x}} = \begin{bmatrix} 1 & 0 & 0 \end{bmatrix} \dot{\bar{x}}$$

$$= x_1^2 + e^{-2t}e^{x_2} + \quad (x_1-1) \quad 0 \quad (f(\bar{x},t) + G(\bar{x},t)\bar{w})$$

$$\nabla y_1 B(\bar{x},t) = \begin{bmatrix} (x_1-1) & 0 \end{bmatrix} \neq 0$$

$$\rho_1 = 1$$

$$\nabla y_1 a(\bar{x},t) = x_1^2 + e^{-2t}e^{x_2}$$

Differentiating the second output:

$$y_2 = x_3$$

$$y_2^{(1)} = \begin{bmatrix} 0 & 0 & 1 \end{bmatrix} \dot{x} = x_2^2$$

$$\nabla y_2 B(\bar{x},t) = \begin{bmatrix} 0 & 0 \end{bmatrix} = 0$$

continue

$$y_2^{(2)} = \begin{bmatrix} 0 & 2x_2 & 0 \end{bmatrix} \dot{x}$$

$$= 2x_2 \tan x_2 + \begin{bmatrix} 2x_2^2 e^{x_1} & 2x_2 \end{bmatrix} (f(\bar{x},t) + G(\bar{x},t)\bar{w})$$

$$\nabla y_2^{(1)} B(\bar{x},t) = \begin{bmatrix} 2x_2^2 e^{x_1} & 2x_2 \end{bmatrix} = 0$$

$$\rho_2 = 2$$

$$\nabla y_2^{(1)} a(\bar{x},t) = 2x_2 \tan x_2$$

From (2.6) and Theorem 1

$$D^*(\bar{x},t) = \begin{bmatrix} (x_1 - 1) & 0 \\ 2x_2^2 e^{x_1} & 2x_2 \end{bmatrix} \tag{B.6}$$

$$\det D^*(\bar{x},t) = 2x_2(x_1 - 1)$$

$$H = \{\bar{x}: x_2 \neq 0, x_1 \neq 1\}$$

Thus the system can theoretically be decoupled over the entire state space except the points $x_2 = 0$ and $x_1 = 1$.

Collecting the terms from the differentiation process for $a^*(\bar{x},t)$ given by (2.9)

$$a^*(\bar{x},t) = \begin{bmatrix} x_1^2 + e^{-2t}e^{x_2} \\ \\ 2x_2 \tan x_2 \end{bmatrix} \tag{B.7}$$

From (2.16) in the synthesis procedure, $r(\bar{x},t)$ for a linear input-output decoupled system is given by

$$r(\bar{x},t) = \begin{bmatrix} m_{10}x_1 \\ \\ m_{20}x_3 + m_{21}x_2^2 \end{bmatrix} \tag{B.8}$$

Letting $\Lambda = I$ (Identity matrix) in the synthesis procedure then (B.4) and (B.5) become

$$G(\bar{x},t) = D^{*-1}(\bar{x},t) = \frac{1}{2x_2(x_1-1)} \begin{bmatrix} 2x_2 & 0 \\ -2x_2^2 e^{x_1} & (x_1-1) \end{bmatrix} \tag{B.9}$$

and

$$f(\bar{x},t) = \begin{bmatrix} f_1(\bar{x},t) \\ \\ f_2(\bar{x},t) \end{bmatrix} \tag{B.10}$$

where

$$f_1(\bar{x},t) = m_{10}x_1/(x_1-1) - (x_1^2 + e^{-2t}e^{x_2})/(x_1-1)$$

$$f_2(\bar{x},t) = -m_{10}x_1x_2e^{x_1}/(x_1-1) + (m_{20}x_3 + m_{21}x_2^2)/2x_2$$

$$+ x_2e^{x_1}(x_1^2 + e^{-2t}e^{x_2})/(x_1-1) - (2x_2\tan x_2)/2x_2$$

Substituting for $f(\bar{x},t)$ and $G(\bar{x},t)$ into the system closed loop equation (B.3) gives the following input-state relation--ships.

$$\dot{x}_1 = m_{10}x_1 + w_1$$

$$\dot{x}_2 = m_{20}x_3/2x_2 + \tfrac{1}{2}m_{21}x_2 + w_2/2x_2 \qquad (B.11)$$

$$\dot{x}_3 = x_2$$

Note that, besides being nonlinear, the input-state relation--ships of (B.11) do not constitute a completely controllable system since $\dot{x}_3$ can only be driven in a positive direction. This is evident from the fact that $\dot{x}_3 = x_2^2$ in (B.11).

The input-output relationships from the synthesis procedure are

$$\dot{y}_1 = m_{10}y_1 + w_1$$

$$\qquad (B.12)$$

$$\ddot{y}_2 = m_{20}y_2 + m_{21}\dot{y}_2 + w_2$$

The input-output relationships can be made stable by choosing the m's > 0 in (B.12). However, for the decoupled system to be stable, the input-state relationships must also be stable.

From (B.11), it is apparent that x_1 will be stable if $m_{10} > 0$. The stability of the equations for $\dot{x}_2$ and $\dot{x}_3$ in (B.11) is not so obvious. If we consider only constant values of input w_2, the equations for $\dot{x}_2$ and $\dot{x}_3$ constitute an autonomous system and can be represented as a single first order differential equation by

$$\frac{dx_2}{dx_3} = \tfrac{1}{2}(m_{20}x_3/x_2^3 + m_{21}/x_2 + w_2/x_2^3) \qquad \text{(B.13)}$$

The stability of this equation can now be determined for different values of m_{20}, m_{21} and w_2 using phase plane analysis. Trajectories are located on the $x_2 - x_3$ plane by solving for the slope from $\dfrac{dx_2}{dx_3}$ at a number of points.

The technique is fairly straightforward and the interested reader is referred to Cunningham.[56]

Class 2 System Example

The Class 2 system of Chapter 2 is given by

$$\dot{\bar{x}} = a(\bar{x},t) + b(\bar{x},\bar{u},t)$$

$$\bar{y} = c(\bar{x},t)$$

(B.14)

This system is decoupled by solving the following vector feedback equation for all the components of $\bar{u}$:

$$d(\bar{x},\bar{u},t) = f(\bar{x},t) + \bar{w}$$

(B.15)

For linear decoupling, (B.15) becomes

$$d(\bar{x},\bar{u},t) = r(\bar{x},t) - a^*(\bar{x},t) + \Lambda \bar{w}$$

(B.16)

as given in the synthesis procedure for Class 2 systems.

The entries for vector functions of (B.14) are

$$a(\bar{x},t) = \begin{bmatrix} \tan x_1 \\ x_2 \end{bmatrix} \;,\; b(\bar{x},\bar{u},t) = \begin{bmatrix} u_1 + u_1 u_2 \\ u_2^2 \end{bmatrix} \;,\; c(\bar{x},t) = \begin{bmatrix} x_1 \\ 2x_1 + x_2 \end{bmatrix}$$

According to the theory for Class 2 systems, the entries of $d(\bar{x},\bar{u},t)$ and $a^*(\bar{x},t)$ are generated by differentiating the outputs.

Differentiating the first output:

$$y_1 = x_1$$

$$y_1^{(1)} = \nabla y_1 \dot{x} = \begin{bmatrix} 1 & 0 \end{bmatrix} \dot{x} = \tan x_1 + u_1 + u_1 u_2$$

$$\nabla y_1 b(\bar{x}, \bar{u}, t) = u_1 + u_1 u_2$$

Therefore $\rho_1 = 1$

$$\nabla y_1 a(\bar{x}, t) = \tan x_1$$

Differentiating the second output:

$$y_2 = 2x_1 + x_2$$

$$y_2^{(1)} = \begin{bmatrix} 2 & 1 \end{bmatrix} \dot{x} = 2\tan x_1 + x_2 + 2u_1 u_2 + 2u_1 + u_2^2$$

$$\nabla y_2 b(\bar{x}, \bar{u}, t) = 2u_1 u_2 + 2u_1 + u_2^2 \neq 0$$

Therefore $\rho_2 = 1$

$$\nabla y_2 a(\bar{x}, t) = 2\tan x_1 + x_2$$

From the above differentiation process and Theorem 2 in Chapter 2, the entries for $d(\bar{x}, \bar{u}, t)$ and $a^*(\bar{x}, t)$ are

$$d(\bar{x},\bar{u},t) = \begin{bmatrix} u_1 + u_1 u_2 \\ 2u_1 u_2 + 2u_1 + u_2^2 \end{bmatrix} \tag{B.17}$$

$$\text{and} \quad a^*(\bar{x},t) = \begin{bmatrix} \tan x_1 \\ 2\tan x_1 + x_2 \end{bmatrix} \tag{B.18}$$

Application of the sufficient condition for decoupling given in Theorem 2 to (B.17) gives

$$J_d(\bar{x},\bar{u},t) = \begin{vmatrix} 1 & 1 \\ 2 + 2u_2 & 2u_1 + 2u_2 \end{vmatrix} = 2u_1 - 2 \neq 0$$

Therefore a solution set exists to the vector feedback equa-
-tion of (B.15) and also for (B.16).

Applying the synthesis procedure to linearly decouple the
system gives

$$r(\bar{x},t) = \begin{bmatrix} m_{10} x_1 \\ m_{20} (x_1 + x_2) \end{bmatrix} \tag{B.19}$$

and for simplicity we let $\Lambda = I$. In a physical system where the input vector $\bar{w}$ consisted of say pressures and voltages whose magnitudes were not large enough to yield the desired system response, then we would not choose $\Lambda = I$.

Combining (B.17), (B.18) and (B.19), the components of the vector feedback equation (B.16) are

$$u_1 + u_2 = m_{10}x_1 - \tan x_1 + w_1 \tag{B.20}$$

$$u_2^2 + 2u_1u_2 + 2u_1 = m_{20}(2x_1 + x_2) - 2\tan x_1 - x_2 + w_2 \tag{B.21}$$

The above equations must be solved for u_1 and u_2 to decouple the system by state variable feedback. Solution of these two equations results in rather lengthy expressions for u_1 and u_2 which will not be included here. The solution set does impose some restrictions. For the solution to be real, the space H is restricted to

$$H = \bar{x} : (2m_{10}x_1 - 2m_{10}\tan x_1 + 2w_1)^2 - 12(2m_{10}x_1$$

$$- 2m_{10}\tan x_1 + 2w_1 - m_{20}(2x_1 + x_2) + 2\tan x_1$$

$$+ x_2 - w_2) \geq 0 \tag{B.22}$$

Substituting the solution for the inputs u_1 and u_2 into (B.14)

for the input-state relationships gives

$$\dot{x}_1 = m_{10}x_1 + w_1$$

$$\dot{x}_2 = (m_{20} - 2m_{10})x_1 + m_{20}x_2 - 2w_1 + w_2$$

(B.23)

and for the input-output relationships

$$\dot{y}_1 = m_{10}y_1 + w_1$$

$$\dot{y}_2 = m_{20}y_2 + w_2$$

(B.24)

Choosing the m's > 0 in (B.23) and (B.24) will give a decoupled linear system which is completely stable, controllable and observable.[45,51]

APPENDIX C

COMPUTER PROGRAMS

```
PROGRAM NO. 1

TITLE ROLL-SURGE COUPLED SYSTEM RESPONSE
INITIAL
     U1=1.64
     U2=0.
DYNAMIC
X1 IS THE SURGE VELOCITY
X2 IS THE ROLL ANGLE
     X1DOT=-4.55E-3*X1*X1-.0129*X1*U1+.168*U1*U1
     C1=-.444*X2-.0443*X1*X3-.781*X3*ABS(X3)-.958E-4*X1*X1
     X3DOT=C1-1.54E-4*X1*U1+.0155*U1*U1+1.05E-4*U2
     X3=INTGRL(0.,X3DOT)
     X2=INTGRL(0.,X3)
     X1=INTGRL(0.,X1DOT)
TIMER PRDEL=.2,OUTDEL=.2,FINTIM=40.
PRINT X1,X2,X3
PRTPLT X1,X2
END
STOP
ENDJOB


PROGRAM NO. 2

TITLE DECOUPLED ROLL - SURGE WITH INPUT CONSTRAINTS NOT INCLUDED
PARAMETER W1=(.2,.3,.45)
     M10=-1./17.
     M20=-.4
     M21=-.88
     W2=0.
DYNAMIC
     X1DOT=-4.55E-3*X1*X1-.0129*X1*U1+.168*U1*U1
     C1=-.444*X2-.0443*X1*X3-.781*X3*ABS(X3)-.958E-4*X1*X1
     X3DOT=C1-1.54E-4*X1*U1+.0125*U1*U1+1.05E-4*COS(X2)*U2
     X3=INTGRL(0.,X3DOT)
     X2=INTGRL(0.,X3)
     X1=INTGRL(0.,X1DOT)
     C3=(.0129*X1)**2+.672*(M10*X1+4.55E-3*X1*X1+W1)
     U1=(.0129*X1+SQRT(C3))/.336
     U2=(-C1-.0125*U1*U1+1.54E-4*X1*U1+M20*X2+M21*X3)/1.05E-4*COS(X2)
TIMER PRDEL=.2,OUTDEL=.2,FINTIM=30.
PRINT U1,U2,X1DOT,X1,X2
PRTPLT X1,X2
END
STOP
ENDJOB


PROGRAM NO. 3

TITLE DECOUPLED ROLL-SURGE. INPUT CONSTRAINTS INCLUDED.
PARAMETER W1=.47
     M10=-1./17.
     M20=-.4
     M21=-.88
     W2=0.
DYNAMIC
     X1DOT=-4.55E-3*X1*X1-.0129*X1*U1+.168*U1*U1
```

```
      C1=-.444*X2-.0443*X1*X3-.781*X3*ABS(X3)-.954E-4*X1*X1
      X3DOT=C1-1.54E-4*X1*U1+.0125*U1*U1+1.05E-4*COS(X2)*U2
      X3=INTGRL(0.,X3DOT)
      X2=INTGRL(0.,X3)
      X1=INTGRL(0.,X1DOT)
      C3=(.0129*X1)**2+.672*(M10*X1+4.55E-3*X1*X1+W1)
      U1DOT=2.*(MC-U1)
       U1=INTGRL(0.,U1DOT)
      MC=(.0129*X1+SQRT(C3))
      C4=(-C1-.0125*U1+1.54E-4*X1*U1+M20*X2+M21*X3)/1.05E-4*COS(X2)
      WPDOT=DERIV(0.,C4)
NOSORT
      IF(WPDOT.LT.-56.4) WPDOT=-56.4
      IF(WPDOT.GT.56.4) WPDOT=56.4
SORT
TIMER PRDEL=.2,OUTDEL=.2,FINTIM=25.
PRINT X1,X2,WPDOT
PRTPLT X1,X2,WPDOT
END
STOP
ENDJOB


PROGRAM NO.3-A

MODIFICATIONS TO COMPENSATE THE NEW SYSTEM IMPUTS W1 AND W2.
NOTE W1C AND W2C ARE THE NEW SYSTEM IMPUTS.
      W1DOT=.5*(W1C-W1)
      W1=INTGRL(0.,W1DOT)
      W2DOT=.5*(W2C-W2)
      W2=INTGRL(0.,W2DOT)


PROGRAM 4

TITLE DSRV TURNING CIRCLE SIMULATION FULL 360 DEGREE TURN
INITIAL
ASSIGNMENT OF NUMERICAL VALUES TO CONSTANTS
      C4=1./4.507E3
      C1=8083.*C4
      C2=-16.7*C4
      C3=-830.*C4
      LS=46.95
      L1=23.4
      KS=L1/LS
      C14=1./8683.
      C5=-3323.*C14
      C6=-124.*C14
      RO=1.992
      C7=RO*LS*LS*(-.142)/2.
      C8=C7*LS*(2.*KS-1.)
      C9=C7*LS*LS*(1.-3.*KS+3.*KS*KS)/3.
      C10=2.*C7/(3.*LS)
      C11=C7*(2.*KS-1.)
      C12=C7*LS*((1.-KS)**2+KS*KS)
      C13=C7*LS*LS*(1.-KS+KS*KS)*(2.*KS-1.)
      C24=1./8.6E5
      C15=-3600.*C24
      C16=(-3.2E4)*C24
      CA=RO*LS*LS*(-.142)*C24/2.
      C17=CA*LS**3*(KS**4+(1.-KS)**4)/4.
      C18=CA*LS*(KS*KS+(1.-KS)**2)/2.
```

```
      C19=CA/(2.*LS)
      C20=2.*CA*LS*LS*(KS**3-(1.-KS)**3)/3.
      C21=2.*CA*LS*LS*(KS**3+(1.-KS)**3)/3.
      C22=CA*LS*(KS*KS-(1.-KS)**2)/2.
      C23=CA*LS**3*(KS**4-(1.-KS)**4)/4.
      XS=-(23.55+1.83302)
      CS=RO*R.*1.83
      TS=0.5
  UI=5.5
  N=1.5
      DELY=15.*CP
      TR=3.0
      CP=3.14159/180.
  D=7.0
  FSX=RO*D**3*N*(0.95*N*D-1.19*U)
      FI=755.*N*N
DYNAMIC
EQUATION FOR SURGE
      UDOT=C1*R*V+C2*U*U+C3*R*R+C4*(FPX+FSX)
      U=INTGRL(UI,UDOT)
EQUATION FOR SWAY
      VDOT=C5*R*U+C6*V*U+C1V+C2V+C14*(FPY+FSY)
      V=INTGRL(0.,VDOT)
EQUATION FOR YAW
      RDOT=C15*U*V+C16*R*U+CR1+CR2+C24*(NP+NS)
      R=INTGRL(0.,RDOT)
DECISION BLOCK FOR CONSTANTS IN YAW - SWAY DRAG TERMS
NOSORT
      IF(ABS(R).LT.1.E-7) GO TO 14
      IF(ABS(V).LT.1.E-8) GO TO 16
      KB=0.5*LS*ABS(R)
      IF(ABS(V).LT.KB) GO TO 11
      GO TO 5
   11 C2V=0.
      C1V=C10*V**3/ABS(R)+C11*R*V*V/ABS(R)+C12*V*ABS(R)+C13*R*ABS(R)
      CR2=0.
      CRO=C17*R*ABS(R)+C18*R*V*V/ABS(R)
      CR1=CRO+C19*ABS(R)*V**4/R**3+C20*ABS(R)*V
      GO TO 9
    5 C1V=0.
      C2V=ABS(V)*(C7*V+C8*R+C9*R*R/V)
      CR1=0.
      CR2=ABS(V)*(C21*R+C22*V+C23*R*R/V)
      GO TO 9
   14 C1V=0.
      C2V=C7*ABS(V)*V
      CR1=0.
      CR2=C22*ABS(V)*V
      GO TO 9
   16 C1V=0.
      C2V=C13*R*ABS(R)
      CR1=0.
      CR2=C17*R*ABS(R)
    9 CONTINUE
SORT
CONSTANT FORWARD VELOCITY CONTROL BLOCK
NOSORT
      NPO=N
      IF(U.GT.5.6) N=NPO-.0001
      IF(U.GT.5.7) N=NPO-.0002
      IF(U.GT.5.8) N=NPO-.0003
      IF(U.GT.5.9) N=NPO-.0004
```

```
      IF(U.LT.5.4) N=NPO+.0001
      IF(U.LT.5.3) N=NPO+.0002
      IF(U.LT.5.2) N=NPO+.0003
      IF(U.LT.5.1) N=NPO+.0004
      IF(N.GT.1.80) N=1.6
      IF(N.LT.1.0) N=0.4
SORT
*CALCULATION OF FORCES FOR PROPELLER AND TILTABLE SHROUD
NOSORT
      THETA=ATAN((V+XS*R)/U)
      ALPHS=DELY+THETA
      AD=ALPHS/CP
      IF(ABS(AD).LT.1.E-6) GO TO 15
      IF(ABS(AD).LE.15.0) GO TO 2
      CL=1.21*ABS(AD)/AD-.21*(AD-15.0*ABS(AD)/AD)/14.
      GO TO 3
   2  CL=1.21*AD/15.0
   3  CONTINUE
      V2=U*U+(V+XS*R)**2
      IF(AD.GT.26.)CL=1.0
      LIFT=CL*CS*V2
      IF(ABS(AD).LE.10.) GO TO 12
      CD=.12+(ABS(AD)-10.)*.68/30.
      GO TO 13
  12  CD=.05+(7.E-4)*AD*AD
      GO TO 13
  15  V2=U*U+(V+XS*R)**2
      CD=.05
  13  CONTINUE
      DRAG=CD*CS*V2
      FSX=-LIFT*SIN(THETA)-DRAG*COS(THETA)
      FSY=LIFT*COS(THETA)-DRAG*SIN(THETA)
      NS=FSY*XS
      VP=V+XS*R
      FPX=755.*N*N-58.*U*N-3.8*U*U
      FPY=0.
      NP=FPY*XS
SORT
TRANSFORMATIONS TO FIXED AXIS SYSTEM
      CHI=INTGRL(0.,R)
      XDOT=U*COS(CHI)-V*SIN(CHI)
      YDOT=U*SIN(CHI)+V*COS(CHI)
      X=INTGRL(0.,XDOT)
      Y=INTGRL(0.,YDOT)
      VAVE=INTGRL(0.,U)
      YAW=CHI/CP
      YC=-YAW
TIMER DELT=1.E-5,DELMIN=1.E-7,PRDEL=.5,OUTDEL=.5,FINTIM=300.
FINISH YC=105.
PRINT X,Y,N,U,V,R,YAW,VAVE
END
STOP
ENDJOB


PROGRAM 4-A

CALCULATION OF FORCES FOR THE WAKE STEERING NOZZLE AND PRO-
PELLER. THIS BLOCK REPLACES THE BLOCK FOR CALCULATING THE FORCES
FOR THE PROPELLER AND TILTABLE SHROUD.
NOSORT
      FPX=0.
```

```
      FPY=0.
      N=.996*U/(.788*D)
      RK=RO*D)**3*M
      FSX=RK*(0.788*N*D-0.996*U)
      FSY=RK*(.215*N*D-.0771*U+.683*U*U/(N*D))
  22  NS=FSY*XS
      NP=FPY*XS
SORT


PROGRAM 4-B

THE ACCELERATING FORCE CONTROL BLOCK. THIS BLOCK REPLACES THE
FORWARD VELOCITY CONTROL BLOCK FOR THE 90 DEGREE ACCELERATED TURN
      NPO=N
      FT=FPX+FSX
      IF(FT.GT.(FI+2.))  N=NPO-.0002
      IF(FT.GT.(FI+4.))  N=NPO-.0005
      IF(FT.GT.(FI+6.))  N=NPO-.0008
      IF(FT.LT.(FI-2.))  N=NPO+.0002
      IF(FT.LT.(FI-4.))  N=NPO+.0005
      IF(FT.LT.(FI-6.))  N=NPO+.0008
      IF(N.GT.7.) N=7.
      IF(N.LT.1.0) N=1.0
SORT


PROGRAM 4-C

THE DECCELERATED FORCE CONTROL BLOCK. THIS BLOCK REPLACES
THE FORWARD VELOCITY CONTROL BLOCK FOR THE 90 DEGREE DECCELE-
RATED TURN.
NOSORT
      NPO=N
      FT=FPX+FSX
      IF(FT.GT.(FI+5.))  N=NPO-.0002
      IF(FT.GT.(FI+10.))  N=NPO-.0005
      IF(FT.LT.(FI-5.))  N=NPO+.0002
      IF(FT.LT.(FI-10.))  N=NPO+.0005
SORT
THE END)
```

APPENDIX D

COMPARISON OF A WSN AND TILTABLE SHROUD

In this appendix, equations are developed which enable a comparison of the steering characteristics of a WSN and the tiltable shroud on the DSRV. The equations of motion given in Appendix A are simplified by a number of assumptions to describe vehicle motion in the horizontal plane. Information on the steering forces developed by the DSRV tiltable shroud is taken from the Lockheed report.[20] Data on the steering characteristics of the WSN is taken from Chapter V of this thesis describing forward velocity tests.

The Reduced Equations of Motion

For the purpose of comparing the tiltable shroud and a WSN, the equations of motion for the DSRV are simplified by the following assumptions:

1) Only motion in the horizontal plane is considered and motion in the roll degree of freedom is assumed zero. Therefore, $w = p = q = \emptyset = \Theta = 0$. This assumption is not overly restrictive since most standard turning maneuvers are performed in the horizontal plane.

2) The center of mass and the center of gravity of the vessel are assumed to coincide in the horizontal plane. Therefore, $x_G = y_G = 0$.

3) The cross-coupling acceleration terms $Y_{\dot{r}}\dot{r}$ and $N_{\dot{v}}\dot{v}$ in Equations A.3 and A.5 respectively, can be neglected as indicated in Table 1, Chapter III.

4) The ducted thrusters are not used in any of the maneuvers. Therefore, $X_t = Y_t = Z_t = 0$

With these simplifying assumptions, the equations of motion in the remaining three degrees of freedom are:

Surge:

$$m(\dot{u} - rv) = X_{\dot{u}}\dot{u} + X_{rv}rv + X_{u|u|}u|u| + X_{rr}r^2 + X_p + X_s \qquad (D.1)$$

Sway:

$$m(\dot{v} + ru) = Y_{\dot{v}}\dot{v} + Y_{r|u|}r|u| + Y_{v|u|}v|u| + (C_{1v}v|v| + C_{2v}r|v|$$

$$+ C_{3v}\frac{v}{|v|}r^2)^{**} + (C_{4v}\frac{r}{|r|}\frac{v^3}{r} + C_{5v}\frac{r}{|r|}v^2 + C_{6v}v|r|$$

$$+ C_{7v}r|r|)^* + Y_p + Y_s \qquad (D.2)$$

Yaw:

$$I_z\dot{r} = N_{u|v|}u|v| + N_{r|u|}r|u| + (C_{1r}r|r| + C_{2r}\frac{r}{|r|}v^2$$

$$+ C_{3r}\frac{r}{|r|}\frac{v^4}{r^2} + C_{4r}r|v|)^* + (C_{5r}v|r| + C_{6r}v|v|$$

$$+ C_{7r}\frac{v}{|v|}r^2)^{**} + x_s Y_s + N_p \qquad (D.3)$$

* Terms are cancelled when $-\frac{v}{rL_s} > k_s$ or $-\frac{v}{rL_s} < k_s - 1$

** Terms are cancelled when $k_s \geqq -\frac{v}{rL_s} \geqq k_s - 1$

Propeller-Nozzle Characteristics

The Tiltable Shroud-Main Propeller

The tiltable shroud lift and drag forces, F_ℓ and F_d, are given by

$$F_\ell = \frac{\rho}{2} C_\ell A_c V^2 \qquad (D.4)$$

and $\quad F_d = \frac{\rho}{2} C_d A_c V^2 \qquad (D.5)$

where A_c = characteristic area

C_ℓ = lift coefficient

C_d = drag coefficient

V = velocity of the fluid

The characteristic area A_c is given as 52.3 ft.^{2} [20]

The shroud lift and drag coefficients as a function of the angle of attack of the fluid α_s are plotted in Figure 41 from data in the Lockheed report.[20] The relevent geometric angles and fluid velocities used to describe the steering forces of the tiltable shroud are shown in Figure 42.

The angle θ_w is the angle of approach of the fluid measured relative to the vessel surge axis and observed from a point on the tail of the submersible. The angle δ_y represents the angular mechanical deflection of the shroud relative to the vehicle sway axis.

With these definitions, the equations for X_s in (D.1) and Y_s in (D.2) and (D.3) become

$$X_s = - F_\ell \sin \Theta_w - F_d \cos \Theta_w \qquad (D.6)$$

$$Y_s = F_\ell \cos \Theta_w - F_d \sin \Theta_w \qquad (D.7)$$

The main propeller force X_p in the surge direction in (D.1) is given by (A.16). The main propeller force in the sway direction Y_p and the yaw moment due to the main propeller N_p are small by comparison and these terms were dropped from (D.2) and (D.3).

Selection of a WSN Size and Type

Figures 31 and 32 in Chapter V show the efficiency of and axial and radial thrust coefficients, K_{TA} and K_{TR}, plotted as a function of advance ratio J for a number of different propeller pitch to diameter ratios in Nozzles A2 and A3. Based on these test results, a nozzle and propeller combination must be selected for use in the simulations which is compatible with the operating characteristics of the DSRV and as optimum as possible in terms of efficiency and steering ratio K_{TR-A}.

The procedure in selecting a WSN is basically the same as that used by a submersible designer in selecting a thruster for any vessel, except for the additional parameter, the steering

ratio. The procedure is largely trial and error where the designer must select a propulsor to satisfy specified thrust requirements efficiently within certain constraints such as size and rotational speed.

One immediately apparent constraint which must be placed on the WSN is the physical size of the device. The diameter of the tiltable shroud is 6 feet and its length is 1.83 feet. Since the WSN tested have a length to diameter ratio of 2.5, a 6 foot diameter WSN would have the unwieldly length of 15 feet. The full length of the DSRV is only 50 feet. Consequently, the choice of diameter was restricted to a range of 2 to 3 feet. This results in comparable shroud external surface areas.

The necessary insight for selecting the best nozzle-propeller combination is gained by considering the equations relating the WSN thrust and the thrust required to propel the submersible.

From Figures 31 and 32, the equations for axial thrust for each WSN can be derived from the curves for the axial thrust coefficient K_{TA}. The equation for K_{TA} for a particular nozzle-propeller combination is given by

$$K_{TA} = C_o - C_1 J \qquad (D.8)$$

where the C_o and C_1 are positive constants representing the intercept and slope of the thrust coefficient curve.

Using the equations defining the axial thrust coefficient ($K_{TA} = F_x / \rho n^2 D^4$) and advance ratio ($J = u/nD$) given in Chapter IV, (D.8) becomes

$$F_x = \rho C_o D^4 n^2 - \rho C_1 D^3 un \qquad \text{(D.9)}$$

The thrust F_x must be sufficient to propel the submersible during cruising in straight ahead motion. For straight ahead, constant velocity motion, (D.1) becomes

$$X_p = F_x = X_{u|u|} u^2 \qquad \text{(D.10)}$$

Combining (D.9) and D.10) and substituting the numerical values for the fluid density ρ and coefficient of drag $X_{u|u|}$, taken from Table 9 , Appendix A, gives

$$C_o D^4 n^2 - C_1 Dun - 6.17u^2 = 0 \qquad \text{(D.11)}$$

Equation (D.11) can be rewritten in terms of the advance ratio J as

$$J^2 + .162C_1 D^2 J - .162C_o D^2 = 0 \qquad \text{(D.12)}$$

The two variables, u and n, do not appear directly in this equation but are contained in J. This is particularly advantageous since the two parameters we want to maximize, the efficiency and steering ratio K_{TR-A}, are both plotted as functions of advance ratio J.

Equation (D.12) can be solved for J as a function of nozzle diameter D giving

$$J = D^2 \left(-.081C_1 + \sqrt{(.041C_1)^2 + .162C_o/D^2} \right) \qquad \text{(D.13)}$$

where only the positive root has been retained since we are considering only motion in the forward direction.

The next step in the procedure of selecting an optimum WSN is essentially a trial and error iteration back and forth between the curves of Figures 31 , 32 , and 33 and Equation (D.13).

The procedure is as follows:

1) A nozzle-propeller combination is selected from either Figure 31 or Figure 32 and the constants, C_o and C_1, are determined from the K_{TA} curve for this combination.

2) Values of advance ratio J for this WSN are calculated using Equation (D.13) over the constrined range of nozzle diameters of 2 feet to 3 feet.

3) The efficiency and steering ratio for the WSN over this range of advance ratios is obtained from the curves of Figures 31, 32 and 33 and is used as the basis of comparison.

Repeating this procedure for the nozzle-propeller combinations in Figures 31 and 32 led to the selection of nozzle A3 operating with propeller no.4 at a diameter of 2.75 feet as the

optimum choice. This choice results in operation at an advance ratio of about .43.

The equations developed in this appendix were simulated on the digital computer using CSMP.[52] The programs are given in Appendix C. The results of these simulations are presented in Figures 36,37 and 38 in Chapter 6.